Level Set Method in Medical Imaging Segmentation

Taylor & Francis
Taylor & Francis Group
http://taylorandfrancis.com

Level Set Method in Medical Imaging Segmentation

Authored by

Ayman El-Baz and Jasjit S. Suri

CRC Press
Taylor & Francis Group
Boca Raton London New York

CRC Press is an imprint of the
Taylor & Francis Group, an **informa** business

CRC Press
Taylor & Francis Group
6000 Broken Sound Parkway NW, Suite 300
Boca Raton, FL 33487-2742

Printed on acid-free paper

International Standard Book Number-13: 978-1-138-55345-3 (Hardback)

Library of Congress Cataloging-in-Publication Data

Names: El-Baz, Ayman S., editor. | Suri, Jasjit S. editor.
Title: Level set method in medical imaging segmentation / [edited by] Ayman El-Baz and Jasjit S. Suri.
Description: Boca Raton : Taylor & Francis, 2019. | Includes bibliographical references.
Identifiers: LCCN 2019005809 | ISBN 9781138553453 (hardback : alk. paper) | ISBN 9781315148595 (ebook)
Subjects: | MESH: Image Interpretation, Computer-Assisted—methods | Image Processing, Computer-Assisted—methods | Mathematical Computing
Classification: LCC RC78.7.D53 | NLM WN 182 | DDC 616.07/54—dc23
LC record available at https://lccn.loc.gov/2019005809

Visit the Taylor & Francis Web site at
http://www.taylorandfrancis.com

and the CRC Press Web site at
http://www.crcpress.com

With love and affection to my mother and father,
whose loving spirit sustains me still

Ayman El-Baz

To my late loving parents, my wife, and loving children

Jasjit S. Suri

Contents

Preface

In the medical imaging field, accurate segmentation of structures is crucial in many applications; for example, in detecting lesions and abnormalities. However, segmentation is highly challenging due to such factors as the low contrast between different tissues types that makes it difficult to even segment the desired object manually, and the motion artifacts associated with the scans which adds noise to images. This book covers the state-of-the-art approaches for medical imaging segmentation based on the level set technique that was implemented by Osher and Sethian. The level set technique mainly relies on the theory of curve and surface evolution, in addition to the link between front propagation and hyperbolic conservation laws. This makes it easy to follow shapes that change topology.

Among numerical techniques, level sets are significantly powerful at interpreting interface motion. Level set methods have provided great advances to clinicians in assessing abnormalities through computer-aided diagnostic (CAD) systems that can analyze images from these different modalities; for example computed tomography (CT), magnetic resonance imaging (MRI), and optical coherence tomography (OCT). Different modalities will be discussed in this book for different applications.

In summary, the main aim of this book is to survey an illustrative subset of past and current applications of level set technique in medical imaging segmentation. It focuses on major trends and challenges in this area, identifies new techniques and presents their use in biomedical image analysis.

Ayman El-Baz
Jasjit S. Suri

Biographies

Ayman El-Baz is a professor, university scholar, and Chair of the Bioengineering Department at the University of Louisville, Kentucky. Dr. El-Baz earned his B.Sc. and M.Sc. degrees in electrical engineering in 1997 and 2001, respectively. He earned his Ph.D. in electrical engineering from the University of Louisville in 2006. In 2009, Dr. El-Baz was named a Coulter Fellow for his contributions to the field of biomedical translational research. Dr. El-Baz has 17 years of hands-on experience in the fields of bio-imaging modeling and non-invasive computer-assisted diagnosis systems. He has authored or coauthored more than 500 technical articles (133 journals, 25 books, 57 book chapters, 212 refereed-conference papers, 143 abstracts, and 27 US patents and disclosures).

Jasjit S. Suri is an innovator, scientist, visionary, industrialist and an internationally known world leader in biomedical engineering. Dr. Suri has spent over 25 years in the field of biomedical engineering/devices and its management. He received his Ph.D. from the University of Washington, Seattle and his Business Management Sciences degree from Weatherhead, Case Western Reserve University, Cleveland, Ohio. Dr. Suri was awarded the President's Gold medal in 1980 and made Fellow of the American Institute of Medical and Biological Engineering for his outstanding contributions. In 2018, he was awarded the Marquis Life Time Achievement Award for his outstanding contributions and dedication to medical imaging and its management.

Acknowledgements

The completion of this book could not have been possible without the participation and assistance of many people; all of whose names may not be enumerated. Their contributions are sincerely appreciated and gratefully acknowledged. However, the editors would like to express their deep appreciation and indebtedness particularly to Dr. Ali H. Mahmoud and Ahmed ElTanboly for their endless support.

Ayman El-Baz
Jasjit S. Suri

Contributors

Sebastian Bautista
Computer Science Department
Engineering School, Universidad de Cuenca
Cuenca, Ecuador

Tien D. Bui
Department of Computer Science and Software Engineering
Concordia University
Montréal, Quebec

Elisabetta Carlini
Mathematics Department, "Sapienza"
University of Rome
Rome, Italy

Yuncheng Du
Department of Chemical and Biomolecular Engineering
Clarkson University
Potsdam, New York

Dongping Du
Department of Industrial, Manufacturing, and System Engineering
Texas Tech University
Lubbock, Texas

Ahmed ElTanboly
Bioimaging Laboratory, University of Louisville
Louisville, Kentucky

Magdi El-Azab
Department of Engineering Mathematics
Mansoura University
Mansoura, Egypt

Ayman El-Baz
Department of Bioengineering
University of Louisville
Louisville, Kentucky

Maurizio Falcone
Mathematics Department, "Sapienza"
University of Rome
Rome, Italy

Bin Fang
Department of Computer Science
Chongqing University
Chongqing, China

Jiangxiong Fang
Department of Measure and Control
East China University of Technology
Nanchang, China

Aly A. Farag
Electrical and Computer Engineering Department
University of Louisville
Louisville, Kentucky

Roberto Ferretti
Mathematics Department
"Sapienza"
University of Rome
Rome, Italy

Thomas Fevens
Department of Computer Science
and Software Engineering
Concordia University
Montréal, Quebec

Mohammed Ghazal
Department of Electrical and
Computer Engineering
Abu Dhabi University
Abu Dhabi, UAE
and
Bioengineering Department
University of Louisville
Louisville, Kentucky

Deepak K. Ghodgaonkar
RF Lab, DA-IICT
Gandhinagar, Gujarat
India

Hassan Hajjdiab
Department of Electrical and
Computer Engineering
Abu Dhabi University
Abu Dhabi, UAE

Robert Keynton
Bioengineering Department
University of Louisville
Louisville, Kentucky

Alexandra La Cruz
GBBA
Universidad Simón Bolívar
Caracas, Venezuela

Laquan Li
School of Automation
Huazhong University of Science
and Technology
Wuhan, China

Ali Mahmoud
Bioengineering Department
University of Louisville
Louisville, Kentucky

Ruben Medina
Biomedical Engineering Group
(GIBULA)
Electronics and Communications
Department
Universidad de Los Andes
Merida, Venezuela

Villie Morocho
Computer Science Department
Engineering School, Universidad
de Cuenca
Cuenca, Ecuador

Hossam Abd El Munim
Computer and Systems Engineering
Department
Ain Shams University
Cairo, Egypt

Padmasini N
Department of Biomedical
Engineering
Rajalakshmi Engineering
College
Chennai, India

Hardik N. Patel
RF Lab, DA-IICT
Gandhinagar, Gujarat
India

Françoise Peyrin
Creatis Laboratory
INSA-Lyon
University of Lyon
Lyon, France

Ahmed Shalaby
Bioengineering Department
University of Louisville
Louisville, Kentucky

Mohamed Yacin Sikkandar
Department of Medical Equipment Technology
CAMS
Majmaah University
Kingdom of Saudi Arabia

Manavi D Sindal
Senior Consultant
Vitreo-Retina Services
Aravind Eye Hospital
Pondicherry, India

Bruno Sixou
Creatis Laboratory
INSA-Lyon
University of Lyon
Lyon, France

Jasjit S. Suri
Global Biomedical Technologies, Inc.
Roseville, California
and
AtheroPoint LLC
Roseville, California
and
Department of Electrical Engineering
Idaho State University
Pocatello, Idaho

Shaghayegh Taheri
Department of Computer Science and Software Engineering
Concordia University
Montréal, Quebec

Umamaheswari R
Department of Electrical and Electronics Engineering
Velammal Engineering College
Chennai, India

Lin Wang
Creatis Laboratory
INSA-Lyon
University of Lyon
Lyon, France

Shenhai Zheng
Department of Computer Science
Chongqing University
Chongqing, China

1

Tomography Reconstructions With Stochastic Level-Set Methods

Bruno Sixou, Lin Wang, and Françoise Peyrin

CONTENTS

1.1 Introduction

The level-set methods are now a well-known tool for the computation of evolving boundaries since their introduction by Osher and Sethian [1]. They have been designed newly to reconstruct solutions of inverse problems with non-smooth and piecewise constant solutions [2–4]. The numerical results indicate their sucess. Yet, inverse problems with piecewise constant solution are non-convex and the reconstructed solution is a local minimum of the regularization functional. It may be interesting to escape this local minimum with global optimization methods. Stochastic algorithms based on stochastic differential equations have been proposed for the global optimization of non-convex functions [5–9]. Let $(\Omega, \mathcal{F}, P)$ be a probability space, in order to obtain the global minimum of a function $g : \mathbb{R}^m \to \mathbb{R}^m$, a random trajectory $X(t)$ governed by the following diffusion process is often used [5–9]:

$$dX(t) = -\nabla g(X(t))dt + \mu(t)dW(t) \tag{1.1}$$

where $W = (W_1(t), \ldots., W_m(t))$ is the standard m-dimensional Brownian motion and $\mu(t)$ the noise strength. For an appropriate annealing schedule $\mu(t)$ and under appropriate condition on g, the probability law of $X(t)$ converges weakly to a probability law which has its support on the set of the global minimizers of g [5–9]. In the field of image processing, stochastic partial differential equations applied to level-set functions have been used for segmentation tasks [10]. The right way to study stochastic evolutions in the level-set framework is through the Stratonovich integral so that evolution of the boundary curve is independent of the level-set function used for its representation [10]. The aim of this chapter is to show that this type of approach can be generalized to inverse problems with piecewise constant solutions.

In the first section, we summarize some results about stochastic calculus and the level-set regularization of inverse problems. Then, the stochastic level-set approach is applied to the binary tomography and to the phase contrast tomography inverse problem.

1.2 Preliminaries

In this first section, we present the level-set regularization approach of inverse problems and some aspects of stochastic calculus.

1.2.1 Level-Set Regularization of Inverse Problems

In this section, we detail the level-set regularization approach of inverse problems. Let $R : H_1 \to H_2$, a linear operator mapping two Hilbert spaces H_1 and H_2, and $g \in H_2$. Our aim is to find a piecewise constant solution f of the inverse problem:

$$Rf = g \tag{1.2}$$

For Ω a bounded Lipschitz open subset in $\mathbb{R}^2$, we assume that the function to be reconstructed f is the characteristic function of a regular set $\Omega_1 \subset \Omega$, $f = \chi_{\Omega_1}$. It can be represented with the Heaviside distribution and with a level-set function $\theta \in H_1(\Omega)$ as $f = H(\theta)$, where $H_1(\Omega)$ is the first-order Sobolev space and with $H(\theta) = 1$ if $\theta > 0$ and 0 otherwise.

Assuming that the noisy data are such that $\|g^\delta - g\| \le \delta$, where δ is the noise level, the reconstruction problem becomes nonlinear and consists in determining the level-set function θ minimizing the regularization functional:

$$E(\theta) = \frac{\|RH(\theta) - g^\delta\|_2^2}{2} + F(\theta) \tag{1.3}$$

where F is a regularization term for the level-set function. We have considered here a Total Variation-H_1 regularization functional [2,3]:

$$F(\theta) = \beta_1 |H(\theta)|_{TV} + \beta_2 \|\theta\|_{H_1}^2 \tag{1.4}$$

where $|.|_{TV}$ is the Total Variation semi-norm. The regularization parameters β_1, β_2 determine the relative weights of the stabilizing terms.

Since H is discontinuous, it is necessary to consider generalized minimizers of the regularization functional [2, 3]. These minimizers can be approximated by minimizers of smoothed regularization functional with an approximation H_ϵ. The following smooth approximations of the Heaviside function H has been used $H_\epsilon(x) = \frac{1+2\epsilon}{2}(erf(x/\epsilon) + 1) - \epsilon$ where ϵ is a real positive constant. The smoothed regularization functional is given by:

$$E_\epsilon(\theta) = \frac{\left\|RH_\epsilon(\theta) - g^\delta\right\|_2^2}{2} + \beta_1 |H_\epsilon(\theta)|_{TV} + \beta_2 \|\theta\|_{H_1}^2 \tag{1.5}$$

The minimizers of the Tikhonov functionals are found with a first-order optimality condition for the smoothed functionals, $E'_\epsilon(\theta) = 0$, with:

$$E'_\epsilon(\theta) = H'_\epsilon R^*\left(RH_\epsilon(\theta) - g^\delta\right) + \beta_2 (I - \Delta)(\theta) + \beta_1 \frac{\partial |H_\epsilon(\theta)|_{TV}}{\partial\theta} \tag{1.6}$$

where R^* denotes the adjoint of the forward operator. From the current estimate θ_k, the update $\theta_{k+1} = \theta_k + \delta\theta$ is obtained with a classical Gauss-Newton method with a linearization of the condition $G(\theta_k + \delta\theta) = 0$ [22].

This method can be generalized to nonlinear operators and R must be replaced by the Fréchet derivative of the direct operator. For high noise levels, the solution θ may be trapped in a local minima. In that case, the data term

$\|RH_\epsilon(\theta) - g^\delta\|$ at the end of the optimization is largely higher than the noise level δ and the many reconstruction errors are still present. In order to escape from these stationary points, we propose stochastic global optimization methods.

1.2.2 Some Notions of Stochastic Calculus

The stochastic evolution of the level-set function is based on the Stratonovich integral. In this first section, we summarize some useful notions of stochastic calculus [11, 12]. We explain the difference between the Itô and Stratonovich stochastic integrals. Let $(\Omega, \mathcal{F}, \mathcal{F}_t, P)$ represent a probability space and $W_{t\geq 0}$ a one-dimensional Brownian motion. The paths of the Brownian motion are only $\frac{1}{2}$-Hölder continous and nowhere differentiable, and in order to define $dW(t)$, it is usual to start with the stochastic integral. Given a square integrable process $(\phi(s,\omega))_{s\geq 0}$ and a subdivision $\Delta = \{0 = t_1 < \ldots . < t_n = t\}$, the stochastic Itô integral $\int_0^t \phi(s,\omega)dW(s)$ with respect to the Brownian motion is defined as the limit of the Riemann sum:

$$\sum_{1\leq i\leq n} \phi(t_i,\omega)(W(t_{i+1}) - W(t_i)) \tag{1.7}$$

when $|\Delta| = min|t_{i+1} - t_i| \to 0$. The limit obtained $\{I(\phi)\}_{t\geq 0}$ is a square integrable martingale. This definition can be extended to an arbitrary dimension.

Considering a process $X = (X_t)_{t\geq 0}$ and a smooth function α of class C^2, the process $Y_t = (\alpha(X_t))$ satisfies the Itô formula:

$$dY(t) = \alpha'(X(t))dt + \frac{1}{2}\alpha'' d < X, X > (t) \tag{1.8}$$

The drift term involves the quadratic variation $< X, X >$ of the process X which depends on the stochastic part of the dynamics. For a stochastic process, $X(t) = \int_0^t f(s)dW(s) + A(t)$, where f is a continuous square integrable function and $A(t)$ is continuous and increasing, the quadratic variation can be calculated as:

$$< X, X > (t) = \int_0^t f(s)^2 ds \tag{1.9}$$

It is possible to give another definition of the stochastic integral so that the classical chain rule is satisfied. Considering two processes $X(t) = M(t) + B(t)$, $Y(t) = N(t) + C(t)$ where M, N are local continuous martingales and B, C are increasing processes, the Stratonovich integral of Y with respect to X is given by the formula

$$\int_0^t Y(s) o dX(s) = \int_0^t Y(s)dX(s) + \frac{1}{2} < M, N > (t) \tag{1.10}$$

Then, it can be shown that the classical chain rule formula is satisfied [11,12]:

$$\alpha(X_t) = \alpha(X_0) + \int_0^t \alpha'(X(s)) o dX(s) \tag{1.11}$$

The principle of the stochastic level-set evolution framework is to transfer the contour evolution to the level-set function. The dynamics of the level-set contour should not be modified by a change of the level-set function. This invariance property is not guaranted by the Itô rule. If the Itô integral is replaced by the Stratonovich for the stochastic evolution, the additional drift term disappears and the invariance property is verified.

The Stratonovich evolution equation can be implemented with an implicit scheme. The Stratonovich integral with respect to the Brownian motion W can be approximated as:

$$\int_0^T Y(s) o dW(s) = \lim_{|\Delta| \to 0} \sum_{1 \le i \le n} Y\left(\frac{t_i + t_{i+1}}{2}\right)(W(t_{i+1}) - W(t_i)) \tag{1.12}$$

with $W(t_{i+1}) - W(t_i) \sim \sqrt{(t_{i+1} + t_i)}\mathcal{N}(0,1)$, where $\mathcal{N}(0,1)$ is a Gaussian of standard deviation 1.

In [10], it was proposed to simulate the Stratonovich evolution with the Itô formalism and an additional drift term. Using the formula Eq. 1.10, it can be shown that, for a level-function θ:

$$\begin{aligned} |\nabla\theta(x,t)| o dW(t) &= |\nabla\theta(x,t)| dW(t) \\ &\quad + \frac{1}{2}(\Delta\theta(x,t) - |\nabla\theta(x,t)| div\left(\frac{\nabla\theta(x,t)}{|\nabla\theta(x,t)|}\right) \end{aligned} \tag{1.13}$$

This evolution equation has been used for image segmentation tasks leading to stochastic active contours [10]. It is the basis of the approaches presented in the following. Some proper type of solutions can be defined for these equations with stochastic viscosity solutions [10].

1.3 Binary Tomography Reconstructions of Bone Microstructure from Few Projections with Stochastic Level-Set Methods

1.3.1 The Binary Tomography Problem

The tomographic reconstruction from few projections is a very ill-posed problems with many applications in medical imaging or material science. The binary tomography methods can be used to set a simpler inverse problem [13]. The binary tomography problem can be formulated as an under-determined linear system of equations with the linear Radon projection operator R and binary constraints:

$$Rf = p^{\delta} \quad f = (f_1, \ldots\ldots f_n) \in \{0, 1\}^n \tag{1.14}$$

relating the pixel values $(f_i)_{1 \leq i \leq n}$ of the image and the noisy projection data p^{δ}. Very often it is assumed that the non-noisy projections p are corrupted by an additive Gaussian noise.

Various approaches have been investigated to solve this reconstruction problem [14, 15, 19, 20]. The minimization of a functional with a data term and a binary constraint may be performed with stochastic techniques [16] or convex analysis optimization [17, 18]. A variational method based on Total Variation regularization can also be used for this reconstruction problem [21–23].

Yet, the discrete tomography problem is non-convex and the reconstructed solution may be trapped in local minima of the regularization functional. The reconstruction errors are very often localized on the boundaries [22]. We use here stochastic level-set methods for the discrete tomography problem to improve the reconstruction obtained with a deterministic level-set scheme [22, 23]. The reconstruction results obtained with this new approach are compared with the ones obtained with the classical simulated annealing method [24–26] in terms of reconstruction quality and convergence speed.

1.3.2 Global Optimization with Stochastic Level-Set Evolution and Simulated Annealing

1.3.2.1 Stochastic Level-Set Evolution

We use here the level-set regularization and represent the function f with a level-set function $\theta, f = H(\theta)$. Let Ω be the domain of the image to be reconstructed, we propose to improve the reconstruction image with the following stochastic partial differential equation for the level-set function θ, for $x \in \Omega$, given by:

$$d\theta(x,t) = \delta\theta(x,t) + \mu(t)|\nabla\theta(x,t)|odW(t) \tag{1.15}$$

where o denotes the Stratanovich convention [12] and $\delta\theta$ is the gradient calculated as explained in Section II.A, Eq. 1.6.

As explained in Section II.B, using the definition of the Stratonovich integral, the equation can be transformed to get the following Itô stochastic differential equation:

$$\begin{aligned} d\theta(x,t) = \delta\theta &+ |\nabla\theta(x,t)|dW(t) \\ &+ \frac{1}{2}(\Delta\theta(x,t) - |\nabla\theta(x,t)|div\left(\frac{\nabla\theta(x,t)}{|\nabla\theta(x,t)|}\right) \end{aligned} \tag{1.16}$$

The level-set and stochastic level-set schemes are applied successively on random time intervals. In the framework of the intermittent diffusion algorithm, the coefficient for the intermittent diffusion is defined as:

$$\mu(t) = \sum_j \mu_j I_{[S_j,T_j]}(t) \tag{1.17}$$

where $I_{[S_j,T_j]}$ is the characteristic function of the interval $[S_j, T_j]$. The time intervals length and the diffusion strengths μ_j are chosen at random in the range $[0, T]$ and $[0, \mu_{max}]$ where $\mu_{\max}$ is the scale for the diffusion strength and T is the scale for the diffusion time [8]. With probability arbitrarily close to 1, the intermittent diffusion method can find the global minimum of the regularization functional in a finite simulation time.

1.3.2.2 Classical Simulated Annealing

Simulated annealing methods are reviewed extensively in [24–26]. Let f_b be the binary reconstructed image, and U the data term $U = \|Rf_b - p^\delta\|$, our aim is to minimize the objective function U on a finite configuration space E which is the set of binary images:

$$E = \{f_b = (f_k)_{1\leq k\leq N} \quad f_k \in \{0,1\} \quad \forall k \in [1,N]\} \tag{1.18}$$

The classical simulated annealing algorithm is based on the definition of a Markov chain, $(f^n)_{n\in\mathbb{N}}$ on the finite state space E. Each point f^n in the state space is defined by the set $(f_k^n)_{0\leq k\leq N}$ of the pixel values. A stochastic search is performed on E with a "cooling down" algorithm. The boundary between the 0 and the 1 regions is first calculated with a Sobel filter. Then one pixel is selected at random on the boundary and is changed and this rule defines the neighborhood system $N(f_b)$ of a point $f_b \in E$:

$$g_b \in N(f_b) \iff \exists! k, f_k \neq g_k \tag{1.19}$$

It is thus possible to define a communication kernel $q_0(f,g)$, in which all the new states in the neighbourhood of f are equiprobable:

$$q_0(f_b, g_b) = \begin{cases} \frac{1}{|N(f_b)|} & \text{if} \quad g_b \in N(f_b) \\ 0 & \text{otherwise} \end{cases} \tag{1.20}$$

The classical simulated annealing algorithm defines an inhomogeneous Markov chain, with transitions constructed recursively as follows: $P(f^{n+1} = g|f^n = f) = q(f,g)$ with

$$q(f,g) = \begin{cases} q_0(f,g)exp(-\beta_n(U(g) - U(f))^+ & \text{if } g \neq f \\ 1 - \sum_{h\neq f} q(f,h) & \text{if } g = f \end{cases} \tag{1.21}$$

where [a]+=max(a,0), $(\beta_n)_{n\in\mathbb{N}}$ the cooling schedule, f^0 an arbitrary initial point.

From the current state f^n, a test image f_{test} is sampled randomly according to Eqs. 1.20 and 1.21. If $U(f_{test}) > U(f^n)$ the proposal f_{test} may be accepted. In the beginning of the simulation, the temperature is high and the state space is explored freely. As β increases, the images distribution is more and more concentrated around the minima of U [24–26]. Under some restricting conditions on the cooling schedule, the convergence towards the global minimum is obtained by the convergence rate may be very slow. Several techniques have been used to speed up the simulated annealing method but the modifications are rather empirical [27, 28] and the results obtained seems to be very dependent on the complexity of the objective function. They will not be considered here.

1.3.3 Comparison of the Algorithms: Results and Discussion

1.3.3.1 Simulation Details

The simulated annealing algorithm and stochastic level-set methods have applied to simulated projections of an experimental bone cross-section acquired with synchrotron micro-CT (voxel size:15 μm) [29]. Figure 1.1 displays the 256×256 bone cross-section f^* reconstructed from 400 projections with 400 rays per projections with Filtered Back Projection (FBP). The discrete approximation of the Radon transform is the operator implemented in the Matlab Toolbox.

First, the deterministic level-set scheme regularization is applied. To obtain a good accuracy, the ϵ was set to $\epsilon = 0.03$. The initial level-set function chosen is $\theta_0 = 0$. The regularization parameters were chosen to obtain the best decrease of the regularization functional. The iterations are stopped when the iterates stagnate, $\|f_{k+1} - f_k\|_2 < 0.01$. At the end of this first optimization step,

FIGURE 1.1
Reconstruction of the bone cross-section from 400 projections with the FBP algorithm. The bone fraction is 14.20%.

the Morozov discrepancy principle [30] is not satisfied. The discrepancy term is much higher than the noise level, $||p^\delta - Rf|| >> \delta$. This image is the initial image used for the application of the stochastic algorithms. For the simulated annealing algorithm, the initial temperature value is chosen so that most transitions are accepted, with an acceptance ratio around 0.8.

For the simulation of Eq. 1.16, we use an explicit scheme with finite differences, the WENO scheme with $\Delta x = 0.5$ and $\Delta t = 0.1$. The noise strength μ and the number of iterations T are chosen randomly with a uniform distribution in $[0.01, 0.1]$ and $[1, 100]$. A binary image is then obtained by thresholding and a signed distance is then used for reinitializations before the stochastic level-set step. The optimization method was applied for M equally spaced noisy projections, with $M = 10$ and $M = 15$, with N = 367 rays per projections and with a Gaussian noise added to the projections with a standard deviation $\sigma_p = 3$ (PSNR=20 dB) and $\sigma_p = 6.5$ (PSNR=7 dB). The noise level δ can estimated by $\delta = \sqrt{MN}\sigma_p$.

1.3.3.2 Numerical Results

The reconstructed cross-sections obtained with 10 projections and 367 rays per projection, for the standard deviation $\sigma_p = 3$ after the level-set algorithm and after the stochastic level-set algorithm are displayed in Figure 1.2a and Figure 1.3a respectively. The difference maps are displayed in Figure 1.2b and Figure 1.3b. The reconstruction errors on the boundaries of the homogeneous regions are reduced.

At the end of the deterministic optimization, the discrepancy term $||Rf - p^\delta||$ is well-above the noise level for different number of projections. A local minimum is obtained and the level-set algorithm can not escape this

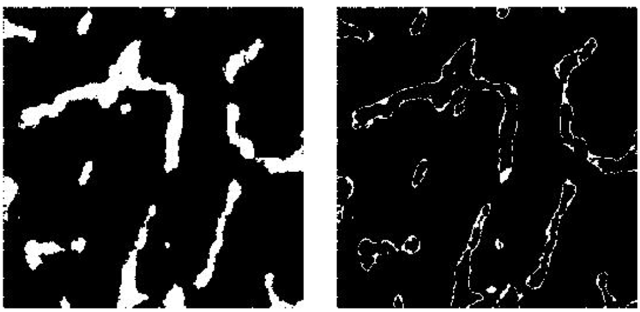

(a) (b)

FIGURE 1.2
(a) Reconstruction of the bone cross-section from 10 noisy projections ($\sigma_p = 3$) with the level-set regularization method. The misclassification rate is 3.29% and the bone fraction is 12.27% (b) Error map.

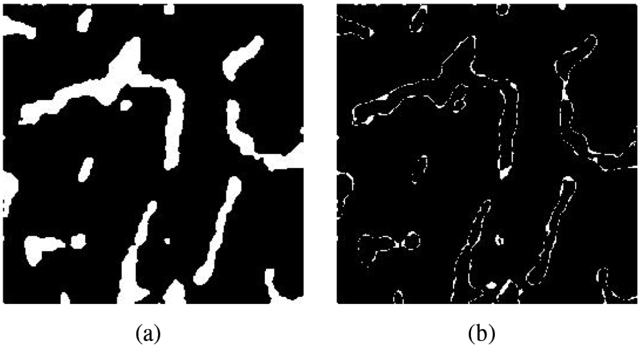

FIGURE 1.3
(a) Reconstruction of the bone cross-section from 10 noisy projections ($\sigma_p = 3$) with the stochastic level-set regularization method. The misclassification rate is 2.56% and the bone fraction is 14.14% (b) Error map.

local minimum. With the iterations, a significant decrease of the data term is obtained towards these noise levels for both stochastic methods.

The decrease of the misclassification rate as a function of the number of iterations is displayed in Figure 1.4 for the same number of projections and noise levels. The misclassification rates obtained at the end of the simulations are summarized in Table 1.1. Better reconstruction results are obtained with

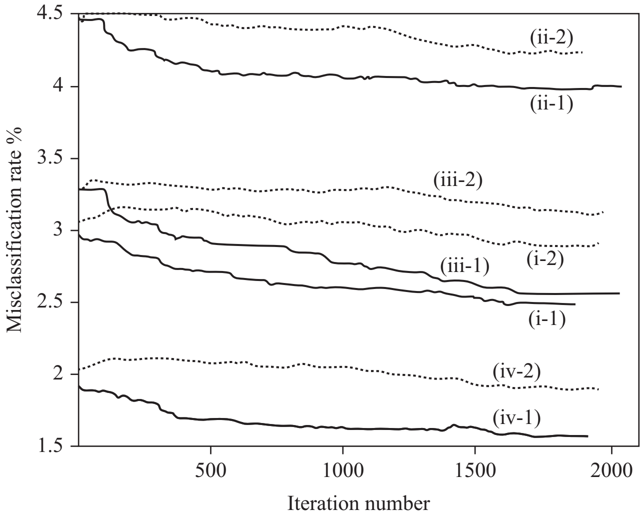

FIGURE 1.4
Evolution of the misclassification rate with the iteration number (i) M = 15, $\sigma_p = 6.5$ (ii) M = 10, $\sigma_p = 6.5$ (iii) M = 15, $\sigma_p = 3$ (iv) M = 10, $\sigma_p = 3$. The dotted lines corresponds to the simulated annealing and the plain lines to the stochastic level method.

TABLE 1.1

Misclassification Rates Obtained with the Stochastic Algorithms

	Simulated Annealing	Stochastic Level-Set
$\sigma_p = 3$, M = 15	1.89	1.56
$\sigma_p = 3$, M = 10	3.12	2.55
$\sigma_p = 6.5$, M = 15	2.9	2.48
$\sigma_p = 6.5$, M = 10	4.23	3.97

the stochastic level-set algorithm than with the simulated annealing minimization, for all noise levels and numbers of projections. At the end of the simulations, the errors on the boundary of the images are much lower.

1.4 Stochastic Level-Set Reconstruction in Nonlinear Phase Contrast Tomography

In this section, we detail the results obtained with stochastic level-set methods for phase contrast tomography. The inverse problem considered is nonlinear but the optimization methodology is very similar to the one applied to the binary tomography problem.

1.4.1 Nonlinear Phase Contrast Tomography

X-ray in-line phase contrast tomography is a very sensitive technique for soft tissues within dense materials. This imaging technique is based on a coupling of tomography and phase retrieval [31, 32] and it aims at reconstructing the complex refractive index [33]. For coherent X-rays obtained with synchrotrons, the Fresnel intensity is recorded for one or several propagation distances and for several projection angles after interaction of the X-rays with the object [34,35]. The inverse problem set by the reconstruction of the refractive index is nonlinear.

For volumes with several homogeneous materials, the imaginary and real part of the index are piecewise constant [33], and the level-set regularization can account for this a priori on the index map. Assuming that the discrete real and imaginary parts of the index are known, the inverse problem is then formulated as a shape optimization problem. Yet, the nonlinear phase contrast tomography problem is non-convex and the reconstructed solution obtained with the deterministic level-set regularization is a local minimum. We investigate here stochastic perturbations of the boundaries performed with tools similar to the ones used for binary tomography in [36] to improve the reconstruction and escape the critical point of the cost functional obtained with the deterministic method.

1.4.2 Level-Set Regularization in In-Line Phase Contrast Tomography

The real and imaginary parts of the complex refractive index to reconstruct from the Fresnel intensity measurements, denoted as δ and β are defined on a 3D bounded domain (Σ) with spatial coordinates (x, y, z). We denote (x_θ, y_θ, z) be the rotated spatial coordinate system for an angle θ around the z-axis (Figure 1.5). The sample is irradiated with a monochromatic, coherent, parallel X-ray beam propagating in the y_θ direction with the wavelength λ. The complex refractive index is given by [37,38]:

$$n(x, y, z) = 1 - \delta(x, y, z) + i\beta(x, y, z) \tag{1.22}$$

where δ is the refractive index decrement and β is the absorption index. Let $X_\theta = (x_\theta, z)$, the intensity detected at a distance D after the sample is given by the squared modulus of the following convolution product [33]:

$$I_{D,\theta}(X_\theta) = |T_\theta(X_\theta) * P_D(X_\theta)|^2 \tag{1.23}$$

where the Fresnel propagator is written:

$$P_D(X_\theta) = \frac{1}{i\lambda D} exp\left(i\frac{\pi}{\lambda D}|X_\theta|^2\right). \tag{1.24}$$

The transmittance function T_θ is given by:

$$T_\theta(X_\theta) = \exp[-B_\theta(X_\theta) + i\varphi_\theta(X_\theta)] \tag{1.25}$$

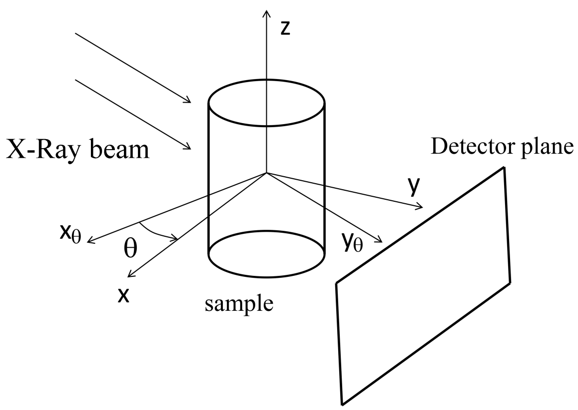

FIGURE 1.5
Experimental set-up in propagation based phase contrast tomography with a single propagation-distance showing the X-ray beam, the rotated coordinate system (x_θ, y_θ, z) for a rotation angle θ, the sample, and the detector.

with

$$B_\theta(X_\theta) = \frac{2\pi}{\lambda} \int \beta(y_\theta, X_\theta) dy_\theta \tag{1.26}$$

and

$$\varphi_\theta(X_\theta) = \frac{2\pi}{\lambda} \int (1 - \delta(y_\theta, X_\theta)) dy_\theta \tag{1.27}$$

Let $L(\theta, x_\theta)$ the line defined by $L(\theta, x_\theta) = \{y_\theta \bar{\theta}^* + x_\theta \bar{\theta} : \tau \in \mathbb{R}\}$, with $\bar{\theta} = (cos(\theta), sin(\theta))$ and $\bar{\theta}^* = (-sin(\theta), cos(\theta))$, for parallel beam projection, with a beam parallel to the $X = (x, y)$ plane and $f \in L^1(\Sigma)$, the Radon transform of f is defined as:

$$Rf(\theta, x_\theta, z) = R_\theta f(x_\theta) = \int_{t \in L(\theta, x_\theta, z) \cap \Sigma} f(t) dt \tag{1.28}$$

where $L(\theta, x_\theta, z)$ is the $L(\theta, x_\theta)$ line for the coordinate z. The intensity $I_{D,\theta}$ can be reformulated with the Radon transform R.

For simplicity, we assume that δ and β are piecewise constant and that they can take two values δ_1, δ_2 and β_1, β_2 on disjoint subsets Σ_1, Σ_2 such that $\Sigma = \Sigma_1 \cup \Sigma_2$. In order to represent the unknown functions δ and β, we have used a level-set function of the first order Sobolev space $\eta \in H_1(\Sigma)$:

$$\beta = \beta_1 + H(\eta)(\beta_2 - \beta_1) \tag{1.29}$$

$$\delta = \delta_1 + H(\eta)(\delta_2 - \delta_1) \tag{1.30}$$

A variational approach is considered with the following regularization functional:

$$F[\eta] = \|I_{D,\theta}[\eta] - I_{\delta_n}\|_2^2 + \alpha_1 \left(\|\eta\|_{L_2}^2 + \||\nabla \eta|\|_{L_2}^2 \right) \tag{1.31}$$

where I_{δ_n} are the noisy intensity data and α_1 a regularization parameter.

The minimizers of the regularization are found numerically with first order optimality conditions for the smoothed functional where the Heaviside function is replaced by its approximation:

$$I'^*_{D,\theta}[\eta][I_{D,\theta}[\eta] - I_{\delta_n}] + \alpha_1 (I - \Delta)[\eta] = 0 \tag{1.32}$$

where I'^*_D denotes the adjoint of the Fréchet derivative of the intensity operator with respect to L_2 spaces. I represent identity and Δ the Laplacian operator. The solutions of the optimality system are obtained with a Gauss-Newton method. The update is given by $\eta_{k+1} = \eta_k + \delta\eta$ and $\delta\eta$ is obtained with the linear system:

$$\left([I'^*_{D,\theta}[\eta^k] I'_{D,\theta}[\eta^k] \right) \delta\eta + \alpha_1 (I - \Delta) \delta\eta = -F'[\eta^k] \tag{1.33}$$

An explicit formula can be derived for the Fréchet derivative of the intensity $I_D[\delta, \beta]$ and its adjoint are given in [39].

1.4.3 Stochastic Level-Set Methods for Phase Contrast Tomography

Stochastic level-set evolution The deterministic optimization of the level-set function is often stopped in local minima. We propose to improve the reconstruction image obtained with the deterministic level-set evolution with the following stochastic partial differential equation for the level-set function η, for $\vec{r} \in \Sigma$ by:

$$d\eta(\vec{r},t) = \delta\eta(\vec{r},t) + \rho(t)|\nabla\eta(\vec{r},t)| o dW(t) \tag{1.34}$$

where o denotes the Stratanovitch convention and $\delta\eta$ is the deterministic change calculated with the Gauss-Newton method of Eqs. 1.32, 1.33 as explained in the former section. We obtain the following Itô stochastic differential equation with the definition of the Stratonovich integral:

$$\begin{aligned} d\eta(\vec{r},t) = \delta\eta + \rho(t)|\nabla\eta(\vec{r},t)|dW(t) + \frac{1}{2}\rho(t)(\Delta\eta(\vec{r},t) \\ - |\nabla\eta(\vec{r},t)| div\left(\frac{\nabla\eta(\vec{r},t)}{|\nabla\eta(\vec{r},t)|}\right) \end{aligned} \tag{1.35}$$

The deterministic level-set and stochastic level-set schemes are applied successively on random time intervals with an intermittent diffusion similar to the one proposed for the binary tomography. For the stochastic evolution, the time interval lengths and the diffusion strengths ρ are chosen at random with a uniform distribution in the range $[0, T_{max}]$ and $[0, \rho_{max}]$ where $\rho_{\max}$ is the scale for the diffusion strength and T_{max} is the scale for the diffusion time.

The minimization scheme is summarized in Algorithm 1:

Algorithm 1

Let Δt be the time step of the discretization of Eq. 1.35,
For k=1 to Maxiter:

Step 1: chose a projection angle θ at random with a uniform distribution, chose at random $t \in [0, T_{max}]$, and $\rho \in [0, \rho_{max}]$, for the iteration number $N_{iter,sto} = t/\Delta t$, use the discrete version of Eq. 1.35.

Step 2: calculate $\delta\eta$ with Eqs. 1.32, 1.33, for $N_{iter,deterministic} = 100$ iterations.

Step 3: reinitialize the level-set function η with the signed distance function.

end

The derivative in Eq. 1.32 and Eq. 1.33 describes the sensitivity of the regularization functional with respect to deterministic changes of shape of the boundary between the regions of constant values of the index. The equation Eq. 1.35 corresponds to stochastic perturbations of the geometry. Topology changes like splitting and merging of domains can be obtained with the level-set approach [40]. It has also been proposed to add some new components or small holes far from the boundaries to modify the topology of the reconstructed images [39].

1.4.4 Numerical Results and Discussion

In the following, we compare the deterministic level-set algorithm with the modified algorithms with the stochastic evolution.

1.4.4.1 Simulation Details

The deterministic and intermittent stochastic level-set algorithms and the deterministic algorithm are compared in this section on one multi-material object made up of two homogeneous materials. It is possible to extend these results to objects with more than two materials with multi-level regularization.

The simulated test object (O_1) consists of an Al cylinder of 20 μm in diameter and 110 μm in height embedded in PMMA. Some horizontal sections of the β and δ maps of the simulated object (O_1) are displayed in Figure 1.6.

Let $\mu = \frac{4\pi\beta}{\lambda}$, the δ and μ values used for PMMA and Al for 24 keV X-rays are summarized in Table 1.2. The β and δ values were discretized on a regular grid with a pixel size of 1.5 μm. The cylinder is included in a rectangular volume of size $N_1 \times N_1 \times N_2$ pixels with $N_1 = 74$ and $N_2 = 109$ used for the simulations. The number of projection angles N_θ used for the simulation are $N_\theta = 75, 125$ and 180. A single sample-to-detector distance D = 100 mm is considered. The Radon transform is the projection operator implemented in the Mablab Toolbox. The intensity data were corrupted with additive Gaussian white noise. This noise distribution corresponds to the noise measured experimentally. The signal to noise ratio was measured with the peak-to-peak signal to noise ratio (PPSNR). To obtain a good accuracy, the ϵ parameter of the smooth approximation of the Heaviside function was fixed to $\epsilon = 0.03$.

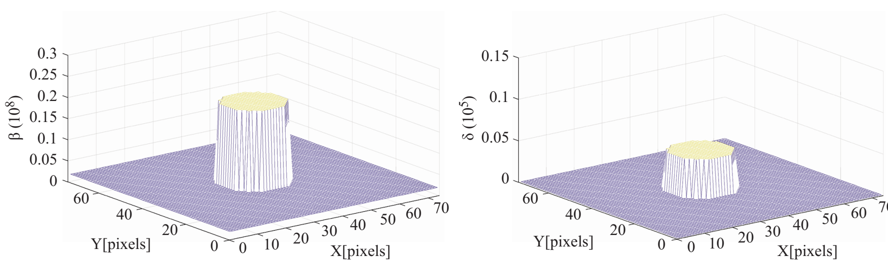

FIGURE 1.6
Ground truth β and δ maps for the object (O_1).

TABLE 1.2
Values of the δ and μ Values for the Materials in the Object, at 24 keV X-rays from http://henke.lbl.gov/optical_constants

Material	$\delta(10^{-7})$	$\mu(\mathrm{m}^{-1})$
PMMA	4.628	41.2
Al	9.396	502.6

In order to evaluate the efficiency of the reconstruction, the relative mean square errors (RMSE) using the $L_2(\Sigma)$ norm, $\|\delta^* - \delta\|_2/\|\delta^*\|_2$ and $\|\beta^* - \beta\|_2/\|\beta^*\|_2$ have been studied. Let $D_k = \frac{\|I_{D,\theta}[\eta_k]-I_{\delta_n}\|}{\|I_{\delta_n}\|}$ the value of the data term for the projection angle θ and the value η_k. The iterations are stopped when the average value of the variation of the data term $D_{k+1} - D_k$ evaluated on 10 iterations is below 0.05.

1.4.4.2 Numerical Results for Deterministic Level-Set Method

For piecewise constant δ and β maps, the reconstruction results are improved with the level-set regularization with respect to Tikhonov regularization because some a priori information on the possible values of δ and β is included. Some simulations have been performed to reconstruct the object (O_1) with an initial diameter of the central Al cylinder equal to 40 μm, twice the diameter of the cylinder to be reconstructed and noise levels of 30 and 48 dB. With this starting map for the refractive index, the inverse problem is an easier shape optimization problem in which only the possible discrete values of the real and imaginary parts of the refractive index are known but not the shape of the regions where the refractive index takes constant values.

Figure 1.7 displays the horizontal section of the initial β and δ maps. Figure 1.8 presents some horizontal sections of the errors for the real and imaginary part of the reconstructed index map for a PPSNR of 48 dB after 500 iterations. These figures show that the reconstruction errors have been significantly reduced. Some errors are still present on the boundaries between the

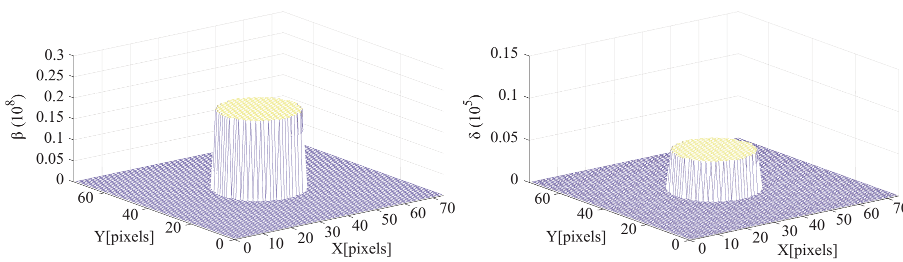

FIGURE 1.7
Horizontal section of the initial β and δ maps for the object (0_1).

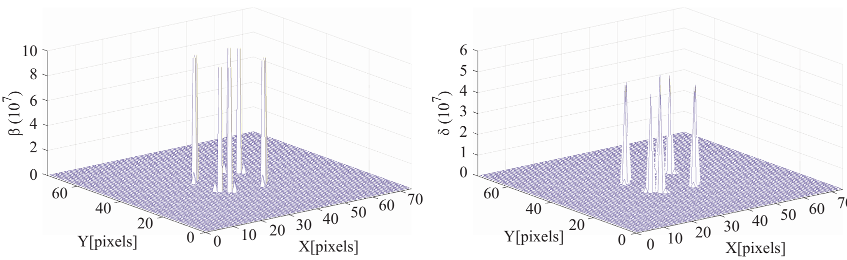

FIGURE 1.8
Horizontal section of the final error map for β and δ for a PPSNR of 48 dB.

two materials. Similar results are obtained for the other sections and the noise level of 30 dB with reconstruction errors at the interface between the different regions.

In order to have more quantitative information about the convergence of the method, the evolution of the relative mean square errors (RMSE) $\|\delta^* - \delta\|_2/\|\delta^*\|_2$ and $\|\beta^* - \beta\|_2/\|\beta^*\|_2$, are displayed as a function of the number of iterations for a PPSNR of 30 dB and 48 dB in Figures 1.9 and 1.10. The relative mean square errors on the two components β and δ of the refractive index are much decreased.

1.4.4.3 Deterministic Level-Set versus Stochastic Level-Set Algorithm

For higher noise levels and initializations maps with very different shape from the ground truth, the level-set regularization algorithm may be stuck in local optima. The stochastic level-set algorithm improves the reconstruction results. In order to perform a comparison of the deterministic and stochastic level-set algorithm, a first reconstruction is performed on the simulated

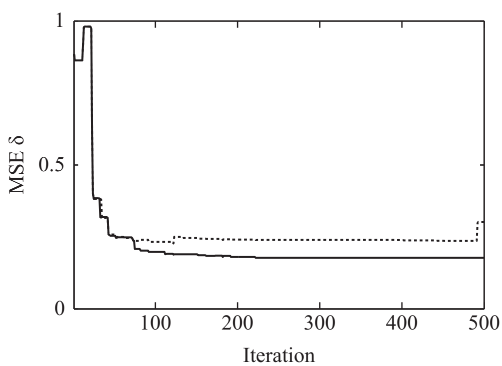

FIGURE 1.9
Evolution of the RMSE on δ with the iterations for the noise levels 30 dB (dotted line) and 48 dB (plain line).

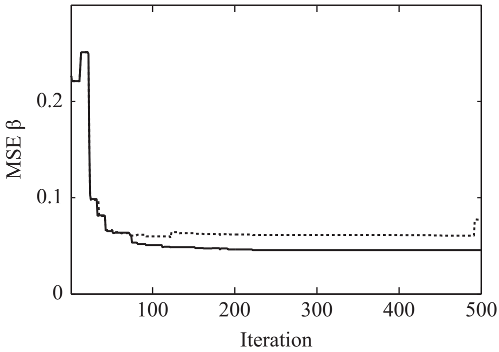

FIGURE 1.10
Evolution of the RMSE on β with the iterations for the noise levels 30 dB (dotted line) and 48 dB (plain line).

object (O_1). The initial guess is a large cylinder with a diameter twice the diameter of the object (0_1). Then algorithm 1 is applied to this initial reconstruction for PPSNR of 24 and 18 dB. Following algorithm 1, the numbers of stochatic iterations are chosen randomly with a uniform distribution between 1 and 50 and the noise strength in the range $[1, 10^{-3}]$. For the simulation of Eq. 1.35, we use an explicit scheme with finite differences, the WENO scheme [41] with $\Delta x = 0.1$ and $\Delta t = 0.01$. An iterated deterministic minimization is performed for comparison with periodic reinitialization of the level-set function and projection angles chosen at random.

The evolutions of the data term, $\|I_{D,\theta}[\eta] - I_{\delta_n}\|/\|I_{\delta_n}\|$ are displayed in Figure 1.11 for the deterministic and intermittent stochastic algorithms

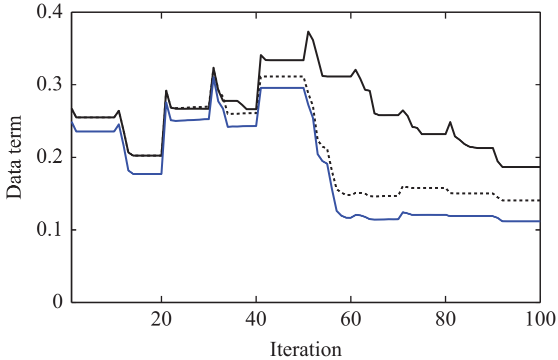

FIGURE 1.11
Evolution of the data term for the deterministic level-set algorithm for 24 dB (black line), for the intermittent stochastic level-set algorithm for 24 dB (blue line) and for the intermittent stochastic level-set algorithm for 18 dB (dotted line).

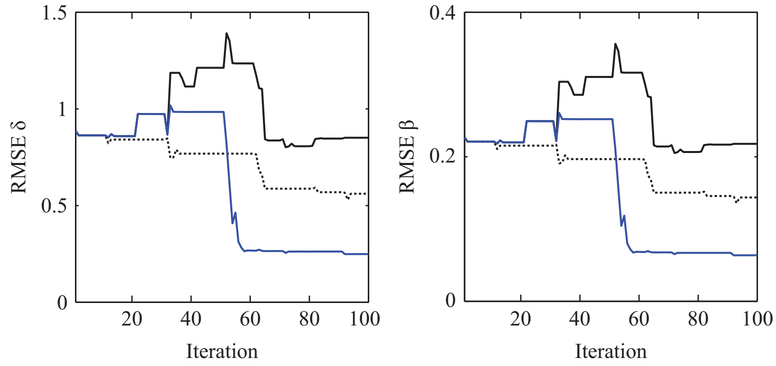

FIGURE 1.12
Evolution of the RMSE for β and δ for the deterministic level-set algorithm for 24 dB (black line), for the intermittent stochastic level-set algorithm for 24 dB (blue line) and for the intermittent stochastic level-set algorithm for 18 dB (dotted line).

starting from the initial reconstruction for the noise levels 18 dB and 24 dB. The deterministic algorithm is not efficient to achieve lower reconstruction errors. Different behaviours are obtained depending on the random projection angles θ for similar noise levels. Yet, after hundred iterations, only small fluctuations are observed on the real and imaginary parts of the refractive index, β and δ, and the uncertainty on the RMSE given in the Tables is below 5% for a given noise level.

The evolution of the normalized mean square error, $\|\delta^* - \delta\|_2/\|\delta^*\|_2$ and $\|\beta^* - \beta\|_2/\|\beta^*\|_2$, are displayed as a function of the number of iterations for the deterministic and stochastic algorithms in Figure 1.12. The iterated deterministic minimization can not escape the local minimum corresponding to the initial reconstructed δ and β volumes. A larger decrease is obtained with the stochastic scheme. Table 1.3 presents the reconstution quality results for different noise levels and the different algorithms. The results correspond to an average over three trials. This table shows the efficiency of the stochastic optimization.

Some horizontal sections of the difference image between the ground truth image and the reconstructed real index map obtained for the minimum of the discrepancy term for 24 dB with the stochastic or the deterministic methods are displayed in Figure 1.13. These figures show that the

TABLE 1.3
RMSE for β and δ for Deterministic Level-Set and Stochastic Level-Set

	RMSE β, LS	RMSE δ,LS	RMSE β, Stochastic LS	RMSE δ, Stochastic LS
PPSNR=18 dB	0.28	0.85	0.15	0.55
PPSNR=24 dB	0.22	0.80	0.06	0.26

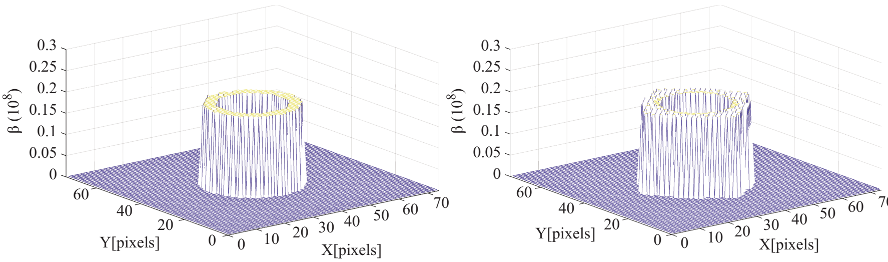

FIGURE 1.13
Horizontal section of the difference image between the ground truth and the reconstructed β maps with the stochastic and the deterministic level-set algorithms for the noise level 24 dB.

reconstruction errors have been significantly reduced. Similar results are obtained for the imaginary part of the refractive index.

1.4.5 Conclusion

We have studied some aspects of the nonlinear inverse problem associated with the reconstruction of the real and imaginary parts of the refractive index in phase contrast tomography and with the binary tomographic reconstruction problem. Both are regularized with level-set functions and with Total-Sobolev penalty term. The deterministic optimization of the regularization functional leads to local minima with large reconstruction errors. The reconstruction results are improved with a stochastic perturbation of the shape of the reconstructed regions with a stochastic level-set evolution. The evolution is based on a stochastic partial differential equation with the Stratonovich formulation. The stochastic algorithm leads to a decreased reconstruction errors localized on the boundaries for different noise levels. The method gives better reconstruction results than the classical simulated annealing method.

References

1. J. A. Sethian, "Level Set Methods and Fast Marching Methods", Cambridge Monograph on Applied and Computational Mathematics, Cambridge University Press, 1999.
2. A. Egger and L. Leitao, "Nonlinear regularization for ill-posed problems with piecewise constant or strongly varying solutions", *Inverse Problems*, vol. 25, pp. 115014, 2009.
3. A. DeCezaro, A. Leitao and X. C. Tai, "On multiple level-set regularization methods for inverse problems", *Inverse Problems*, vol. 25, pp. 035004, 2009.
4. M. Burger, "A level set method for inverse problems", *Inverse Problems*, vol. 17, pp. 1327–1355, 2001.

5. S. Geman and C. R. Hwang, "Diffusion for global optimization", *J. Control Optim.*, vol. 24, pp. 1031–1043, 1986.
6. B. Gidas, "Metropolis-type Monte Carlo simulation algorithm and simulated annealing", *Topics in Contemporary Probability and Its Applications*, Probability Stochastics Series, CRC, Boca Raton, FL. pp. 159–232, 1995.
7. P. Parpas, B. Rustem, "Convergence analysis a a global optimization algorithm using stochastic differential equations", *J. Control Optim.*, vol. 45, pp. 95–110, 2009.
8. S. Chow, T. Yang and H. Zhou, "Global optimization by intermittent diffusion", National Science Council Tunghai University Endowment Fund for Academic Advancement Mathematics Research Promotion Center vol. 121, 2009.
9. T. S. Chiang, C. R. Hwang and S. J. Sheu, "Diffusion for global optimization in $\mathbb{R}^n$" *SIAM J. Control Optim.*, vol. 25, pp. 737–753, 1987.
10. O. Juan, R. Keriven and G. Postelnicu, "Stochastic Motion and the Level-Set Method in Computer Vision: Stochastic Active Contours", *International Journal of Computer Vision*, vol. 69, pp. 7–25, 2006.
11. I. Karatzas and S. Shreve, *Brownian motion and stochastic calculus*, Springer Verlag, New York, 1991.
12. G. Da Prato and J. Zabczyk, "Stochastic equations in infinite dimensions", *Encyclopedia of Mathematics and Its Applications*, Cambridge:Cambridge University Press, 1992.
13. G. T. Herman and A. Kuba, "Advances in discrete tomography and its applications", Birkhauser Boston, 2007.
14. K. J. Batenburg and J. Sijbers, "Generic iterative subset algorithm for discrete tomography", *Discrete Applied Mathematics*, vol. 157, pp. 438–451, 2009.
15. W. Cai and L. Ma, "Comparison of approaches based on optimization and algebraic iteration for binary tomography", *Computer Physics Communications*, vol. 181, pp. 1974–1981, 2010.
16. L. Rusko and A. Kuba, "Multi-resolution methods for binary tomography", *Electonics Notes in Discrete Mathematics*, vol. 20, pp. 299–311, 2005.
17. T. D. Capricelli and P. L. Combettes, "A convex programing algorithm for noisy discrete tomography", *Advances in discrete tomography and its applications*, Boston, MA, pp. 207–226, 2007.
18. T. Schule, C. Schnorr, S. Weber and J. Hornegger, "Discrete tomogrphy by convex-concave regularization and D. C programming", *Discrete Applied Mathematics*, vol. 151, pp. 229–243, 2005.
19. H. Y. Liao and G. T. Herman, "Automated estimation of the parameters of the Gibbs priors to be uses in binary tomography", *Discrete Applied Mathematics*, pp. 149–170, 2004.
20. E. Gouillart, F. Krzakala, M. Mezard and L. Zdebrova, "Belief propagation reconstruction for discrete tomography", *Inverse Problems*, vol. 29, pp. 035003, 2013.
21. L. I. Rudin, S. Osher, E. Fatemi, "Nonlinear total variation based noise removal algorithms", *Phys. D*, vol. 60, pp. 259–268, 1992.
22. B. Sixou, L. Wang and F. Peyrin, "Binary tomographic reconstruction of bone microstructure from few projections with level-set regularization", *IEEE Symposium on Biomedical Imaging*, San Francisco, 2013.
23. Sixou B. "Binary tomography reconstruction with stochastic level-set methods" *IEEE Signal Processing Letters* vol. 22, pp. 920–924, 2015.

24. R. Azencott, "Sequential simulated annealing: speed of convergence and acceleration techniques", *Simulated annealing:parallelization techniques* Wiley, New York, pp. 1–10, 1992.
25. O. Catoni, "Rough large deviation estimates for simulated annealing algorithms", *Annals of Probability*, vol. 20, pp. 1109–1146, 1992.
26. C. Cot and O. Catoni, "Piecewise constant triangular cooling schedule for generalized annealing algorithms", *Annals of Applied probability*, vol. 8, pp. 375–396, 1998.
27. R. Szu and R. Hartley, "Fast simulated annealing", *Physics Letters A*, vol. 122, pp. 157–162, 1987.
28. L. Ingber, "Very fast simulated annealing", *Journal of Mathematical Computer Modelling*, vol. 12, pp. 967–973, 1989.
29. L. Apostol, V. Boudousq, O. Basset, C. Odet, S. Yot, J. Tabary, J. M. Dinten, E. Boller, P. O. Kotzki and F. Peyrin, "Relevance of 2D radiographic texture analysis for the assessment of 3D bone microarchitecture", *Medical Physics*, vol. 33, pp. 3546–3556, 2006.
30. H. W. Engl, M. Hanke and A. Neubauer, "Regularization of Inverse Problems", Dordrecht: Kluwer Academic, 1996.
31. A. Momose, T. Takeda, Y. Tai, Y. Yoneyama and K. Hirano, "Phase-contrast tomographic imaging using an X-ray interferometer", *J. Synchrotron. Rad.* vol. 5, pp. 309–314, 1998.
32. P. Cloetens, M. Pateyron-Salome, J. Y. Buffiere, G. Peix, J. Baruchel, F. Peyrin and M. Schlenker, "Observation of microstructure and damage in materials by phase sensitive radiography and tomography" *J. Appl. Phys.* vol. 81, pp. 5878–5886, 1997.
33. M. Langer, P. Cloetens, A. Pacureanu and F. Peyrin, "X-ray in-line phase tomography of multimaterial objects" *Optics Letters* vol. 37, pp. 2151–2154, 2102.
34. B. Sixou, V. Davidoiu, M. Langer, F. Peyrin, "Absorption and phase retrieval in phase contrast imaging with nonlinear Tikhonov regularization and joint sparsity constraint regularization" *Inverse Problems and Imaging* vol. 7, pp. 267–282, 2013.
35. K. A. Nugent, "Coherent methods in the X-rays science" *Advances in Physics* vol. 59, pp. 1–99, 2010.
36. L. Wang, B. Sixou and F. Peyrin, "Binary tomography reconstruction with stochastic level-set method" *Signal Processing Letters* vol. 22, pp. 922–924, 2015.
37. M. Born and E. Wolf "Principles of Optics". Cambridge University Press; 1997.
38. J. W. Goodman "Intoduction fo Fourier Optics" Roberts, Greenwood Village, CO; 2005.
39. B. Sixou, "Deterministic versus stochastic level-set regularization in nonlinear phase contrast tomography" *Inverse Problems in Science and Engineering* 2016.
40. S. Osher and R. P. Fedkiw, "The Level-Set method and Dynamic Implic Surfaces" Springer, New York; 1988.
41. G. S. Jiang and D. Peng, "Weigthed ENO schemes for Hamilton-Jacobi equations" *SIAM J. Control Optim.* vol. 21, pp. 2126–2143, 2000.

References

2

Application of 3D Level Set Based Optimization in Microwave Breast Imaging for Cancer Detection

1. Ferlay, Jacques, Isabelle Soerjomataram, Rajesh Dikshit, Sultan Eser, Colin Mathers, Marise Rebelo, Donald Maxwell Parkin, David Forman, and Freddie Bray. "Cancer incidence and mortality worldwide: sources, methods and major patterns in GLOBOCAN 2012," *International Journal of Cancer*, Vol. 136, no. 5, pp. 359–386, March 2015.
2. Elise C. Fear, Paul M. Meaney, and Maria A. Stuchly. "Microwaves for breast cancer detection," *IEEE Potentials*, Vol. 22, no. 1, pp. 12–18, 2003.
3. Campbell, A. M., and D. V. Land. "Dielectric properties of female human breast tissue measured in vitro at 3.2 GHz," *Physics in Medicine and Biology*, Vol. 37, no. 1, pp. 193–210, 1992.
4. Lazebnik, Mariya, Leah McCartney, Dijana Popovic, Cynthia B. Watkins, Mary J. Lindstrom, Josephine Harter, Sarah Sewall et al. "A large-scale study of the ultra-wideband microwave dielectric properties of normal breast tissue obtained from reduction surgeries," *Physics in Medicine and Biology*, Vol. 52, no. 10, pp. 2637–2656, 2007.
5. Lazebnik, Mariya, Dijana Popovic, Leah McCartney, Cynthia B. Watkins, Mary J. Lindstrom, Josephine Harter, Sarah Sewall et al. "A large-scale study of the ultra-wideband microwave dielectric properties of normal, benign and malignant breast tissues obtained from cancer surgeries," *Physics in Medicine and Biology*, Vol. 52, no. 20, pp. 6093–6115, 2007.
6. Robert A. Jesinger, MD, MSE "Breast Anatomy for the Interventionalist," *Techniques in Vascular and Interventional Radiology*, Elsevier, Vol. 17, no. 1, pp. 3–9, March 2014.
7. Douglas Hanahan and Robert A. Weinberg, "Hallmarks of Cancer: The Next Generation," Elsevier, *Cell Press*, Vol. 144, no. 5, pp. 646–674, March 2011.
8. Zhou, Chuan, Heang-Ping Chan, Nicholas Petrick, Mark A. Helvie, Mitchell M. Goodsitt, Berkman Sahiner, and Lubomir M. Hadjiiski. "Computerized image analysis: estimation of breast density on mammograms," *Medical Physics*, Vol. 28, no. 6, pp. 1056–1069, 2001.

9. Vacek, Pamela M., and Berta M. Geller. "A prospective study of breast cancer risk using routine mammographic breast density measurements," *Cancer Epidemiology and Prevention Biomarkers*, Vol. 13, no. 5, pp. 715–722, 2004.
10. Boyd, Norman F., Gina A. Lockwood, Jeff W. Byng, David L. Tritchler, and Martin J. Yaffe. "Mammographic densities and breast cancer risk," *Cancer Epidemiology and Prevention Biomarkers*, Vol. 7, no. 12, pp. 1133–1144, 1998.
11. Vachon, Celine M., Carla H. Van Gils, Thomas A. Sellers, Karthik Ghosh, Sandhya Pruthi, Kathleen R. Brandt, and V. Shane Pankratz. "Mammographic density, breast cancer risk and risk prediction," *Breast Cancer Research*, Vol. 9, no. 6, pp. 217–225, 2007.
12. Freer, Phoebe E. "Mammographic breast density: impact on breast cancer risk and implications for screening," *Radiographics*, Vol. 35, no. 2, pp. 302–315, 2015.
13. Nelson, Heidi D., Ellen S. O'meara, Karla Kerlikowske, Steven Balch, and Diana Miglioretti. "Factors Associated With Rates of False-Positive and False-Negative Results From Digital Mammography Screening: An Analysis of Registry DataFalse-Positive and False-Negative Digital Mammography Screening Results," *Annals of Internal Medicine*, Vol. 164, no. 4, pp. 226–235, 2016.
14. Zastrow, E., S. K. Davis, M. Lazebnik, F. Kelcz, B. D. Van Veen, and S. C. Hagness, "Development of anatomically realistic numerical breast phantoms with accurate dielectric properties for modelling microwave interactions with the human breast," *IEEE Transactions on Biomedical Engineering*, Vol. 55, no. 12, pp. 2792–2800, 2008.
15. Lazebnik, M., M. Okoniewski, J. H. Booske, and S. C. Hagness, "Highly accurate Debye models for normal and malignant breast tissue dielectric properties at microwave frequencies," *IEEE Microwave and Wireless Components Letters*, Vol. 17, no. 12, pp. 822–824, 2007.
16. David W. Winters, Jacob D. Shea, Panagiotis Kosmas, Barry D. VanVeen, Susan C. Hagness, "Three-dimensional microwave breast imaging: dispersive dielectric properties estimation using patient-specific basis functions," *IEEE Transactions on Medical Imaging*, Vol. 28, no. 7, pp. 969–981, July 2009.
17. J. D., Shea, P. Kosmas, S. C. Hagness, and B. D. Van Veen, "Three-dimensional microwave imaging of realistic numerical breast phantoms via a multiple-frequency inverse scattering technique," *Medical Physics*, Vol. 37, no. 8, pp. 4210–4226, 2010.
18. S. Osher, J.A. Sethian, "Fronts propagating with curvature-dependent speed: algorithms based on Hamilton-Jacobi formulations," *Journal of Computational Physics*, Vol. 79, pp. 12–49, 1988.
19. S. Osher and R. Fedkiw, "Level set methods and dynamic implicit surfaces," *Applied Mathematical Sciences*, 2003 Springer-Verlag New York Inc.
20. Fadil Santosa, "A level-set approach for inverse problems involving obstacles," *EASIM: Control, Optimization and calculus of variations*, Vol. 1, pp. 17–33, January 1996.
21. Oliver Dorn, Eric L Miller and Carey M Rappaport, "A shape reconstruction method for electromagnetic tomography using adjoint fields and level sets," *Inverse Problems*, Vol. 16, No. 5, October 2000.
22. Martin Burger, "A level set method for inverse problems," *Inverse Problems*, Volume 17, Number 5, August 2001.

23. R. Ferraye, J.-Y. Dauvignac, C. Pichot, "An inverse scattering method based on contour deformations by means of a level set method using frequency hopping technique," *IEEE Transactions on Antennas and Propagation*, Vol. 51, No. 5, pp. 1100–1113, July 2003.
24. Martin burger and stanley j. osher, "A survey on level set methods for inverse problems and optimal design," *European Journal of Applied Mathematics*, Vol. 16, No. 2, pp. 263–301, April 2005.
25. Oliver Dorn and Dominique Lesselier, "Level set methods for inverse scattering," *Inverse Problems*, Volume 22, Number 4, June 2006.
26. Natalia Irishina, Oliver Dorn, Miguel, "A level set evolution strategy in microwave imaging for early breast cancer detection," *Computers & Mathematics with Applications*, Elsevier, Volume 56, Issue 3, pp. 607–618, August 2008.
27. Natalia Irishina, Miguel Moscoso, Oliver Dorn, "Microwave Imaging for Early Breast Cancer Detection Using a Shape-based Strategy," *IEEE Transactions on Biomedical Engineering*, Vol. 56, No.4, pp. 1143–1153, January 2009.
28. Alireza Aghasi, Misha Kilmer, and Eric L. Miller, "Parametric Level Set Methods for Inverse Problems," *SIAM Journal on Imaging Sciences*, Vol. 4, No. 2, 618–650, 2011.
29. Oguz Semerci, Eric L. Miller, "A Parametric Level-Set Approach to Simultaneous Object Identification and Background Reconstruction for Dual-Energy Computed Tomography," *IEEE transactions on Image Processing*, Vol. 21, No. 5, pp. 2719–2734, February 2012.
30. Timothy J. Colgan, Susan C. Hagness, Barry D. Van Veen, "A 3-D Level Set Method for Microwave Breast Imaging," *IEEE Transactions on Biomedical Engineering*, Vol. 62, No. 10, pp. 2526–2534, Oct. 2015.
31. Mohammad Reza Eskandari, Mojtaba Dehmollaian, Reza Safian, "Simultaneous Microwave Imaging and Parameter Estimation Using Modified Level-Set Method," *IEEE Transactions on Antennas and Propagation* Vol. 64, No. 8, pp. 3554–3564, June 2016.
32. Natalia Irishina, "Microwave medical imaging using level set techniques," PhD Thesis, University of Carlos, Spain, 2009.
33. H. N. Patel and D. K. Ghodgaonkar, "3D level set based optimization of inverse scattering problem for microwave breast imaging", IEEE MTT-S International Microwave Bio Conference, 15-17 May 2017, Gothenburg, Sweden, pp. 1–4.
34. H. N. Patel and D. K. Ghodgaonkar, "Study of effect of numerical breast phantom heterogeneity on dielectric profile reconstruction using microwave imaging," *Progress In Electromagnetics Research* M, Vol. 58, pp. 135–145, 2017.
35. Hua, Ping, Eung Je Woo, John G. Webster, and Willis J. Tompkins. "Iterative reconstruction methods using regularization and optimal current patterns in electrical impedance tomography," *IEEE Transactions on Medical Imaging*, Vol. 10, no. 4, pp. 621–628, 1991.
36. Zhang, Hua, Jing Huang, Jianhua Ma, Zhaoying Bian, Qianjin Feng, Hongbing Lu, Zhengrong Liang, and Wufan Chen. "Iterative reconstruction for X-ray computed tomography using prior-image induced nonlocal regularization," *IEEE Transactions on Biomedical Engineering*, Vol. 61, no. 9, pp. 2367–2378, 2014.
37. Zhao, Shan, and Imad L. Al-Qadi. "Development of regularization methods on simulated ground-penetrating radar signals to predict thin asphalt overlay thickness," *Signal Processing, Elsevier*, Vol. 132, pp. 261–271, March 2017.

38. Jurgen De Zaeytijd, Ann Franchois, Christelle Eyraud, and Jean-Michel Geffrin, "Full-Wave Three-Dimensional Microwave Imaging With a Regularized Gauss-Newton Method-Theory and Experiment," *IEEE Transactions on Antennas and Wave Propagation*, Vol. 55, no. 11, pp. 3279–3292, November 2007.
39. Park, C. S. and B. S. Jeong, "Reconstruction of a high contrast and large object by using the hybrid algorithm combining a Levenberg-Marquardt algorithm and a genetic algorithm," *IEEE Transactions on Magnetics*, Vol. 35, no. 3, pp. 1582–1585, May 1999.
40. Rubk, T., P. M. Meaney, P. Meincke, and K. D. Paulsen, "Nonlinear microwave imaging for breast-cancer screening using Gauss-Newton's method and the CGLS inversion algorithm," *IEEE Transactions on Antennas and Propagation*, Vol. 55, no. 8, pp. 2320–2331, August 2007.

3

A Modified Global and Elastic ICP Shape Registration for Medical Imaging Applications

1. A.A. Farag, H.E. Abd El Munim, J.H. Graham, A.A. Farag: A *Novel Approach for Lung Nodules Segmentation in Chest CT using Level Sets*, IEEE Trans. on Image Processing, 22(12):5202–5213, 2013.
2. A.H. Yousef and H.E. Abd El Munim, "An accelerated shape based segmentation approach adopting the pattern search optimizer, Ain Shams Engineering Journal," 2016, http://dx.doi.org/10.1016/j.asej.2016.11.002.
3. A.H. Yousef and H.E. Abd El Munim, "A GPU-Based Elastic Shape Registration Approach in Implicit Spaces," *Journal of Real-Time Image Processing*, pp. 1–13, August, 2017.
4. R. Veltkamp and M. Hagedoorn, "State of the Art in Shape Matching,"*Technical Report*, UU-CS-19999-27, Utrecht University, Sept. 1999.
5. Nikos Paragios, Mikael Rousson and Visvanathan Ramesh, "Matching Distance Functions: A Shape-to-Area Variational Approach for Global-to-Local Registration,"*European Conference in Computer Vision*, Copenhagen, Denmark, Jun. 2002.
6. P. Besl and N. Mckay, "A Method for Registration of 3-D Shapes,"*IEEE Tr. on PAMI*, 14(2):239–256, 1992.
7. Z. Zhang, "Iterative Point Matching for Registration of Free-form Curves and Surfaces," *Ph.D. International Journal of Computer Vision*, vol. 13, no. 2, pp. 119–152, 1994.
8. I. Cohen and I. Herlin, "Curve Matching Using Geodesic Paths,"*In IEEE CVPR*, pp 741–746, Santa Barbara, USA, 1998.
9. A. Fitzgibbon, "Robust Registration of 2D and 3D Points Sets,"*In Proceeding of The British Machine Vision Conference (BMVC)*, vol. 2, pp 411–420, University of Manchester, UK, 2001.
10. D. Kozinska, O. Tretika, J. Nissanov, and C. Ozturk, "Multidimensional Alignment Using the Euclidean Distance Transform, "*Graphical Models and Image Processing*, pp 6:373–385, 1997.
11. Z. Xie and G. E. Farin, "Image Registration Using Hierarchical B-Splines,"*IEEE Transaction on Visualization and Computer Graphics*, Vol. 10, NO. 1, 2004.
12. M. Rousson, N. Paragios and R. Deriche. "Implicit Active Shape Models for 3D Segmentation in MRI Imaging," *Medical Image Computing and Computer Assisted Intervention (MICCAI)*, Part 1, pp 209–216, Saint-Malo, France, September 26-29, 2004.

13. T. Sederberg and S. Parry, "Free-Form Deformation of Solid Geometric Models,"*in ACM SIGGRAPH*, 1986, pp. 151–160.
14. D. Rueckert, L. Sonoda, C. Hayes, D. Hill, M. Leach, and D. Hawkes, "Non-rigid Registration Using Free-Form Deformations: Application to Breast MR Images,"*IEEE Transactions on Medical Imaging*, vol. 8, pp. 712–721, 1999.
15. Tim McInerney and Demetri Terzopoulos, "Deformable Models in Medical Image Analysis: A Survey," *In Medical Image Analysis*, 1(2):91–108, 1996.
16. Sakae Nagasawa, Takamitsu Yoshida, Kaoru Tamura, Masatoshi Yamazoe, Yoshinori Arai Keigo Hayano, Hirohito Yamada, Etsuo Kasahara, and Michio Ito, "Construction of database for three-dimensional human tooth models and its ability for education and research - carious tooth models," *Dental Materials Journal*, vol. 29, 2010.
17. H. E. Abd El Munim and A. A. Farag, "A Shape-Based Segmentation Approach: An Improved Technique Using Level Sets ," *(ICCV'05)*, pp. 930–935.
18. H. E. Abd El Munim and A. A. Farag, "Curve/Surface Representation and Evolution using Vector Level Sets with Application to the Shape-based Segmentation Problem ," *PAMI*, Vol. 29, No. 6, pp. 945–958, June 2007.
19. G. Mori and J. Malik,, "Recovering 3D Human Body Configurations Using Shape Contexts, "*PAMI*, VOL. 28, NO. 7, pp. 1052–1062, July 2006.
20. N. Hasler, H. Ackermann, B. Rosenhahn, T. Thormahlen, and H. Seidel, "Multilinear pose and body shape estimation of dressed subjects from image sets,"*CVPR*, Page(s): 1823–1830.
21. R. Sagawa, K. Akasaka, Y. Yagi, H. Hamer, and L. Van Gool, "Elastic convolved ICP for the registration of deformable objects,"*ICCV*, Page(s): 1558–1565, Kyoto, Japan, Sep. 27 to Oct. 4, 2009.
22. Xiaolei Huang, N. Paragios, and D.N. Metaxas, "Shape registration in implicit spaces using information theory and free form deformations ," *TPAMI*, Vol. 28, Issue 8, Aug. 2006 Page(s): 1303–1318.

4

Robust Nuclei Segmentation Using Statistical Level Set Method with Topology Preserving Constraint

1. C. Wählby, I.-M. Sintorn, F. Erlandsson, G. Borgefors, and E. Bengtsson, "Combining intensity, edge and shape information for 2D and 3D segmentation of cell nuclei in tissue sections," *Journal of Microscopy*, vol. 215, no. 1, pp. 67–76, 2004.
2. S. Di Cataldo, E. Ficarra, A. Acquaviva, and E. Macii, "Automated segmentation of tissue images for computerized IHC analysis," *Computer Methods and Programs in Biomedicine*, vol. 100, no. 1, pp. 1–15, 2010.
3. C. Jung and C. Kim, "Segmenting clustered nuclei using H-minima transform-based marker extraction and contour parameterization," *IEEE Transactions on Biomedical Engineering*, vol. 57, no. 10, pp. 2600–2604, Oct 2010.
4. J. Cheng and J. Rajapakse, "Segmentation of clustered nuclei with shape markers and marking function," *IEEE Transactions on Biomedical Engineering*, vol. 56, no. 3, pp. 741–748, March 2009.
5. H. Irshad, A. Veillard, L. Roux, and D. Racoceanu, "Methods for nuclei detection, segmentation, and classification in digital histopathology: A review – current status and future potential," *IEEE Reviews in Biomedical Engineering*, vol. 7, pp. 97–114, 2014.
6. H. Kong, M. Gurcan, and K. Belkacem-Boussaid, "Partitioning histopathological images: an integrated framework for supervised color-texture segmentation and cell splitting," *IEEE Transactions on Medical Imaging*, vol. 30, no. 9, pp. 1661–1677, 2011.
7. A. Rosenfeld and J. L. Pfaltz, "Sequential operations in digital picture processing," *J. ACM*, vol. 13, no. 4, pp. 471–494, Oct. 1966. [Online]. Available: http://doi.acm.org/10.1145/321356.321357
8. C. Jung, C. Kim, S. W. Chae, and S. Oh, "Unsupervised segmentation of overlapped nuclei using bayesian classification," *IEEE Transactions on Biomedical Engineering*, vol. 57, no. 12, pp. 2825–2832, 2010.
9. D. Ballard, "Generalizing the Hough transform to detect arbitrary shapes," *Pattern Recognition*, vol. 13, no. 2, pp. 111–122, 1981. [Online]. Available: http://www.sciencedirect.com/science/article/pii/0031320381900091
10. R. O. Duda and P. E. Hart, "Use of the Hough transformation to detect lines and curves in pictures," *Commun. ACM*, vol. 15, no. 1, pp. 11–15, Jan. 1972. [Online]. Available: http://doi.acm.org/10.1145/361237.361242

11. E. Cosatto, M. Miller, H. Graf, and J. Meyer, "Grading nuclear pleomorphism on histological micrographs," in *19th International Conference on Pattern Recognition (ICPR)*, Dec 2008, pp. 1–4.
12. Y. M. George, B. M. Bagoury, H. H. Zayed, and M. I. Roushdy, "Automated cell nuclei segmentation for breast fine needle aspiration cytology," *Signal Processing*, vol. 93, no. 10, pp. 2804–2816, 2013.
13. O. Dzyubachyk, W. van Cappellen, J. Essers, W. Niessen, and E. Meijering, "Advanced level-set-based cell tracking in time-lapse fluorescence microscopy," *IEEE Transactions on Medical Imaging*, vol. 29, no. 3, pp. 852–867, March 2010.
14. F. Tek, A. Dempster, and I. Kale, "Blood cell segmentation using minimum area watershed and circle Radon transformations," in *Mathematical Morphology: 40 Years On*, ser. Computational Imaging and Vision, C. Ronse, L. Najman, and E. Decencière, Eds. Springer Netherlands, 2005, vol. 30, pp. 441–454. [Online]. Available: http://dx.doi.org/10.1007/1-4020-3443-1_40
15. T. Esteves, P. Quelhas, A. M. Mendonça, and A. Campilho, "Gradient convergence filters and a phase congruency approach for in vivo cell nuclei detection," *Machine Vision and Applications*, vol. 23, no. 4, pp. 623–638, 2012.
16. H. Kobatake and S. Hashimoto, "Convergence index filter for vector fields," *IEEE Transactions on Image Processing*, vol. 8, no. 8, pp. 1029–1038, 1999.
17. C. Pereira, H. Fernandes, A. Mendonça, and A. Campilho, "Detection of lung nodule candidates in chest radiographs," *Pattern Recognition and Image Analysis*, pp. 170–177, 2007.
18. J. Wei, Y. Hagihara, and H. Kobatake, "Detection of cancerous tumors on chest X-ray images-candidate detection filter and its evaluation," in *International Conference on Image Processing (ICIP)*, vol. 3. IEEE, 1999, pp. 397–401.
19. R. A. Russell, N. M. Adams, D. A. Stephens, E. Batty, K. Jensen, and P. S. Freemont, "Segmentation of fluorescence microscopy images for quantitative analysis of cell nuclear architecture," *Biophysical journal*, vol. 96, no. 8, pp. 3379–3389, 2009.
20. M. N. Gurcan, T. Pan, H. Shimada, and J. Saltz, "Image analysis for neuroblastoma classification: Segmentation of cell nuclei," in *28th Annual International Conference of the IEEE Engineering in Medicine and Biology Society (EMBS)*. IEEE, 2006, pp. 4844–4847.
21. F. Cloppet and A. Boucher, "Segmentation of complex nucleus configurations in biological images," *Pattern Recognition Letters*, vol. 31, no. 8, pp. 755–761, 2010.
22. O. Schmitt and M. Hasse, "Radial symmetries based decomposition of cell clusters in binary and gray level images," *Pattern Recognition*, vol. 41, no. 6, pp. 1905–1923, 2008.
23. F. Meyer, "Topographic distance and watershed lines," *Signal Processing*, vol. 38, no. 1, pp. 113–125, 1994.
24. J. B. Roerdink and A. Meijster, "The watershed transform: Definitions, algorithms and parallelization strategies," *Fundamenta Informaticae*, vol. 41, no. 1,2, pp. 187–228, Apr. 2000. [Online]. Available: http://dl.acm.org/citation.cfm?id=2372488.2372495
25. S. Osher and J. A. Sethian, "Fronts propagating with curvature-dependent speed: algorithms based on Hamilton-Jacobi formulations," *Journal of Computational Physics*, vol. 79, no. 1, pp. 12–49, 1988.

26. M. Kass, A. Witkin, and D. Terzopoulos, "Snakes: Active contour models," *International Journal of Computer Vision*, vol. 1, no. 4, pp. 321–331, 1988.
27. V. Caselles, R. Kimmel, and G. Sapiro, "Geodesic active contours," *International Journal of Computer Vision*, vol. 22, no. 1, pp. 61–79, 1997.
28. D. Mumford and J. Shah, "Optimal approximations by piecewise smooth functions and associated variational problems," *Communications on Pure and Applied Mathematics*, vol. 42, no. 5, pp. 577–685, 1989.
29. T. E. Chan and L. Vese, "A level set algorithm for minimizing the Mumford-Shah functional in image processing," in *IEEE Workshop on Variational and Level Set Methods in Computer Vision*. IEEE, 2001, pp. 161–168.
30. T. F. Chan and L. Vese, "Active contours without edges," *IEEE Transactions on Image Processing*, vol. 10, no. 2, pp. 266–277, 2001.
31. S. Gao and T. D. Bui, "A multistage image segmentation and denoising method–based on the Mumford and Shah variational approach," in *Image Analysis and Recognition*. Springer, 2004, pp. 82–89.
32. A. C. Ruifrok and D. A. Johnston, "Quantification of histochemical staining by color deconvolution," *Analytical and Quantitative Cytology and Histology*, vol. 23, no. 4, pp. 291–299, 2001.
33. J. Ni, M. Singh, and C. Bahlmann, "Fast radial symmetry detection under affine transformations," in *IEEE Conference on Computer Vision and Pattern Recognition (CVPR)*, June 2012, pp. 932–939.
34. X. Han, C. Xu, and J. L. Prince, "A topology preserving level set method for geometric deformable models," *IEEE Transactions on Pattern Analysis and Machine Intelligence*, vol. 25, no. 6, pp. 755–768, 2003.
35. G. Loy and A. Zelinsky, "Fast radial symmetry for detecting points of interest," *IEEE Transactions on Pattern Analysis and Machine Intelligence*, vol. 25, no. 8, pp. 959–973, August 2003.
36. D. Cremers, M. Rousson, and R. Deriche, "A review of statistical approaches to level set segmentation: integrating color, texture, motion and shape," *International Journal of Computer Vision*, vol. 72, no. 2, pp. 195–215, 2007.
37. T. Brox, M. Rousson, R. Deriche, and J. Weickert, "Colour, texture, and motion in level set based segmentation and tracking," *Image and Vision Computing*, vol. 28, no. 3, pp. 376–390, 2010. [Online]. Available: http://www.sciencedirect.com/science/article/pii/S0262885609001334
38. G. Bertrand, "Simple points, topological numbers and geodesic neighborhoods in cubic grids," *Pattern Recognition Letters*, vol. 15, no. 10, pp. 1003–1011, 1994. [Online]. Available: http://www.sciencedirect.com/science/article/pii/0167865594900329
39. L. Coelho, A. Shariff, and R. Murphy, "Nuclear segmentation in microscope cell images: A hand-segmented dataset and comparison of algorithms," in *IEEE International Symposium on Biomedical Imaging: From Nano to Macro (ISBI)*, June 2009, pp. 518–521.
40. A. E. Carpenter, T. R. Jones, M. R. Lamprecht, C. Clarke, I. H. Kang, O. Friman, D. A. Guertin, J. H. Chang, R. A. Lindquist, J. Moffat *et al.*, "Cellprofiler: image analysis software for identifying and quantifying cell phenotypes," *Genome Biology*, vol. 7, no. 10, p. R100, 2006.

5

Level Set Methods in Segmentation of SDOCT Retinal Images

1. Abramoff, M. D., Garvin, M. K., & Sonka, M. (2010). Retinal imaging and image analysis. *IEEE Reviews in Biomedical Engineering*, 3, 169–208.
2. Padmasini, N., Umamaheswari, R., & Sikkandar, M. Y. (2018). State-of-the-Art of Level-Set Methods in Segmentation and Registration of Spectral Domain Optical Coherence Tomographic Retinal Images. In *Soft Computing Based Medical Image Analysis*. Chapter: 10 Publisher: Academic Press pp. 163 –181.
3. Tsantis, S., Dimitropoulos, N., Ioannidou, M., Cavouras, D., & Nikiforidis, G. (2007). Inter-scale wavelet analysis for speckle reduction in thyroid ultrasound images. *Computerized Medical Imaging and Graphics*, *31*(3), 117–127.
4. Hitesh H. Vandra & Pandya, H.N. (2010). Comparative analysis on Speckle noise reduction techniques on computed tomographic images. *Oriental Journal of Computer Science & Technology*, 3(2), 261–264.
5. Schmitt, J. M., Xiang, S. H., & Yung, K. M. (1999). Speckle in optical coherence tomography. *Journal of Biomedical Optics*, 4(1), 95–105.
6. Padmasini, N., Abbirame, K. S., Yacin, S. M., & Umamaheswari, R. (2014, November). Speckle noise reduction in spectral domain optical coherence tomography retinal images using anisotropic diffusion filtering. *2014 IEEE International Conference* In *Science Engineering and Management Research (ICSEMR)*, (pp. 1–5).
7. Fu, K. S., & Mui, J. K. (1981). A survey on image segmentation. *Pattern Recognition*, 13(1), 3–16.
8. Pavlidis, T. (2012). *Algorithms for graphics and image processing*, Springer Science & Business Media.
9. Bankhead, P., McGowan, J., & Curtis, T. (2009). "Fast retinal vessel detection and measurement using wavelets and edge location refinement", *PLoS ONE*, 7, p. e32435.
10. Rossant, F., Badellino, M., Chavillon, A., Bloch, I., & Paques, M. (2011). A morphological approach for vessel segmentation in eye fundus images, with quantitative evaluation. *J. Med. Imag. Health. Inf.*, 1, 42–49.
11. Al-Diri, B., Hunter, A., & Steel, D. (2009, September). An active contour model for segmenting and measuring retinal vessels. *IEEE Trans. Med. Imag.*, 28(9), 1488–1497.

12. B. Dizdaroglu et al. (2012). Level sets for retinal vasculature segmentation using seeds from ridges and edges from phase maps, in *Proc. IEEE Int. Workshop Mach. Learn. Signal Process*, 1–6.
13. Osher S., & Sethian, J.A. (1988). Fronts propagating with curvature-dependent speed: algorithms based on Hamilton–Jacobi formulation. *Journal of Computational Physics*, 79(1):12–49.
14. Mumford, D., & Shah, J. (1989), Optimal approximations by piecewise smooth functions and associated variational problems. Communications on pure and applied mathematics, 42(5), 577–685.
15. Sethian, J.A. *Level set methods and fast marching methods*, Cambridge University Press, 1996.
16. Malladi, R., & Sethian, J. A. (1995). Image processing via level set curvature flow. *Proceedings of the National Academy of Sciences*, 92(15), 7046–7050.
17. Kass, M., Witkin, A., & Terzopoulos, D. (1988). Snakes: Active contour models. *International Journal of Computer Vision*, 1:321–331.
18. Precioso, F., Barlaud, M., Blu, T., & Unser, M. (2005). Robust real-time segmentation of images and videos using a smooth-spline snake-based algorithm. *IEEE Transactions on Image Processing*, 14(7):910–924.
19. Osher, S., & Sethian, J.A. (1988). Fronts propagating with curvature-dependent speed: algorithms based on Hamilton-Jacobi formulations. *Journal of Computational Physics*, 79(1):12–49.
20. Caselles, V., Kimmel, R., & Sapiro, G. (1997). Geodesic Active Contours. *International Journal of Computer Vision*, 22(1):61–79.
21. Chan, T. F., & Vese, L.A. (2001). Active contours without edges. IEEE Transactions on Image Processing, 10(2):266–277.
22. Kass, M., Witkin, A., & Terzopoulos, D. (1988). Snakes: active contour models. *Int. J. Comput. Vis.*, 1 (4), 321–331.
23. Osher, S., & Fedkiw, R. (2006). Level set methods and dynamic implicit surfaces (Vol. 153). Springer Science & Business Media.
24. Li, C., Xu, C., Gui, C., & Fox, M. D. (2005, June). Level set evolution without re-initialization: a new variational formulation. In *Computer Vision and Pattern Recognition*, 2005. CVPR 2005. IEEE Computer Society Conference ,Vol. 1, pp. 430–436.
25. Cremers, D., Rousson, M., & Deriche, R. (2007). A review of statistical approaches to level set segmentation: integrating color, texture, motion and shape. *International Journal of Computer Vision*, 72(2), 195–215.
26. Kass, M., Witkin, A., & Terzopoulos, D. (1987, June), Snakes: Active contour models. In *Proc. 1st Int. Conf. on Computer Vision* (Vol. 259, p. 268).
27. Zhu, C., Zou, B., Zhao, R., Cui, J., Duan, X., Chen, Z., & Liang, Y. (2017). Retinal vessel segmentation in colour fundus images using Extreme Learning Machine. Computerized Medical Imaging and Graphics, 55, 68–77.
28. Yazdanpanah, A., Hamarneh, G., Smith, B.R., & Sarunic, M.V. (2011). Segmentation of intra-retinal layers from optical coherence tomography images using an active contour approach. *IEEE Trans. Med. Imaging*, 30(2), 484–496.
29. Vermeer, K. A., Van der Schoot, J., Lemij, H. G., & De Boer, J. F. (2011). Automated segmentation by pixel classification of retinal layers in ophthalmic OCT images. *Biomedical optics express*, 2(6), 1743–1756.
30. Crandall, M.G., Ishii, H., & Lions, P.-L. (1992). User's guide to viscosity solutions of second order partial differential equations. *Bull. Amer. Math. Soc.* (N.S.), 27(1):1–67.

31. Luminita A.V. & Chan, T.F. (2002). A new multiphase level set framework for image segmentation via the Mumford and Shah model. *International Journal of Computer Vision*, 50(3):271–293.
32. Novosel, J., Vermeer, K. A., Thepass, G., Lemij, H. G., & Van Vliet, L. J. (2013, April). Loosely coupled level sets for retinal layer segmentation in optical coherence tomography. In *Biomedical Imaging (ISBI), 2013 IEEE 10th International Symposium on* (pp. 1010–1013). IEEE.
33. Mitiche, A., & Ayed, I. B. (2010). *Variational and level set methods in image segmentation* (Vol. 5). Springer Science & Business Media.
34. Novosel, J., Wang, Z., de Jong, H., van Velthoven, M., Vermeer, K. A., & van Vliet, L. J. (2016, April). Locally-adaptive loosely-coupled level sets for retinal layer and fluid segmentation in subjects with central serous retinopathy. In *Biomedical Imaging (ISBI), 2016 IEEE 13th International Symposium on* (pp. 702–705). IEEE.
35. Novosel, J. et al. (2015). Loosely coupled level sets for simultaneous 3d retinal layer segmentation in optical coherence tomography. *Med. Image Anal.*, 26, 146–158.
36. Vermeer, K.A. et al. (2014). Depth-resolved model-based reconstruction of attenuation coefficients in optical coherence tomography. *Biomed. Opt. Express*, 322–337.
37. Droske, M., Meyer, B., Rumpf, M., & Schaller, C. (2001, June). An adaptive level set method for medical image segmentation. In *Biennial International Conference on Information Processing in Medical Imaging* (pp. 416–422). Springer, Berlin, Heidelberg.
38. Zhao, Y. Q., Wang, X. H., Wang, X. F., & Shih, F. Y. (2014). Retinal vessels segmentation based on level set and region growing. *Pattern Recognition*, 47(7), 2437–2446.
39. Chunming Li (Li, C., Xu, C., Gui, C., & Fox, M. D. (2010). Distance regularized level set evolution and its application to image segmentation. *IEEE transactions on image processing*, 19(12), 3243–3254.
40. Zhao, Y., Rada, L., Chen, K., Harding, S. P., & Zheng, Y. (2015). Automated vessel segmentation using infinite perimeter active contour model with hybrid region information with application to retinal images. *IEEE Transactions on Medical Imaging*, 34(9), 1797–1807.
41. Zhang, Y., Matuszewski, B. J., Shark, L. K., & Moore, C. J. (2008, July). Medical image segmentation using new hybrid level-set method. In *BioMedical Visualization, 2008. MEDIVIS'08. Fifth International Conference* (pp. 71–76). IEEE.
42. Paragios, N., & Deriche, R. (2000, June). Coupled geodesic active regions for image segmentation: A level set approach. In *European Conference on Computer Vision* (pp. 224–240). Springer, Berlin, Heidelberg.
43. Wu, H., Geng, X., Zhang, X., Qiu, M., Jiang, K., Tang, L., & Dong, J. (2014). A self-adaptive distance regularized level set evolution method for optical disk segmentation. *Bio-medical Materials and Engineering*, 24(6), 3199–3206.
44. K. Zhang, L. Zhang, H. Song, and W. Zhou. (2010). Active contours with selective local or global segmentation: a new formulation and level set method. *Image and Vision Computing*, 28(4), 668–676.
45. Li, C., Kao, C.-Y., Gore, J.C., & Ding, Z. (2007). Implicit active contours driven by local binary fitting energy. In Proceedings of the IEEE Computer Society Conference on Computer Vision and Pattern Recognition (CVPR '07), Minneapolis, Minn, USA, June 2007.
46. Chen, G., Chen, M., Li, J., & Zhang, E. (2017). Retina image vessel segmentation using a hybrid CGLI level set method. *BioMed Research International*, 2017.

47. Chiu, S.J., Lokhnygina,Y., Dubis, A.M., Dubra, A., Carroll, J., Izatt, J.A., & Farsiu, S. (2013). Automatic cone photoreceptor segmentation using graph theory and dynamic programming. *Biomed. Opt. Express*, 4 (2013) 924–937.
48. Shi, F., Chen, X., Zhao, H., Zhu,W., Xiang, D., Gao, E., & Chen, H. (2015). Automated 3-D retinal layer segmentation of macular optical coherence tomography images with serous pigment epithelial detachments. *IEEE Trans. Med. Imaging*, 34 (2), 441–452.
49. Uji, A., Murakami, T., Unoki, N., Ogino, K., Horii, T., Yoshitake, S., & Yoshimura, N. (2014). Parallelism for quantitative image analysis of photoreceptor–retinal pigment epithelium complex alterations in diabetic macular edema parallelism in DME. *Invest. Ophthalmol. Vis. Sci.*, 55 (5), 3361–3367.
50. Wang,B., Zhang, Q., Lu, R., Zhi, Y. & Yao, X. (2014). Functional optical coherence tomography reveals transient phototropic change of photoreceptor outer segments. *Opt. Lett.*, 39 (24), 6923–6926.
51. Peng, D., Merriman, B., Osher, S., Zhao, H., & Kang, M. (1999). A PDE-based fast local level set method. *Journal of Computational Physics*, 155(2), 410–438.
52. Jia, Y., Bailey, S. T., Wilson, D. J., Tan, O., Klein, M. L., Flaxel, C. J., & Fujimoto, J. G. (2014). Quantitative optical coherence tomography angiography of choroidal neovascularization in age-related macular degeneration. *Ophthalmology*, 121(7), 1435–1444.
53. Hu, Z., Medioni, G.G., Hernandez, M., Hariri, A., Wu, X., & Sadda, S.R. (2013). Segmentation of the geographic atrophy in spectral-domain optical coherence tomography and fundus autofluorescence images geographic atrophy segmentation in SD-OCT and FAF images. *Invest. Ophthalmol. Vis. Sci.*, 54 (13), 8375–8383.
54. Chan, T. F., Sandberg, B. Y., & Vese, L. A. (2000). Active contours without edges for vector-valued images. *Journal of Visual Communication and Image Representation*, 11(2), 130–141.
55. Mohammad, F., Ansari, R., Wanek, J., Francis, A., & Shahidi, M. (2015). Feasibility of level-set analysis of enface OCT retinal images in diabetic retinopathy, *Biomed. Opt. Express*, 6(5), 1904–1918.
56. Al-Qunaieer, F. S., Tizhoosh, H. R., & Rahnamayan, S. (2011). Multi-resolution level set image segmentation using wavelets, *18th IEEE International Conference in Image Processing (ICIP)* (pp. 269–272).
57. He, L., Peng, Z., Everding, B., Wang, X., Han, C. Y., Weiss, K. L., & Wee, W. G. (2008). A comparative study of deformable contour methods on medical image segmentation, *Image and Vision Computing*, 26(2), 141–163.
58. Wei, Y., Xu, X. H., Jia, T., & Zhao, D. Z. (2006, October). An optimal level sets method for lung nodules detection in ct images. In *Intelligent Systems Design and Applications, 2006. ISDA'06. Sixth International Conference on* (Vol. 2, pp. 251–255). IEEE.
59. Pan, S., & Dawant, B.M. (2001). Automatic 3D segmentation of the liver from abdominal CT images: a level-set approach. In *Medical Imaging 2001, International Society for Optics and Photonics*, 2001, pp. 128–138.
60. Lei, Y., Shi, J., & Wu, J. (2017). Region-driven distance regularized level set evolution for change detection in remote sensing images. *Multimedia Tools and Applications*, 76(23), 24707–24722.
61. Rousson, M., & Deriche, R. (2002, December), A variational framework for active and adaptative segmentation of vector valued images. In *Motion and Video Computing, 2002. proceedings. workshop on* (pp. 56–61). IEEE.

62. K. Ni, X. Bresson, T. Chan, and S. Esedoglu. Local histogram based segmentation using the wasserstein distance August 2009, *International Journal of Computer Vision*, 84, 97–111.
63. Villani, C. (2003). Topics in optimal transportation (No. 58). American Mathematical Society.
64. Rabin, J., Delon, J., & Gousseau, Y. (2009). A statistical approach to the matching of local features. *SIAM Journal on Imaging Sciences*, 2(3), 931–958.
65. Delon, J. (2004). Midway image equalization. *Journal of Mathematical Imaging and Vision*, 21(2), 119–134.
66. Rabin, J., Peyré, G., Delon, J., & Bernot, M. (2011, May). Wasserstein barycenter and its application to texture mixing. In International *Conference on Scale Space and Variational Methods in Computer Vision* (pp. 435–446). Springer, Berlin, Heidelberg.
67. Xie, X., & Mirmehdi, M. (2011). Radial basis function based level set interpolation and evolution for deformable modelling. *Image and Vision Computing*, *29*(2-3), 167–177.
68. Li, C., Kao, C. Y., Gore, J. C., & Ding, Z. (2007). Implicit active contours driven by local binary fitting energy. Presented at the Comput. Vis. Pattern Recog.
69. Kaba, D., Wang, Y., Wang, C., Liu, X., Zhu, H., Salazar-Gonzalez, A.G., & Li, Y. (2015). Retina layer segmentation using kernel graph cuts and continuous maxflow, *Opt. Express*, 23 (6), 7366–7384.
70. Farsiu, S., Chiu, S. J., O'Connell, R. V., Folgar, F. A., Yuan, E., Izatt, J. A., & Toth, C. A. (2014). Quantitative classification of eyes with and without intermediate age-related macular degeneration using optical coherence tomography. *Ophthalmology*, 121(1), 162–172.
71. A.M. Andrew, Another efficient algorithm for convex hulls in two dimensions, *Inf. Process. Lett.*, 9 (5), (1979) 216–219.
72. Brown, K.Q. (1979). Voronoi diagrams from convex hulls, *Inf. Process. Lett.*, 9(5), 223–228, https://doi.org/10.1016/0020-0190(79)90074-7.
73. Mishra, A., Wong, A., Bizheva, K., & Clausi, D. A. (2009). Intra-retinal layer segmentation in optical coherence tomography images. *Optics Express*, 17(26), 23719–23728.
74. M.K. Garvin, M.D. Abramoff, X. Wu, S.R. Russell, T.L. Burns, & Sonka, M. (2009). Automated 3-D intraretinal layer segmentation of macular spectral domain optical coherence tomography images, *IEEE Trans. Med. Imaging*, 28 (9),1436–1447.
75. Duan, J., Tench, C., Gottlob, I., Proudlock, F., & Bai, L. (2016). Automated segmentation of retinal layers from optical coherent tomography images using geodesic distance. arXiv preprint arXiv:1609.02214.
76. Kafieh, R., Rabbani, H., Abramoff, M. D., & Sonka, M. (2013). Intra-retinal layer segmentation of 3D optical coherence tomography using coarse grained diffusion map. *Medical Image Analysis*, 17(8), 907–928.
77. G.B. Huang, Q.Y. Zhu, & Siew, C.K. (2006). Extreme learning machine: theory and applications. *Neurocomputing*, 70 (1), 489–501.
78. Shanmugam, V., & Banu, R. D. W. (2013, January). Retinal blood vessel segmentation using an extreme learning machine approach. In *Point-of-Care Healthcare Technologies (PHT), 2013 IEEE* (pp. 318–321). IEEE.
79. Yılmaz Kaya, L. K., & Tekin, R. (2013). A computer vision system for the automatic identification of butterfly species via gabor-filter-based texture features and extreme learning machine: GF+ ELM. *Tem Journal*, 13.

80. Chiu, S. J., Allingham, M. J., Mettu, P. S., Cousins, S. W., Izatt, J. A., & Farsiu, S. (2015). Kernel regression based segmentation of optical coherence tomography images with diabetic macular edema. *Biomedical Optics Express*, 6(4), 1172–1194.
81. Fuller, A., Zawadzki, R., Choi, S., Wiley, D., Werner, J., & Hamann, B. (2007). Segmentation of three-dimensional retinal image data. *IEEE Transactions on Visualization and Computer Graphics*, 13(6), 1719–1726.
82. Lang, A., Carass, A., Hauser, M., Sotirchos, E. S., Calabresi, P. A., Ying, H. S., & Prince, J. L. (2013). Retinal layer segmentation of macular OCT images using boundary classification. *Biomedical Optics Express*, 4(7), 1133–1152.
83. Garvin, M. K., Abràmoff, M. D., Kardon, R., Russell, S. R., Wu, X., & Sonka, M. (2008). Intraretinal layer segmentation of macular optical coherence tomography images using optimal 3-D graph search. *IEEE Transactions on Medical Imaging*, 27(10), 1495–1505.
84. Quellec, G., Lee, K., Dolejsi, M., Garvin, M. K., Abramoff, M. D., & Sonka, M. (2010). Three-dimensional analysis of retinal layer texture: identification of fluid-filled regions in SD-OCT of the macula. *IEEE Transactions on Medical Imaging*, 29(6), 1321–1330.
85. Kafieh, R., Rabbani, H., Hajizadeh, F., Abramoff, M. D., & Sonka, M. (2015). Thickness mapping of eleven retinal layers segmented using the diffusion maps method in normal eyes. *Journal of Ophthalmology*.
86. Caselles, V., Kimmel, R., & Sapiro, G. (1997). Geodesic active contours. In *Computer Vision, 1995. Proceedings. 5th International Conference on*, (pp. 694–699).
87. Caselles, V., Kimmel, R., & Sapiro, G. (1997, February). Geodesic active contours. *International Journal of Computer Vision*, 22(1):61–79.
88. Yezzi, A., Kichenassamy, S., Kumar, A., Olver, P., & Tannenbaum, A. (1997). A geometric snake model for segmentation of medical imagery. *IEEE Transactions on Medical Imaging*, 16(2), 199–209.
89. Kichenassamy, S., Kumar, A., Olver, P., Tannenbaum, A., & Yezzi, A. (1996). Conformal curvature flows: from phase transitions to active vision. *Archive for Rational Mechanics and Analysis*, 134(3), 275–301.
90. Läthén, G., Jonasson, J., & Borga, M. (2010). Blood vessel segmentationusing multi-scale quadrature filtering, *Pattern Recogn. Lett.*, 31, 762–767.
91. Kumar, A., Yezzi, A., Kichenassamy, S., Olver, P., & Tannenbaum, A. (1995, December). Active contours for visual tracking: a geometric gradient based approach. In *Decision and Control, 1995., Proceedings of the 34th IEEE Conference on* (Vol. 4, pp. 4041–4046). IEEE.
92. Yezzi, A. & Mennucci, A. (2005). Conformal metrics and true "gradient ž flows" for curves. *International Conference on Computer Vision*, 1, 913–919.
93. Solem, J. E., & Overgaard, N. C. (2005, April). A geometric formulation of gradient descent for variational problems with moving surfaces. In *International Conference on Scale-Space Theories in Computer Vision* (pp. 419–430). Springer, Berlin, Heidelberg.
94. M. Barchiesi, S. H. Kang, T. M. Le, M. Morini, and M. Ponsiglione, (2010). A variational model for infinite perimeter segmentations based on Lipschitz level set functions: Denoising while keeping finely oscillatory boundaries. *Multiscale Model. Sim.*, 8, 1715–1741.
95. Al-Diri, B., & Hunter, A. (2005). A ribbon of twins for extracting vessel boundaries, eprints.lincoln.ac.uk.

96. Lathen, G., Andersson, T., Lenz, R., & Borga, M. (2009, June). Momentum based optimization methods for level set segmentation. In *International Conference on Scale Space and Variational Methods in Computer Vision* (pp. 124–136). Springer, Berlin, Heidelberg.
97. Wang, C., Wang, Y. X., & Li, Y. (2017), Automatic choroidal layer segmentation using Markov random field and level set method. *IEEE journal of Biomedical and Health Informatics*, 21(6), 1694–1702.
98. Bai, F., Gibson, S. J., Marques, M. J., & Podoleanu, A. (2018, March). Superpixel guided active contour segmentation of retinal layers in OCT volumes. In *2nd Canterbury Conference on OCT with Emphasis on Broadband Optical Sources* (Vol. 10591, p. 1059106). International Society for Optics and Photonics.

6

Numerical Techniques for Level Set Models: an Image Segmentation Perspective

1. L. Alvarez, F. Guichard, P. L. Lions, J. M. Morel, *Axioms and Fundamental Equations of Image Processing*, Arch. for Rational Mechanics, *Arch. for Rational Mechanics*, 123, 199–257 (1993).
2. L. Alvarez, P. L. Lions, J. M. Morel, *Image selective smoothing and edge detection by nonlinear diffusion*, SIAM J. Num. Anal., 29, 845–866 (1992).
3. G. Barles, P.E. Souganidis, *Convergence of approximation schemes for fully nonlinear second-order equations* , Asymp. Anal., 4, 271–283 (1991).
4. E. Carlini, M. Falcone, R. Ferretti, *Convergence of a large time-step scheme for mean curvature motion*, Interfaces and free boundaries, 12, 409–441 (2010).
5. E. Carlini, R. Ferretti, *A semi-Lagrangian approximation for the AMSS model of image processing*, Appl. Num. Math., 73, 16-32 (2013).
6. E. Carlini, R. Ferretti, *A semi-Lagrangian scheme with radial basis approximation for surface reconstruction*, Comput. Vis. Sci. 18 , no. 2-3, 103–112 (2017).
7. V. Caselles, F. Catté, T. Coll, F. Dibos, *A geometric model for active contours in image processing*, Num. Math., 66, 1–31 (1993).
8. V. Caselles, R. Kimmel, G. Sapiro, *Geodesic active contours*, International Journal of Computer Vision, 22, 61–79 (1997).
9. T. Chan, L. Vese, *Active contours without edges*, IEEE Transactions on Image Processing, 10, 266–277 (2001).
10. Y. G. Chen, Y. Giga, S. Goto, *Uniqueness and existence of viscosity solutions of generalized mean curvature flow equation*, J. Diff. Geom, 33, 749–786 (1991).
11. M.G. Crandall, P.L. Lions, *Two approximations of solutions of Hamilton–Jacobi equations*, Math. Comp., 43, 1–19, (1984).
12. J.D. Durou, M. Falcone, M. Sagona, *Numerical Methods for Shape from Shading: a new survey with benchmarks*, Computer Vision and Image Understanding, Elsevier, 109, 22–43 (2008).
13. L.C. Evans, J. Spruck, *Motion of level sets by mean curvature*, I. J. Diff. Geom, 33, 635–681 (1991).
14. M. Falcone, R. Ferretti, Semi-Lagrangian Approximation Schemes for Linear and Hamilton-Jacobi Equations, SIAM, 2013.
15. J. H. Jørgensen. Tomobox, MATLAB Central File Exchange, Retrieved Aug 17, 2010.
16. M. Kass, A. Witkin, D. Terzopoulos. *Snakes: active contour models*, International Journal of Computer Vision, 1, 321–331 (1988).

17. R. Kohn, S. Serfaty, *A deterministic-control-based approach to motion by curvature*, Comm. Pure Appl. Math., 59, 344–407 (2006).
18. R. Malladi, J.A. Sethian, B.C. Vemuri, *A topology independent shape modeling scheme*, in Proc. SPIE Conf. Geometric Methods Computer Vision II, vol. 2031, 246–258 (1993).
19. D. Mumford, J. Shah, *Optimal Approximations by Piecewise Smooth Functions and Associated Variational Problems*, Comm. on Pure and Appl. Math., 42, 577–685 (1989).
20. S. J. Osher, R. P. Fedkiw, Level Set Methods and Dynamic Implicit Surfaces, Applied Mathematical Sciences, 153, Springer-Verlag, New York, (2003).
21. S. J. Osher, J. A. Sethian, *Front propagating with curvature-dependent speed: algorithms based on Hamilton–Jacobi formulation*. J. of Comp. Physics, 79, 12–49 (1988).
22. J. A. Sethian, Level Set Methods and Fast Marching Methods: Evolving Interfaces in Computational Geometry, Fluid Mechanics, Computer Vision, and Materials Science, Cambridge University Press, Cambridge Monograph on Applied and Computational Mathematics, (1999).
23. C.-W. Shu, *High order numerical methods for time dependent Hamilton-Jacobi equations*, in Mathematics and Computation in Imaging Science and Information Processing, S.S. Goh, A. Ron and Z. Shen, eds, Lecture Notes Series, Institute for Mathematical Sciences, National University of Singapore, vol. 11, World Scientific Press, Singapore, 47–91 (2007).
24. L. Vese, T. Chan, *A multiphase level set framework for image segmentation using the Mumford and Shah model*, Int. J. of Comp. Vision., 50, 271–293 (2002).
25. H. Zhao, T. Chan, B. Merriman, S. J. Osher, *A Variational Level Set Approach to Multiphase Motion*, J. of Comp. Physics, 127, 179–195 (1996).
26. H. Zhao, S. J. Osher, B. Merriman, M. Kang, *Implicit and nonparametric shape reconstruction from unorganized points using variational level set method*, Comput. Vis. Image Underst., 80, 295–319 (2000).

7

Level Set Methods for Cardiac Segmentation in MSCT Images

1. A. Frangi, D. Rueckert, and J. Duncan, "Three–dimensional cardiovascular image analysis," *IEEE Transactions on Medical Imaging*, vol. 21, no. 9, pp. 1005–1010, 2002.
2. M. Erdt, S. Steger, and G. Sakas, "Regmentation: A new view of image segmentation and registration," *Journal of Radiation Oncology Informatics*, vol. 4, no. 1, pp. 1–23, 2012.
3. D. L. Pham, C. Xu, and J. L. Prince, "Current methods in medical image segmentation 1," *Annual Review of Biomedical Engineering*, vol. 2, no. 1, pp. 315–337, 2000.
4. O. Ecabert, J. Peters, J. Weese, C. Lorenz, J. von Berg, M. Walker, M. Olszewski, and M. Vembar, "Automatic heart segmentation in ct: current and future applications," *MedicaMundi*, vol. 50, no. 3, pp. 12–17, 2006.
5. J. Fleureau, M. Garreau, A. Hernandez, A. Simon, and D. Boulmier, "Multi–object and N–D segmentation of cardiac MSCT data using SVM classifiers and a connectivity algorithm," *Computers in Cardiology*, vol. 33, no. 1, pp. 817–820, 2006.
6. A. Bravo, M. Vera, M. Garreau, and R. Medina, "Three–dimensional segmentation of ventricular heart chambers from multi–*slice* computerized tomography: An hybrid approach," in *DICTAP*, ser. CCIS. Springer, 2011, vol. 166, pp. 287–301.
7. G. Mühlenbruch, M. Das, C. Hohl, J. E. Wildberger, D. Rinck, T. G. Flohr, R. Koos, C. Knackstedt, R. W. Günther, and A. H. Mahnken, "Global left ventricular function in cardiac ct. evaluation of an automated 3d region-growing segmentation algorithm," *European Radiology*, vol. 16, no. 5, pp. 1117–1123, 2006.
8. M. L. Chuang, P. Gona, G. L. Hautvast, C. J. Salton, S. J. Blease, S. B. Yeon, M. Breeuwer, C. J. O'Donnell, and W. J. Manning, "Left ventricular trabeculae and papillary muscles: Correlation with clinical and cardiac characteristics and impact on cardiovascular magnetic resonance measures of left ventricular anatomy and function," *JACC. Cardiovascular Imaging*, vol. 5, no. 11, p. 1115, 2012.
9. O. Ecabert, J. Peters, H. Schramm, C. Lorenz, J. von Berg, M. Walker, M. Vembar, M. Olszewski, K. Subramanyan, G. Lavi, and J. Weese, "Automatic model–based segmentation of the heart in CT images," *IEEE Transactions on Medical Imaging*, vol. 27, no. 9, pp. 1189–1201, 2008.
10. H. Zhang, A. Wahle, R. Johnson, T. Scholz, and M. Sonka, "4-D cardiac MR image analysis: Left and right ventricular morphology and function," *IEEE Transactions on Medical Imaging*, vol. 29, no. 2, pp. 350–364, 2010.

11. H. Assen, M. Danilouchkine, M. Dirksen, J. Reiber, and B. Lelieveldt, "A 3-D active shape model driven by fuzzy inference: Aplication to cardiac CT and MR," *IEEE Transactions on Information Technology in Biomedicine*, vol. 12, no. 5, pp. 595–605, 2008.
12. H. Kirisli, M. Schaap, S. Klein, L. Neefjes, A. Weustink, T. V. Walsum, and W. Niessen, "Fully automatic cardiac segmentation from 3-D CTA data: a multi–atlas based approach," *Proceedings of SPIE Medical Imaging*, vol. 7623, no. 1, pp. 5–9, 2010.
13. Y. Zheng, A. Barbu, B. Georgescu, M. Scheuering, and D. Comaniciu, "Four–chamber heart modeling and automatic segmentation for 3-D cardiac CT volumes using marginal space learning and steerable features," *IEEE Transactions on Medical Imaging*, vol. 27, no. 11, pp. 1668–1681, 2008.
14. M. Lynch, O. Ghita, and P. Whelan, "Segmentation of the left ventricle of the heart in 3-D MRI data using an optimized nonrigid temporal model," *IEEE Transactions on Medical Imaging*, vol. 27, no. 2, pp. 195–203, 2008.
15. P. Yushkevich, J. Piven, H. Cody, S. Ho, J. Gee, and G. Gerig, "User–guided level set segmentation of anatomical structures with ITK–SNAP," *Insight Journal*, vol. 1, pp. 252–264, 2005, special Issue on ISC/NA-MIC/MICCAI Workshop on Open-Source Software.
16. E. Heiberg, L. Wigstrom, M. Carlsson, A. Bolger, and M. Karlsson, "Time resolved three-dimensional automated segmentation of the left ventricle," in *proceedings of IEEE Computers In Cardiology*, vol. 32, Lyon, France, 2005, pp. 559–602.
17. I. Dydenko, F. Jamal, O. Bernard, J. Dhooge, I. Magnin, and D. Friboulet, "A level set framework with a shape and motion prior for segmentation and region tracking in echocardiography," *Medical Image Analysis*, vol. 10, no. 1, pp. 38–59, 2006.
18. W. Bai, W. Shi, D. P. O'Regan, T. Tong, H. Wang, S. Jamil-Copley, N. S. Peters, and D. Rueckert, "A probabilistic patch-based label fusion model for multi-atlas segmentation with registration refinement: application to cardiac mr images," *IEEE Transactions on Medical Imaging*, vol. 32, no. 7, pp. 1302–1315, 2013.
19. V. Caselles, R. Kimmel, and G. Sapiro, "Geodesic active contours," *International Journal of Computer Vision*, vol. 22, no. 1, pp. 61–79, 1997.
20. S. Zhu and A. Yuille, "Region competition: Unifying snakes, region growing, and Bayes–MDL for multiband image segmentation," *IEEE Transactions on Pattern Analysis and Machine Intelligence*, vol. 18, no. 9, pp. 884–900, 1996.
21. S. Lankton and A. Tannenbaum, "Localizing region-based active contours," *IEEE Transactions on Image Processing*, no. 11, pp. 2029–2039, 2008.
22. T. Chan and L. Vese., "Active contours without edges," *IEEE Transactions on Image Processing*, vol. 10, no. 2, pp. 266–277, 2001.
23. O. Bernard, D. Friboulet, P. Thevenaz, and M. Unser, "Variational b-spline level-set: A linear filtering approach for fast deformable model evolution," *Image Processing, IEEE Transactions on*, vol. 18, no. 6, pp. 1179–1191, June 2009.
24. S. C. Zhu and A. Yuille, "Region competition: Unifying snakes, region growing, and bayes–mdl for multiband image segmentation," *IEEE Transactions on Pattern Analysis and Machine Intelligence*, vol. 18, no. 9, pp. 884–900, 1996.
25. Y. Shi and W. Karl, "A real-time algorithm for the approximation of level-set-based curve evolution," *IEEE Transactions on Image Processing*, vol. 17, no. 5, pp. 645–656, May 2008.

26. T. Dietenbeck, M. Alessandrini, D. Friboulet, and O. Bernard, "Creaseg: A free software for the evaluation of image segmentation algorithms based on level-set," in *Image Processing (ICIP), 2010 17th IEEE International Conference on*, Sept 2010, pp. 665–668.
27. S. Osher and J. Sethian, "Fronts propagating with curvature dependent speed: algorithms based on hamilton–jacobi formulations," *Computational Physics*, vol. 1, pp. 17–33, 1988.
28. R. Tsai and S. Osher, "Review article: Level set methods and their applications in image science," *Commun. Math. Sci.*, vol. 1, no. 4, pp. 1–20, 12 2003. [Online]. Available: http://projecteuclid.org/euclid.cms/1119655349
29. J. A. Sethian, "A fast marching level set method for monotonically advancing fronts," *Proceedings of the National Academy of Sciences*, vol. 93, no. 4, pp. 1591–1595, 1996.
30. R. Malladi and J. A. Sethian, "An o (n log n) algorithm for shape modeling," *Proceedings of the National Academy of Sciences*, vol. 93, no. 18, pp. 9389–9392, 1996.
31. L. Ibañez, "The ITK Software Guide," Kitware Inc., Tech. Rep., July 2005.
32. M. Kass, A. Witkin, and D. Terzopoulos, "Snakes: Active contour models," *International Journal of Computer Vision*, vol. 1, no. 4, pp. 321–331, 1988.
33. D. Adalstein and J. Sethian, "A fast level set method for propagating interfaces," *Computational Physics*, vol. 1, pp. 269–277, 1995.
34. J. Yezzi, A. Tsai, and A.Willsky, "A fully global approach to image segmentation via coupled curve evolution equations," *Journal of Visual Communications and Image Representations*, vol. 13, no. 1, pp. 195–216, 2002.
35. A. Bhattacharyya, "On a measure of divergence between two statistical populations defined by their probability distributions," *Bull. Calcutta Mathematical Society*, vol. 35, pp. 99–110, 1943.
36. J. Sethian, *Level set methods and Fast marching methods*. New York, USA: Springer, 1999.
37. G. Aubert, M. Barlaud, O. Faugeras, and S. Jehan-Besson, "Image segmentation using active contours: Calculus of variations or shape gradients?" *SIAM Journal on Applied Mathematics*, vol. 63, no. 6, pp. 2128–2154, 2003.
38. C. Li, C. Xu, J. C. Gore, and Z. Ding, "Minimization of region-scalable fitting energy for image segmentation," *IEEE Transactions on Image Processing*, vol. 17, no. 10, pp. 1940–1949, 2008.
39. C. Li, C.-Y. Kao, C. Gui, and M. D. Fox, "Distance regularized level set evolution and its application to image segmentation," *IEEE Transactions on Image Processing*, vol. 19, no. 12, pp. 3243–3254, 2010.
40. R. Whitaker, "A level-set approach to 3-D reconstruction from range data," *International Journal of Computer Vision*, vol. 29, no. 3, pp. 203–231, 1998.
41. T. Yoo, *Insight into Images Principles and Practice for Segmentation, Registration, and Image Analysis: A companion to the Insight Toolkit*. MA, USA: AK Peters, 2004.
42. T. S. Yoo, M. J. Ackerman, W. E. Lorensen, W. Schroeder, V. Chalana, S. Aylward, D. Metaxas, and R. Whitaker, "Engineering and algorithm design for an image processing api: a technical report on itk-the insight toolkit," *Studies in Health Technology and Informatics*, pp. 586–592, 2002.

43. A. E. Lefohn, J. M. Kniss, C. D. Hansen, and R. T. Whitaker, "A streaming narrowband algorithm: interactive computation and visualization of level sets," *IEEE Transactions on Visualization and Computer Graphics*, vol. 10, no. 4, pp. 422–433, July 2004.
44. S. Lankton, "Sparse field methods-technical report," *Georgia Institute of Technology*, 2009.
45. R. Medina, S. Bautista, and V. Morocho, "Accuracy of connected confidence left ventricle segmentation in 3-d multi-slice computerized tomography images," in *2017 IEEE Second Ecuador Technical Chapters Meeting (ETCM)*, Oct 2017, pp. 1–6.
46. R. Medina, S. Bautista, P. Vanegas, and V. Morocho, "Left ventricle myocardium segmentation in multi-slice computerized tomography," in *IEEE proceedings of ANDESCON–2016*. IEEE, 2016, pp. 1–4.
47. C. Tsiotsios and M. Petrou, "On the choice of the parameters for anisotropic diffusion in image processing," *Pattern Recognition*, vol. 46, no. 5, pp. 1369–1381, 2013.
48. P. Perona and J. Malik, "Scale-space and edge detection using anisotropic diffusion," *IEEE Transactions on Pattern Analysis and Machine Intelligence*, vol. 12, no. 7, pp. 629–639, 1990.
49. R. Cárdenes, R. de Luis-García, and M. Bach-Cuadra, "A multidimensional segmentation evaluation for medical image data," *Computer Methods and Programs in Biomedicine*, vol. 96, no. 2, pp. 108–124, 2009.
50. A. A. Taha and A. Hanbury, "Metrics for evaluating 3d medical image segmentation: analysis, selection, and tool," *BMC Medical Imaging*, vol. 15, no. 1, pp. 1–29, 2015.
51. K. Babalola, B. Patenaude, P. Aljabar, J. Schnabel, D. Kennedy, W. Crum, S. Smith, T. Cootes, M. Jenkinson, and D. Rueckert, "Comparison and evaluation of segmentation techniques for subcortical structures in brain mri," in *Medical Image Computing and Computer-Assisted Intervention – MICCAI 2008*, ser. Lecture Notes in Computer Science, D. Metaxas, L. Axel, G. Fichtinger, and G. Székely, Eds. Springer Berlin Heidelberg, 2008, vol. 5241, pp. 409–416. [Online]. Available: http://dx.doi.org/10.1007/978-3-540-85988-8_49
52. J. A. Sethian, *Level set methods and fast marching methods: evolving interfaces in computational geometry, fluid mechanics, computer vision, and materials science*. Cambridge University Press, 1999, vol. 3.
53. P. R. Bai, Q. Y. Liu, L. Li, S. H. Teng, J. Li, and M. Y. Cao, "A novel region-based level set method initialized with mean shift clustering for automated medical image segmentation," *Computers in Biology and Medicine*, vol. 43, no. 11, pp. 1827–1832, 2013.
54. J. Huang, F. Jian, H. Wu, and H. Li, "An improved level set method for vertebra ct image segmentation," *Biomedical Engineering Online*, vol. 12, no. 1, p. 48, 2013.
55. X. Jiang, Z. Zhou, X. Ding, X. Deng, L. Zou, and B. Li, "Level set based hippocampus segmentation in mr images with improved initialization using region growing," *Computational and Mathematical Methods in Medicine*, vol. 2017, Article ID 5256346, pp. 1–11, 2017.
56. A. Masood, A. A. Al-Jumaily, and Y. Maali, "Level set initialization based on modified fuzzy c means thresholding for automated segmentation of skin lesions," in *International Conference on Neural Information Processing*. Springer, 2013, pp. 341–351.

57. R. Medina, A. La Cruz, A. Ordoñes, D. Pesántez, V. Morocho, and P. Vanegas, "Level set algorithms comparison for multi-slice ct left ventricle segmentation," in *11th International Symposium on Medical Information Processing and Analysis*, vol. 9681. International Society for Optics and Photonics, 2015, p. 96810O.
58. L. Wang, T. Chitiboi, H. Meine, M. Günther, and H. K. Hahn, "Principles and methods for automatic and semi-automatic tissue segmentation in mri data," *Magnetic Resonance Materials in Physics, Biology and Medicine*, vol. 29, no. 2, pp. 95–110, 2016.
59. M. Lynch, O. Ghita, and P. F. Whelan, "Segmentation of the left ventricle of the heart in 3-d+ t mri data using an optimized nonrigid temporal model," *IEEE Transactions on Medical Imaging*, vol. 27, no. 2, pp. 195–203, 2008.
60. C. Petitjean and J.-N. Dacher, "A review of segmentation methods in short axis cardiac mr images," *Medical Image Analysis*, vol. 15, no. 2, pp. 169–184, 2011.
61. M. Avendi, A. Kheradvar, and H. Jafarkhani, "A combined deep-learning and deformable-model approach to fully automatic segmentation of the left ventricle in cardiac mri," *Medical Image Analysis*, vol. 30, pp. 108–119, 2016.
62. A. Tsai, A. Yezzi, W. Wells, C. Tempany, D. Tucker, A. Fan, W. E. Grimson, and A. Willsky, "A shape-based approach to the segmentation of medical imagery using level sets," *IEEE Transactions on Medical Imaging*, vol. 22, no. 2, pp. 137–154, 2003.
63. A. Yezzi, A. Tsai, and A. Willsky, "A statistical approach to snakes for bimodal and trimodal imagery," in *Computer Vision, 1999. The Proceedings of the Seventh IEEE International Conference on*, vol. 2. IEEE, 1999, pp. 898–903.
64. P.-E. Danielsson, "Euclidean distance mapping," *Computer Graphics and Image Processing*, vol. 14, no. 3, pp. 227–248, 1980.
65. W. H. Kruskal and W. A. Wallis, "Use of ranks in one-criterion variance analysis," *Journal of the American Statistical Association*, vol. 47, no. 260, pp. 583–621, 1952.
66. W. J. Schroeder, L. S. Avila, and W. Hoffman, "Visualizing with vtk: a tutorial," *Computer Graphics and Applications, IEEE*, vol. 20, no. 5, pp. 20–27, 2000.
67. S. G. Myerson, H. E. Montgomery, D. J. Pennell *et al.*, "Left ventricular mass reliability of m-mode and 2-dimensional echocardiographic formulas," *Hypertension*, vol. 40, no. 5, pp. 673–678, 2002.
68. M. Foppa, B. B. Duncan, and L. E. Rohde, "Echocardiography-based left ventricular mass estimation. how should we define hypertrophy?" *Cardiovascular Ultrasound*, vol. 3, no. 1, p. 1, 2005.

8

Deformable Models and Image Segmentation

1. N. Sharma and L. M. Aggarwal,"Automated medical image segmentation techniques," *Journal of Medical Physics/Association of Medical Physicists of India*, vol. 35, no. 1, p. 3, 2010.
2. E. R. Hancock and J. Kittler, "Edge-labeling using dictionary-based relaxation," *IEEE Transactions on Pattern Analysis & Machine Intelligence*, no. 2, pp. 165–181, 1990.
3. Y.-T. Liow, "A contour tracing algorithm that preserves common boundaries between regions," *CVGIP: Image Understanding*, vol. 53, no. 3, pp. 313–321, 1991.
4. T. Law, H. Itoh, and H. Seki, "Image filtering, edge detection, and edge tracing using fuzzy reasoning," *IEEE Transactions on Pattern Analysis & Machine Intelligence*, no. 5, pp. 481–491, 1996.
5. H. Ney, "A comparative study of two search strategies for connected word recognition: Dynamic programming and heuristic search," *IEEE Transactions on Pattern Analysis & Machine Intelligence*, no. 5, pp. 586–595, 1992.
6. E. Oja and L. Xu, "Randomized Hough transform (RHT): basic mechanisms, algorithms, and computational complexities," *CVGIP: Image Understanding*, vol. 57, no. 2, pp. 131–154, 1993.
7. H. Kalviainen, P. Hirvonen, L. Xu, and E. Oja, "Probabilistic and non-probabilistic Hough transforms: overview and comparisons," *Image and Vision Computing*, vol. 13, no. 4, pp. 239–252, 1995.
8. H. T. Nguyen, M. Worring, and R. Van Den Boomgaard, "Watersnakes: Energy-driven watershed segmentation," *IEEE Transactions on Pattern Analysis and Machine Intelligence*, vol. 25, no. 3, pp. 330–342, 2003.
9. L. Najman and M. Schmitt, "Geodesic saliency of watershed contours and hierarchical segmentation," *IEEE Transactions on Pattern Analysis and Machine Intelligence*, vol. 18, no. 12, pp. 1163–1173, 1996.
10. A. M. López, F. Lumbreras, J. Serrat, and J. J. Villanueva, "Evaluation of methods for ridge and valley detection," *IEEE Transactions on Pattern Analysis and Machine Intelligence*, vol. 21, no. 4, pp. 327–335, 1999.
11. M. Kass, A. Witkin, and D. Terzopoulos, "Snakes: Active contour models," *International Journal of Computer Vision*, vol. 1, no. 4, pp. 321–331, 1988.
12. S. Osher and J. A. Sethian, "Fronts propagating with curvature-dependent speed: algorithms based on Hamilton-Jacobi formulations," *Journal of Computational Physics*, vol. 79, no. 1, pp. 12–49, 1988.
13. V. Caselles, R. Kimmel, and G. Sapiro, "Geodesic active contours," *International Journal of Computer Vision*, vol. 22, no. 1, pp. 61–79, 1997.

14. C. Xu, A. Yezzi, and J. L. Prince, "On the relationship between parametric and geometric active contours," in *Signals, Systems and Computers, 2000. Conference Record of the Thirty-Fourth Asilomar Conference on*, 2000, vol. 1, pp. 483–489: IEEE.
15. R. Malladi, J. A. Sethian, and B. C. Vemuri, "Shape modeling with front propagation: A level set approach," *IEEE transactions on pattern analysis and machine intelligence*, vol. 17, no. 2, pp. 158–175, 1995.
16. A. Chakraborty, L. H. Staib, and J. S. Duncan, "Deformable boundary finding in medical images by integrating gradient and region information," *IEEE Transactions on Medical Imaging*, vol. 15, no. 6, pp. 859–870, 1996.
17. J. A. Sethian, *Level set methods and fast marching methods: evolving interfaces in computational geometry, fluid mechanics, computer vision, and materials science*. Cambridge University Press, 1999.
18. G. Sapiro, *Geometric partial differential equations and image analysis*. Cambridge university press, 2006.
19. L. H. Staib and J. S. Duncan, "Boundary finding with parametrically deformable models," *IEEE Transactions on Pattern Analysis & Machine Intelligence*, no. 11, pp. 1061–1075, 1992.
20. J. J. Koenderink and A. J. Van Doorn, "Surface shape and curvature scales," *Image and Vision Computing*, vol. 10, no. 8, pp. 557–564, 1992.
21. R. Kimmel, "Intrinsic scale space for images on surfaces: The geodesic curvature flow," in *International Conference on Scale-Space Theories in Computer Vision*, 1997, pp. 212–223: Springer.
22. G. Tryggvason *et al.*, "A front-tracking method for the computations of multiphase flow," *Journal of Computational Physics*, vol. 169, no. 2, pp. 708–759, 2001.
23. S. Osher and N. Paragios, *Geometric level set methods in imaging, vision, and graphics*. Springer Science & Business Media, 2003.
24. S. Osher and R. Fedkiw, *Level set methods and dynamic implicit surfaces*. Springer Science & Business Media, 2006.
25. J. C. Strikwerda, *Finite difference schemes and partial differential equations*. Siam, 2004.
26. A. Harten, B. Engquist, S. Osher, and S. R. Chakravarthy, "Uniformly high order accurate essentially non-oscillatory schemes, III," in *Upwind and high-resolution schemes*: Springer, 1987, pp. 218–290.
27. C.-W. Shu and S. Osher, "Efficient implementation of essentially non-oscillatory shock-capturing schemes," *Journal of Computational Physics*, vol. 77, no. 2, pp. 439–471, 1988.
28. C.-W. Shu and S. Osher, "Efficient implementation of essentially non-oscillatory shock-capturing schemes, II," in *Upwind and High-Resolution Schemes*: Springer, 1989, pp. 328–374.
29. L. M. Milne-Thomson, *The calculus of finite differences*. American Mathematical Soc., 2000.
30. X.-D. Liu, S. Osher, and T. Chan, "Weighted essentially non-oscillatory schemes," *Journal of Computational Physics*, vol. 115, no. 1, pp. 200–212, 1994.
31. G.-S. Jiang and C.-W. Shu, "Efficient implementation of weighted ENO schemes," *Journal of Computational Physics*, vol. 126, no. 1, pp. 202–228, 1996.
32. G.-S. Jiang and D. Peng, "Weighted ENO schemes for Hamilton–Jacobi equations," *SIAM Journal on Scientific Computing*, vol. 21, no. 6, pp. 2126–2143, 2000.

33. R. P. Fedkiw, B. Merriman, and S. Osher, "Simplified discretization of systems of hyperbolic conservation laws containing advection equations," *Journal of Computational Physics*, vol. 157, no. 1, pp. 302–326, 2000.
34. C. Hu and C.-W. Shu, "Weighted essentially non-oscillatory schemes on triangular meshes," *Journal of Computational Physics*, vol. 150, no. 1, pp. 97–127, 1999.
35. R. J. Spiteri and S. J. Ruuth, "A new class of optimal high-order strong-stability-preserving time discretization methods," *SIAM Journal on Numerical Analysis*, vol. 40, no. 2, pp. 469–491, 2002.
36. M. G. Crandall and P.-L. Lions, "Two Approximations of Solutions of Hamilton-Jacobi Equations," WISCONSIN UNIV-MADISON MATHEMATICS RESEARCH CENTER1982.
37. S. Osher and C.-W. Shu, "High-order essentially nonoscillatory schemes for Hamilton–Jacobi equations," *SIAM Journal on Numerical Analysis*, vol. 28, no. 4, pp. 907–922, 1991.
38. S. Godunov, "A finite difference method for the computation of discontinuous solutions of the equations of fluid dynamics," *Sbornik: Mathematics*, vol. 47, no. 8–9, pp. 357–393, 1959.
39. M. Bardi and S. Osher, "The nonconvex multidimensional Riemann problem for Hamilton–Jacobi equations," *SIAM Journal on Mathematical Analysis*, vol. 22, no. 2, pp. 344–351, 1991.
40. O. P. Agrawal, "Formulation of Euler–Lagrange equations for fractional variational problems," *Journal of Mathematical Analysis and Applications*, vol. 272, no. 1, pp. 368–379, 2002.
41. M. Sussman, P. Smereka, and S. Osher, "A level set approach for computing solutions to incompressible two-phase flow," *Journal of Computational Physics*, vol. 114, no. 1, pp. 146–159, 1994.
42. D. L. Chopp, "Computing minimal surfaces via level set curvature flow," 1991.
43. D. Adalsteinsson and J. A. Sethian, "A fast level set method for propagating interfaces," *Journal of Computational Physics*, vol. 118, no. 2, pp. 269–277, 1995.
44. R. Goldenberg, R. Kimmel, E. Rivlin, and M. Rudzsky, "Fast geodesic active contours," *IEEE Transactions on Image Processing*, vol. 10, no. 10, pp. 1467–1475, 2001.
45. S. Kichenassamy, A. Kumar, P. Olver, A. Tannenbaum, and A. Yezzi, "Conformal curvature flows: from phase transitions to active vision," *Archive for Rational Mechanics and Analysis*, vol. 134, no. 3, pp. 275–301, 1996.
46. X. Bresson, S. Esedoḡlu, P. Vandergheynst, J.-P. Thiran, and S. Osher, "Fast global minimization of the active contour/snake model," *Journal of Mathematical Imaging and Vision*, vol. 28, no. 2, pp. 151–167, 2007.
47. N. Paragyios, O. Mellina-Gottardo, and V. Ramesh, "Gradient vector flow fast geodesic active contour," ed: Google Patents, 2003.
48. C. Xu and J. L. Prince, "Generalized gradient vector flow external forces for active contours1," *Signal Processing*, vol. 71, no. 2, pp. 131–139, 1998.
49. T. F. Chan and L. A. Vese, "Active contours without edges," *IEEE Transactions on Image Processing*, vol. 10, no. 2, pp. 266–277, 2001.
50. D. Mumford and J. Shah, "Optimal approximations by piecewise smooth functions and associated variational problems," *Communications on pure and Applied Mathematics*, vol. 42, no. 5, pp. 577–685, 1989.

51. A. Chambolle, "An algorithm for total variation minimization and applications," *Journal of Mathematical Imaging and Vision*, vol. 20, no. 1–2, pp. 89–97, 2004.
52. A. S. El-Baz, A. A. Farag, H. A. El Munim, and S. E. Yuksel, "Level set segmentation using statistical shape priors," in *Computer Vision and Pattern Recognition Workshop, 2006. CVPRW'06. Conference on*, 2006, pp. 78–78: IEEE.
53. A. El-Baz and G. Gimel'farb, "Image segmentation with a parametric deformable model using shape and appearance priors," in *Computer Vision and Pattern Recognition, 2008. CVPR 2008. IEEE Conference on*, 2008, pp. 1–8: IEEE.
54. D. Jayadevappa, S. Srinivas Kumar, and D. Murty, "Medical image segmentation algorithms using deformable models: a review," *IETE Technical Review*, vol. 28, no. 3, pp. 248–255, 2011.
55. L. He *et al.*, "A comparative study of deformable contour methods on medical image segmentation," *Image and Vision Computing*, vol. 26, no. 2, pp. 141–163, 2008.
56. A. Tsai *et al.*, "A shape-based approach to the segmentation of medical imagery using level sets," *IEEE Transactions on Medical Imaging*, vol. 22, no. 2, pp. 137–154, 2003.
57. C. Pluempitiwiriyawej, J. M. Moura, Y.-J. L. Wu, and C. Ho, "STACS: New active contour scheme for cardiac MR image segmentation," *IEEE transactions on Medical Imaging*, vol. 24, no. 5, pp. 593–603, 2005.
58. J. Montagnat and H. Delingette, "4D deformable models with temporal constraints: application to 4D cardiac image segmentation," *Medical Image Analysis*, vol. 9, no. 1, pp. 87–100, 2005.
59. F. Khalifa, G. Beache, A. El-Baz, and G. Gimel'farb, "Deformable model guided by stochastic speed with application in cine images segmentation," in *Image Processing (ICIP), 2010 17th IEEE International Conference on*, 2010, pp. 1725–1728: IEEE.
60. F. Khalifa, G. M. Beache, G. Gimel'farb, and A. El-Baz, "A novel approach for accurate estimation of left ventricle global indexes from short-axis cine MRI," in *Image Processing (ICIP), 2011 18th IEEE International Conference on*, 2011, pp. 2645–2648: IEEE.
61. F. Khalifa, G. M. Beache, M. Nitzken, G. Gimel'Farb, G. Giridharan, and A. El-Baz, "Automatic analysis of left ventricle wall thickness using short-axis cine CMR images," in *Biomedical Imaging: From Nano to Macro, 2011 IEEE International Symposium on*, 2011, pp. 1306–1309: IEEE.
62. M. G. Uzunbaş, S. Zhang, K. M. Pohl, D. Metaxas, and L. Axel, "Segmentation of myocardium using deformable regions and graph cuts," in *Biomedical Imaging (ISBI), 2012 9th IEEE International Symposium on*, 2012, pp. 254–257: IEEE.
63. F. Khalifa, G. M. Beache, G. Gimelrfarb, G. A. Giridharan, and A. El-Baz, "Accurate automatic analysis of cardiac cine images," *IEEE Transactions on Biomedical Engineering*, vol. 59, no. 2, pp. 445–455, 2012.
64. S. Gopal, Y. Otaki, R. Arsanjani, D. Berman, D. Terzopoulos, and P. Slomka, "Combining active appearance and deformable superquadric models for LV segmentation in cardiac MRI," in *Medical Imaging 2013: Image Processing*, 2013, vol. 8669, p. 86690G: International Society for Optics and Photonics.
65. F. Khalifa, G. M. Beache, G. Gimel'farb, and A. El-Baz, "A novel CAD system for analyzing cardiac first-pass MR images," in *Pattern Recognition (ICPR), 2012 21st International Conference on*, 2012, pp. 77–80: IEEE.

66. F. Khalifa *et al.*, "A new shape-based framework for the left ventricle wall segmentation from cardiac first-pass perfusion MRI," in *Biomedical Imaging (ISBI), 2013 IEEE 10th International Symposium on*, 2013, pp. 41–44: IEEE.
67. F. Khalifa, G. M. Beache, A. Firjani, K. C. Welch, G. Gimel'farb, and A. El-Baz, "A new nonrigid registration approach for motion correction of cardiac first-pass perfusion MRI," in *Image Processing (ICIP), 2012 19th IEEE International Conference on*, 2012, pp. 1665–1668: IEEE.
68. G. M. Beache, F. Khalifa, A. El-Baz, and G. Gimel'farb, "Fully automated framework for the analysis of myocardial first-pass perfusion MR images," *Medical Physics*, vol. 41, no. 10, 2014.
69. H. Sliman *et al.*, "A novel 4D PDE-based approach for accurate assessment of myocardium function using cine cardiac magnetic resonance images," in *Image Processing (ICIP), 2014 IEEE International Conference on*, 2014, pp. 3537–3541: IEEE.
70. H. Sliman *et al.*, "A new segmentation-based tracking framework for extracting the left ventricle cavity from cine cardiac MRI," in *Proceedings of IEEE International Conference on Image Processing, (ICIP'13)*, 2013, pp. 685–689.
71. H. Sliman *et al.*, "Accurate segmentation framework for the left ventricle wall from cardiac cine MRI," in *AIP Conference Proceedings*, 2013, vol. 1559, no. 1, pp. 287–296: AIP.
72. H. Sliman *et al.*, "Myocardial borders segmentation from cine MR images using bidirectional coupled parametric deformable models," *Medical Physics*, vol. 40, no. 9, 2013.
73. S. Ho, E. Bullitt, and G. Gerig, "Level-set evolution with region competition: automatic 3-D segmentation of brain tumors," in *Pattern Recognition, 2002. Proceedings. 16th International Conference on*, 2002, vol. 1, pp. 532–535: IEEE.
74. R. Goldenberg, R. Kimmel, E. Rivlin, and M. Rudzsky, "Cortex segmentation: A fast variational geometric approach," *IEEE Transactions on Medical Imaging*, vol. 21, no. 12, pp. 1544–1551, 2002.
75. Ali, A.M., Farag, A.A., El-Baz, A.: Graph cuts framework for kidney segmentation with prior shape constraints. In: *Proceedings of International Conference on Medical Image Computing and Computer-Assisted Intervention, (MICCAI'07)*. Volume 1., Brisbane, Australia, October 29–November 2 (2007) 384–392.
76. Chowdhury, A.S., Roy, R., Bose, S., Elnakib, F.K.A., El-Baz, A.: Non-rigid biomedical image registration using graph cuts with a novel data term. In: *Proceedings of IEEE International Symposium on Biomedical Imaging: From Nano to Macro, (ISBI'12)*, Barcelona, Spain, May 2–5 (2012) 446–449.
77. El-Baz, A., Farag, A.A., Yuksel, S.E., El-Ghar, M.E.A., Eldiasty, T.A., Ghoneim, M.A.: Application of deformable models for the detection of acute renal rejection. In Farag, A.A., Suri, J.S., eds.: *Deformable Models*. Volume 1. (2007) 293–333.
78. El-Baz, A., Farag, A., Fahmi, R., Yuksel, S., El-Ghar, M.A., Eldiasty, T.: Image analysis of renal DCE MRI for the detection of acute renal rejection. In: *Proceedings of IAPR International Conference on Pattern Recognition (ICPR'06)*, Hong Kong, August 20–24 (2006) 822–825.
79. El-Baz, A., Farag, A., Fahmi, R., Yuksel, S., Miller, W., El-Ghar, M.A., El-Diasty, T., Ghoneim, M.: A new CAD system for the evaluation of kidney diseases using DCE-MRI. In: *Proceedings of International Conference on Medical Image Computing and Computer-Assisted Intervention, (MICCAI'08)*, Copenhagen, Denmark, October 1–6 (2006) 446–453.

80. El-Baz, A., Gimel'farb, G., El-Ghar, M.A.: A novel image analysis approach for accurate identification of acute renal rejection. In: *Proceedings of IEEE International Conference on Image Processing, (ICIP'08)*, San Diego, California, USA, October 12–15 (2008) 1812–1815.
81. El-Baz, A., Gimel'farb, G., El-Ghar, M.A.: Image analysis approach for identification of renal transplant rejection. In: *Proceedings of IAPR International Conference on Pattern Recognition, (ICPR'08)*, Tampa, Florida, USA, December 8–11 (2008) 1–4.
82. El-Baz, A., Gimel'farb, G., El-Ghar, M.A.: New motion correction models for automatic identification of renal transplant rejection. In: *Proceedings of International Conference on Medical Image Computing and Computer-Assisted Intervention, (MICCAI'07)*, Brisbane, Australia, October 29–November 2 (2007) 235–243.
83. Farag, A., El-Baz, A., Yuksel, S., El-Ghar, M.A., Eldiasty, T.: A framework for the detection of acute rejection with Dynamic Contrast Enhanced Magnetic Resonance Imaging. In: *Proceedings of IEEE International Symposium on Biomedical Imaging: From Nano to Macro, (ISBI'06)*, Arlington, Virginia, USA, April 6–9 (2006) 418–421.
84. Khalifa, F., Beache, G.M., El-Ghar, M.A., El-Diasty, T., Gimel'farb, G., Kong, M., El-Baz, A.: Dynamic contrast-enhanced MRI-based early detection of acute renal transplant rejection. *IEEE Transactions on Medical Imaging* 32(10) (2013) 1910–1927 Prostate Cancer Diagnosis using SNCAE 23.
85. Khalifa, F., El-Baz, A., Gimel'farb, G., El-Ghar, M.A.: Non-invasive image-based approach for early detection of acute renal rejection. In: *Proceedings of International Conference Medical Image Computing and Computer-Assisted Intervention, (MICCAI'10)*, Beijing, China, September 20–24 (2010) 10–18.
86. Khalifa, F., El-Baz, A., Gimel'farb, G., Ouseph, R., El-Ghar, M.A.: Shapeappearance guided level-set deformable model for image segmentation. In: *Proceedings of IAPR International Conference on Pattern Recognition, (ICPR'10)*, Istanbul, Turkey, August 23–26 (2010) 4581–4584.
87. Khalifa, F., El-Ghar, M.A., Abdollahi, B., Frieboes, H., El-Diasty, T., El-Baz, A.: A comprehensive non-invasive framework for automated evaluation of acute renal transplant rejection using DCE-MRI. *NMR in Biomedicine* 26(11) (2013) 1460–1470.
88. Khalifa, F., El-Ghar, M.A., Abdollahi, B., Frieboes, H.B., El-Diasty, T., El-Baz, A.: Dynamic contrast-enhanced MRI-based early detection of acute renal transplant rejection. In: *2014 Annual Scientific Meeting and Educational Course Brochure of the Society of Abdominal Radiology, (SAR'14)*, Boca Raton, Florida, March 23–28 (2014) CID: 1855912.
89. Khalifa, F., Elnakib, A., Beache, G.M., Gimel'farb, G., El-Ghar, M.A., Sokhadze, G., Manning, S., McClure, P., El-Baz, A.: 3D kidney segmentation from CT images using a level set approach guided by a novel stochastic speed function. In: *Proceedings of International Conference Medical Image Computing and Computer-Assisted Intervention, (MICCAI'11)*, Toronto, Canada, September 18–22 (2011) 587–594.
90. Khalifa, F., Gimel'farb, G., El-Ghar, M.A., Sokhadze, G., Manning, S., McClure, P., Ouseph, R., El-Baz, A.: A new deformable model-based segmentation approach for accurate extraction of the kidney from abdominal CT images. In: *Proceedings of IEEE International Conference on Image Processing, (ICIP'11)*, Brussels, Belgium, September 11–14 (2011) 3393–3396.

91. Mostapha, M., Khalifa, F., Alansary, A., Soliman, A., Suri, J., El-Baz, A.: Computer-aided diagnosis systems for acute renal transplant rejection: Challenges and methodologies. In El-Baz, A., saba J. Suri, L., eds.: *Abdomen and thoracic imaging*. Springer (2014) 1–35.
92. Shehata, M., Khalifa, F., Hollis, E., Soliman, A., Hosseini-Asl, E., El-Ghar, M.A., El-Baz, M., Dwyer, A.C., El-Baz, A., Keynton, R.: A new non-invasive approach for early classification of renal rejection types using diffusion-weighted mri. In: *IEEE International Conference on Image Processing (ICIP)*, 2016, IEEE (2016) 136–140.
93. Khalifa, F., Soliman, A., Takieldeen, A., Shehata, M., Mostapha, M., Shaffie, A., Ouseph, R., Elmaghraby, A., El-Baz, A.: Kidney segmentation from CT images using a 3D NMF-guided active contour model. In: *IEEE 13th International Symposium on Biomedical Imaging (ISBI)*, 2016, IEEE (2016) 432–435.
94. Shehata, M., Khalifa, F., Soliman, A., Takieldeen, A., El-Ghar, M.A., Shaffie, A., Dwyer, A.C., Ouseph, R., El-Baz, A., Keynton, R.: 3d diffusion mri-based cad system for early diagnosis of acute renal rejection. In: *Biomedical Imaging (ISBI), 2016 IEEE 13th International Symposium on, IEEE* (2016) 1177–1180.
95. Shehata, M., Khalifa, F., Soliman, A., Alrefai, R., El-Ghar, M.A., Dwyer, A.C., Ouseph, R., El-Baz, A.: A level set-based framework for 3d kidney segmentation from diffusion mr images. In: *IEEE International Conference on Image Processing (ICIP)*, 2015, IEEE (2015) 4441–4445. 24 Authors Suppressed Due to Excessive Length.
96. Shehata, M., Khalifa, F., Soliman, A., El-Ghar, M.A., Dwyer, A.C., Gimelfarb, G., Keynton, R., El-Baz, A.: A promising non-invasive cad system for kidney function assessment. In: *International Conference on Medical Image Computing and Computer-Assisted Intervention*. Springer (2016) 613–621.
97. Khalifa, F., Soliman, A., Elmaghraby, A., Gimelfarb, G., El-Baz, A.: 3d kidney segmentation from abdominal images using spatial-appearance models. *Computational and mathematical methods in medicine* 2017 (2017).
98. Hollis, E., Shehata, M., Khalifa, F., El-Ghar, M.A., El-Diasty, T., El-Baz, A.: Towards non-invasive diagnostic techniques for early detection of acute renal transplant rejection: A review. *The Egyptian Journal of Radiology and Nuclear Medicine* 48(1) (2016) 257–269.
99. Shehata, M., Khalifa, F., Soliman, A., El-Ghar, M.A., Dwyer, A.C., El-Baz, A.: Assessment of renal transplant using image and clinical-based biomarkers. In: *Proceedings of 13th Annual Scientific Meeting of American Society for Diagnostics and Interventional Nephrology (ASDIN'17)*, New Orleans, LA, USA, February 10–12, 2017. (2017).
100. Shehata, M., Khalifa, F., Soliman, A., El-Ghar, M.A., Dwyer, A.C., El-Baz, A.: Early assessment of acute renal rejection. In: *Proceedings of 12th Annual Scientific Meeting of American Society for Diagnostics and Interventional Nephrology (ASDIN'16)*, Pheonix, AZ, USA, February 19–21, 2016. (2017).
101. Khalifa, F., Beache, G., El-Baz, A., Gimel'farb, G.: Deformable model guided by stochastic speed with application in cine images segmentation. In: *Proceedings of IEEE International Conference on Image Processing, (ICIP'10)*, Hong Kong, September 26–29 (2010) 1725–1728.

102. Khalifa, F., Beache, G.M., Elnakib, A., Sliman, H., Gimel'farb, G., Welch, K.C., El-Baz, A.: A new shape-based framework for the left ventricle wall segmentation from cardiac first-pass perfusion MRI. In: *Proceedings of IEEE International Symposium on Biomedical Imaging: From Nano to Macro, (ISBI'13)*, San Francisco, CA, April 7–11 (2013) 41–44.
103. Khalifa, F., Beache, G.M., Elnakib, A., Sliman, H., Gimel'farb, G., Welch, K.C., El-Baz, A.: A new nonrigid registration framework for improved visualization of transmural perfusion gradients on cardiac first–pass perfusion MRI. In: *Proceedings of IEEE International Symposium on Biomedical Imaging: From Nano to Macro, (ISBI'12)*, Barcelona, Spain, May 2–5 (2012) 828–831.
104. Khalifa, F., Beache, G.M., Firjani, A., Welch, K.C., Gimel'farb, G., El-Baz, A.: A new nonrigid registration approach for motion correction of cardiac first-pass perfusion MRI. In: *Proceedings of IEEE International Conference on Image Processing, (ICIP'12)*, Lake Buena Vista, Florida, September 30–October 3 (2012) 1665–1668.
105. Khalifa, F., Beache, G.M., Gimel'farb, G., El-Baz, A.: A novel CAD system for analyzing cardiac first-pass MR images. In: *Proceedings of IAPR International Conference on Pattern Recognition (ICPR'12)*, Tsukuba Science City, Japan, November 11–15 (2012) 77–80.
106. Khalifa, F., Beache, G.M., Gimel'farb, G., El-Baz, A.: A novel approach for accurate estimation of left ventricle global indexes from short-axis cine MRI. In: *Proceedings of IEEE International Conference on Image Processing, (ICIP'11)*, Brussels, Belgium, September 11–14 (2011) 2645–2649.
107. Khalifa, F., Beache, G.M., Gimel'farb, G., Giridharan, G.A., El-Baz, A.: A new image-based framework for analyzing cine images. In El-Baz, A., Acharya, U.R., Mirmedhdi, M., Suri, J.S., eds.: *Handbook of multi modality state-of prostate cancer diagnosis using SNCAE 25 the-art medical image segmentation and registration methodologies*. Volume 2. Springer, New York (2011) 69–98.
108. Khalifa, F., Beache, G.M., Gimel'farb, G., Giridharan, G.A., El-Baz, A.: Accurate automatic analysis of cardiac cine images. *IEEE Transactions on Biomedical Engineering* 59(2) (2012) 445–455.
109. Khalifa, F., Beache, G.M., Nitzken, M., Gimel'farb, G., Giridharan, G.A., El-Baz, A.: Automatic analysis of left ventricle wall thickness using short-axis cine CMR images. In: *Proceedings of IEEE International Symposium on Biomedical Imaging: From Nano to Macro, (ISBI'11)*, Chicago, Illinois, March 30–April 2 (2011) 1306–1309.
110. Nitzken, M., Beache, G., Elnakib, A., Khalifa, F., Gimel'farb, G., El-Baz, A.: Accurate modeling of tagged cmr 3D image appearance characteristics to improve cardiac cycle strain estimation. In: *Image Processing (ICIP), 2012 19th IEEE International Conference on*, Orlando, Florida, USA, IEEE (September 2012) 521–524.
111. Nitzken, M., Beache, G., Elnakib, A., Khalifa, F., Gimel'farb, G., El-Baz, A.: Improving full-cardiac cycle strain estimation from tagged cmr by accurate modeling of 3D image appearance characteristics. In: *Biomedical Imaging (ISBI), 2012 9th IEEE International Symposium on, Barcelona, Spain, IEEE* (May 2012) 462–465 (Selected for oral presentation).
112. Nitzken, M.J., El-Baz, A.S., Beache, G.M.: Markov-gibbs random field model for improved full-cardiac cycle strain estimation from tagged cmr. *Journal of Cardiovascular Magnetic Resonance* 14(1) (2012) 1–2.

113. Sliman, H., Elnakib, A., Beache, G., Elmaghraby, A., El-Baz, A.: Assessment of myocardial function from cine cardiac MRI using a novel 4D tracking approach. *J Comput Sci Syst Biol* 7 (2014) 169–173.
114. Sliman, H., Elnakib, A., Beache, G.M., Soliman, A., Khalifa, F., Gimel'farb, G., Elmaghraby, A., El-Baz, A.: A novel 4D PDE-based approach for accurate assessment of myocardium function using cine cardiac magnetic resonance images. In: *Proceedings of IEEE International Conference on Image Processing (ICIP'14)*, Paris, France, October 27–30 (2014) 3537–3541.
115. Sliman, H., Khalifa, F., Elnakib, A., Beache, G.M., Elmaghraby, A., El-Baz, A.: A new segmentation-based tracking framework for extracting the left ventricle cavity from cine cardiac MRI. In: *Proceedings of IEEE International Conference on Image Processing, (ICIP'13)*, Melbourne, Australia, September 15–18 (2013) 685–689.
116. Sliman, H., Khalifa, F., Elnakib, A., Soliman, A., Beache, G.M., Elmaghraby, A., Gimel'farb, G., El-Baz, A.: Myocardial borders segmentation from cine MR images using bi-directional coupled parametric deformable models. *Medical Physics* (9) (2013) 1–13.
117. Sliman, H., Khalifa, F., Elnakib, A., Soliman, A., Beache, G.M., Gimel'farb, G., Emam, A., Elmaghraby, A., El-Baz, A.: Accurate segmentation framework for the left ventricle wall from cardiac cine MRI. In: *Proceedings of International Symposium on Computational Models for Life Science, (CMLS'13)*. Volume 1559., Sydney, Australia, November 27–29 (2013) 287–296.
118. N. Eladawi, M. Elmogy, M.G.O.H.A.A.A.R.S.S.A.E.B.: Classification of retinal diseases based on oct images. *Frontiers in Bioscience Landmark Journal* (2017).
119. A. ElTanboly, M. Ismail, A.S.A.S.S.S.G.G.M.E.A.E.B.: A computer aided diagnostic system for detecting diabetic retinopathy in optical coherence tomography images. *Medical Physics* (2016) 26 Authors Suppressed Due to Excessive Length.
120. Abdollahi, B., Civelek, A.C., Li, X.F., Suri, J., El-Baz, A.: PET/CT nodule segmentation and diagnosis: A survey. In Saba, L., Suri, J.S., eds.: *Multi detector CT imaging*. Taylor, Francis (2014) 639–651.
121. Abdollahi, B., El-Baz, A., Amini, A.A.: A multi-scale non-linear vessel enhancement technique. In: *Engineering in medicine and biology society*, EMBC, 2011 Annual International Conference of the IEEE, IEEE (2011) 3925–3929.
122. Abdollahi, B., Soliman, A., Civelek, A., Li, X.F., Gimel'farb, G., El-Baz, A.: A novel gaussian scale space-based joint MGRF framework for precise lung segmentation. In: *Proceedings of IEEE International Conference on Image Processing, (ICIP'12)*, IEEE (2012). 2029–2032.
123. Abdollahi, B., Soliman, A., Civelek, A., Li, X.F., Gimelfarb, G., El-Baz, A.: A novel 3D joint MGRF framework for precise lung segmentation. In: *Machine learning in medical imaging*. Springer (2012) 86–93.
124. Ali, A.M., El-Baz, A.S., Farag, A.A.: A novel framework for accurate lung segmentation using graph cuts. In: *Proceedings of IEEE International Symposium on Biomedical Imaging: From Nano to Macro, (ISBI'07)*, IEEE (2007) 908–911.
125. El-Baz, A., Beache, G.M., Gimel'farb, G., Suzuki, K., Okada, K.: Lung imaging data analysis. *International Journal of Biomedical Imaging* 2013 (2013).

126. El-Baz, A., Beache, G.M., Gimel'farb, G., Suzuki, K., Okada, K., Elnakib, A., Soliman, A., Abdollahi, B.: Computer-aided diagnosis systems for lung cancer: Challenges and methodologies. *International Journal of Biomedical Imaging* 2013 (2013).
127. El-Baz, A., Elnakib, A., Abou El-Ghar, M., Gimel'farb, G., Falk, R., Farag, A.: Automatic detection of 2D and 3D lung nodules in chest spiral CT scans. *International Journal of Biomedical Imaging* 2013 (2013).
128. El-Baz, A., Farag, A.A., Falk, R., La Rocca, R.: A unified approach for detection, visualization, and identification of lung abnormalities in chest spiral CT scans. In: *International Congress Series*. Volume 1256., Elsevier (2003) 998–1004.
129. El-Baz, A., Farag, A.A., Falk, R., La Rocca, R.: Detection, visualization and identification of lung abnormalities in chest spiral CT scan: Phase-I. In: *Proceedings of International conference on Biomedical Engineering*, Cairo, Egypt. Volume 12. (2002).
130. El-Baz, A., Farag, A., Gimel'farb, G., Falk, R., El-Ghar, M.A., Eldiasty, T.: A framework for automatic segmentation of lung nodules from low dose chest CT scans. In: *Proceedings of International Conference on Pattern Recognition, (ICPR'06)*. Volume 3., IEEE (2006) 611–614.
131. El-Baz, A., Farag, A., Gimelfarb, G., Falk, R., El-Ghar, M.A.: A novel level set-based computer-aided detection system for automatic detection of lung nodules in low dose chest computed tomography scans. *Lung Imaging and Computer Aided Diagnosis* 10 (2011) 221–238.
132. El-Baz, A., Gimel'farb, G., Abou El-Ghar, M., Falk, R.: Appearance-based diagnostic system for early assessment of malignant lung nodules. In: *Proceedings of IEEE International Conference on Image Processing, (ICIP'12)*, IEEE (2012) 533–536.
133. El-Baz, A., Gimel'farb, G., Falk, R.: A novel 3D framework for automatic lung segmentation from low dose CT images. In El-Baz, A., Suri, J.S., eds.: *Lung imaging and computer aided diagnosis*. Taylor, Francis (2011) 1–16.
134. El-Baz, A., Gimel'farb, G., Falk, R., El-Ghar, M.: Appearance analysis for diagnosing malignant lung nodules. In: *Proceedings of IEEE International Symposium on Biomedical Imaging: From Nano to Macro (ISBI'10)*, IEEE (2010) 193–196 Prostate Cancer Diagnosis using SNCAE 27.
135. El-Baz, A., Gimel'farb, G., Falk, R., El-Ghar, M.A.: A novel level set-based CAD system for automatic detection of lung nodules in low dose chest CT scans. In El-Baz, A., Suri, J.S., eds.: Lung Imaging and Computer Aided Diagnosis. Volume 1. Taylor, Francis (2011) 221–238.
136. El-Baz, A., Gimel'farb, G., Falk, R., El-Ghar, M.A.: A new approach for automatic analysis of 3D low dose CT images for accurate monitoring the detected lung nodules. In: *Proceedings of International Conference on Pattern Recognition, (ICPR'08)*, IEEE (2008) 1–4.
137. El-Baz, A., Gimel'farb, G., Falk, R., El-Ghar, M.A.: A novel approach for automatic follow-up of detected lung nodules. In: *Proceedings of IEEE International Conference on Image Processing, (ICIP'07)*. Volume 5., IEEE (2007) V–501.
138. El-Baz, A., Gimel'farb, G., Falk, R., El-Ghar, M.A.: A new CAD system for early diagnosis of detected lung nodules. In: *Image Processing, 2007. ICIP 2007. IEEE International Conference on*. Volume 2., IEEE (2007) II–461.

139. El-Baz, A., Gimel'farb, G., Falk, R., El-Ghar, M.A., Refaie, H.: Promising results for early diagnosis of lung cancer. In: *Proceedings of IEEE International Symposium on Biomedical Imaging: From Nano to Macro, (ISBI'08)*, IEEE (2008) 1151–1154.
140. El-Baz, A., Gimel'farb, G.L., Falk, R., Abou El-Ghar, M., Holland, T., Shaffer, T.: A new stochastic framework for accurate lung segmentation. In: *Proceedings of Medical Image Computing and Computer-Assisted Intervention, (MICCAI'08)*. (2008) 322–330.
141. El-Baz, A., Gimel'farb, G.L., Falk, R., Heredis, D., Abou El-Ghar, M.: A novel approach for accurate estimation of the growth rate of the detected lung nodules. In: *Proceedings of International Workshop on Pulmonary Image Analysis*. (2008) 33–42.
142. El-Baz, A., Gimel'farb, G.L., Falk, R., Holland, T., Shaffer, T.: A framework for unsupervised segmentation of lung tissues from low dose computed tomography images. In: *Proceedings of British Machine Vision, (BMVC'08)*. (2008) 1–10.
143. El-Baz, A., Gimelfarb, G., Falk, R., El-Ghar, M.A.: 3D MGRF-based appearance modeling for robust segmentation of pulmonary nodules in 3D LDCT chest images. In: *Lung imaging and computer aided diagnosis*. chapter (2011) 51–63.
144. El-Baz, A., Gimelfarb, G., Falk, R., El-Ghar, M.A.: Automatic analysis of 3D low dose CT images for early diagnosis of lung cancer. *Pattern Recognition* 42(6) (2009) 1041–1051.
145. El-Baz, A., Gimelfarb, G., Falk, R., El-Ghar, M.A., Rainey, S., Heredia, D., Shaffer, T.: Toward early diagnosis of lung cancer. In: *Proceedings of Medical Image Computing and Computer-Assisted Intervention, (MICCAI'09)*, Springer (2009) 682–689.
146. El-Baz, A., Gimelfarb, G., Falk, R., El-Ghar, M.A., Suri, J.: Appearance analysis for the early assessment of detected lung nodules. In: *Lung imaging and computer aided diagnosis*. chapter (2011) 395–404.
147. El-Baz, A., Khalifa, F., Elnakib, A., Nitkzen, M., Soliman, A., McClure, P., Gimel'farb, G., El-Ghar, M.A.: A novel approach for global lung registration using 3D Markov Gibbs appearance model. In: *Proceedings of International Conference Medical Image Computing and Computer-Assisted Intervention, (MICCAI' 12)*, Nice, France, October 1–5 (2012) 114–121.
148. El-Baz, A., Nitzken, M., Elnakib, A., Khalifa, F., Gimel'farb, G., Falk, R., El-Ghar, M.A.: 3D shape analysis for early diagnosis of malignant lung nodules. In: *Proceedings of International Conference Medical Image Computing and Computer-Assisted Intervention, (MICCAI'11)*, Toronto, Canada, September 18–22 (2011) 175–182.
149. El-Baz, A., Nitzken, M., Gimelfarb, G., Van Bogaert, E., Falk, R., El-Ghar, M.A., Suri, J.: Three-dimensional shape analysis using spherical harmonics for early assessment of detected lung nodules. In: *Lung imaging and computer aided diagnosis*. chapter (2011) 421–438.
150. El-Baz, A., Nitzken, M., Khalifa, F., Elnakib, A., Gimel'farb, G., Falk, R., El-Ghar, M.A.: 3D shape analysis for early diagnosis of malignant lung nodules. In: Proceedings of International Conference on Information Processing in Medical Imaging, (IPMI'11), Monastery Irsee, Germany (Bavaria), July 3–8 (2011) 772–783.
151. El-Baz, A., Nitzken, M., Vanbogaert, E., Gimel'Farb, G., Falk, R., Abo El-Ghar, M.: A novel shape-based diagnostic approach for early diagnosis of lung nodules. In: *Biomedical Imaging: From Nano to Macro, 2011 IEEE International Symposium on*, IEEE (2011) 137–140.

152. El-Baz, A., Sethu, P., Gimel'farb, G., Khalifa, F., Elnakib, A., Falk, R., El-Ghar, M.A.: Elastic phantoms generated by microfluidics technology: Validation of an imaged-based approach for accurate measurement of the growth rate of lung nodules. *Biotechnology Journal* 6(2) (2011) 195–203.
153. El-Baz, A., Sethu, P., Gimel'farb, G., Khalifa, F., Elnakib, A., Falk, R., El-Ghar, M.A.: A new validation approach for the growth rate measurement using elastic phantoms generated by state-of-the-art microfluidics technology. In: *Proceedings of IEEE International Conference on Image Processing, (ICIP'10)*, Hong Kong, September 26–29 (2010) 4381–4383.
154. El-Baz, A., Sethu, P., Gimel'farb, G., Khalifa, F., Elnakib, A., Falk, R., Suri, M.A.E.G.J.: Validation of a new imaged-based approach for the accurate estimating of the growth rate of detected lung nodules using real CT images and elastic phantoms generated by state-of-the-art microfluidics technology. In El-Baz, A., Suri, J.S., eds.: *Handbook of lung imaging and computer aided diagnosis*. Volume 1. Taylor & Francis, New York (2011) 405–420.
155. El-Baz, A., Soliman, A., McClure, P., Gimel'farb, G., El-Ghar, M.A., Falk, R.: Early assessment of malignant lung nodules based on the spatial analysis of detected lung nodules. In: *Proceedings of IEEE International Symposium on Biomedical Imaging: From Nano to Macro, (ISBI'12)*, IEEE (2012) 1463–1466.
156. El-Baz, A., Yuksel, S.E., Elshazly, S., Farag, A.A.: Non-rigid registration techniques for automatic follow-up of lung nodules. In: *Proceedings of Computer Assisted Radiology and Surgery, (CARS'05)*. Volume 1281., Elsevier (2005) 1115–1120.
157. El-Baz, A.S., Suri, J.S.: *Lung imaging and computer aided diagnosis*. CRC Press (2011).
158. Soliman, A., Khalifa, F., Shaffie, A., Liu, N., Dunlap, N., Wang, B., Elmaghraby, A., Gimelfarb, G., El-Baz, A.: Image-based cad system for accurate identification of lung injury. In: *Proceedings of IEEE International Conference on Image Processing, (ICIP'16)*, IEEE (2016) 121–125.
159. Soliman, A., Khalifa, F., Dunlap, N., Wang, B., El-Ghar, M., El-Baz, A.: An isosurfaces based local deformation handling framework of lung tissues. In: *Biomedical Imaging (ISBI), 2016 IEEE 13th International Symposium on*, IEEE (2016) 1253–1259.
160. Soliman, A., Khalifa, F., Shaffie, A., Dunlap, N., Wang, B., Elmaghraby, A., El-Baz, A.: Detection of lung injury using 4d-ct chest images. In: *Biomedical Imaging (ISBI), 2016 IEEE 13th International Symposium on*, IEEE (2016) 1274–1277 Prostate Cancer Diagnosis using SNCAE 29.
161. Dombroski, B., Nitzken, M., Elnakib, A., Khalifa, F., El-Baz, A., Casanova, M.F.: Cortical surface complexity in a population-based normative sample. *Translational Neuroscience* 5(1) (2014) 17–24.
162. El-Baz, A., Casanova, M., Gimel'farb, G., Mott, M., Switala, A.: An MRI-based diagnostic framework for early diagnosis of dyslexia. *International Journal of Computer Assisted Radiology and Surgery* 3(3–4) (2008) 181–189.
163. El-Baz, A., Casanova, M., Gimel'farb, G., Mott, M., Switala, A., Vanbogaert, E., McCracken, R.: A new CAD system for early diagnosis of dyslexic brains. In: *Proc. International Conference on Image Processing (ICIP'2008)*, IEEE (2008) 1820–1823.
164. El-Baz, A., Casanova, M.F., Gimel'farb, G., Mott, M., Switwala, A.E.: A new image analysis approach for automatic classification of autistic brains. In: *Proc. IEEE International Symposium on Biomedical Imaging: From Nano to Macro (ISBI'2007)*, IEEE (2007) 352–355.

165. El-Baz, A., Elnakib, A., Khalifa, F., El-Ghar, M.A., McClure, P., Soliman, A., Gimel'farb, G.: Precise segmentation of 3-D magnetic resonance angiography. *IEEE Transactions on Biomedical Engineering* 59(7) (2012) 2019–2029.
166. El-Baz, A., Farag, A.A., Gimel'farb, G.L., El-Ghar, M.A., Eldiasty, T.: Probabilistic modeling of blood vessels for segmenting mra images. In: *ICPR* (3). (2006) 917–920.
167. El-Baz, A., Farag, A.A., Gimelfarb, G., El-Ghar, M.A., Eldiasty, T.: A new adaptive probabilistic model of blood vessels for segmenting mra images. In: *Medical image computing and computer assisted intervention–MICCAI 2006*. Volume 4191., Springer (2006) 799–806.
168. El-Baz, A., Farag, A.A., Gimelfarb, G., Hushek, S.G.: Automatic cerebrovascular segmentation by accurate probabilistic modeling of tof-mra images. In: *Medical image computing and computer-assisted intervention–MICCAI 2005*. Springer (2005) 34–42.
169. El-Baz, A., Farag, A., Elnakib, A., Casanova, M.F., Gimel'farb, G., Switala, A.E., Jordan, D., Rainey, S.: Accurate automated detection of autism related corpus callosum abnormalities. *Journal of Medical Systems* 35(5) (2011) 929–939.
170. El-Baz, A., Farag, A., Gimelfarb, G.: Cerebrovascular segmentation by accurate probabilistic modeling of tof-mra images. In: *Image Analysis*. Volume 3540., Springer (2005) 1128–1137.
171. El-Baz, A., Gimelfarb, G., Falk, R., El-Ghar, M.A., Kumar, V., Heredia, D.: A novel 3D joint Markov-gibbs model for extracting blood vessels from PC–mra images. In: *Medical image computing and computer-assisted intervention– MICCAI 2009*. Volume 5762., Springer (2009) 943–950.
172. Elnakib, A., El-Baz, A., Casanova, M.F., Gimel'farb, G., Switala, A.E.: Image-based detection of corpus callosum variability for more accurate discrimination between dyslexic and normal brains. In: *Proc. IEEE International Symposium on Biomedical Imaging: From Nano to Macro (ISBI'2010)*, IEEE (2010) 109–112.
173. Elnakib, A., Casanova, M.F., Gimel'farb, G., Switala, A.E., El-Baz, A.: Autism diagnostics by centerline-based shape analysis of the corpus callosum. In: *Proc. IEEE International Symposium on Biomedical Imaging: From Nano to Macro (ISBI'2011)*, IEEE (2011) 1843–1846.
174. Elnakib, A., Nitzken, M., Casanova, M., Park, H., Gimel'farb, G., El-Baz, A.: Quantification of age-related brain cortex change using 3D shape analysis. In: *Pattern Recognition (ICPR)*, 2012 21st International Conference on, IEEE (2012) 41–44. 30 Authors Suppressed Due to Excessive Length.
175. Mostapha, M., Soliman, A., Khalifa, F., Elnakib, A., Alansary, A., Nitzken, M., Casanova, M.F., El-Baz, A.: A statistical framework for the classification of infant dt images. In: *Image Processing (ICIP)*, 2014 IEEE International Conference on, IEEE (2014) 2222–2226.
176. Nitzken, M., Casanova, M., Gimel'farb, G., Elnakib, A., Khalifa, F., Switala, A., El-Baz, A.: 3D shape analysis of the brain cortex with application to dyslexia. In: *Image Processing (ICIP)*, 2011 18th IEEE International Conference on, Brussels, Belgium, IEEE (September 2011) 2657–2660 (Selected for oral presentation. Oral acceptance rate is 10 percent and the overall acceptance rate is 35 percent).
177. El-Gamal, F.E.Z.A., Elmogy, M., Ghazal, M., Atwan, A., Barnes, G., Casanova, M., Keynton, R., El-Baz, A.: A novel cad system for local and global early diagnosis of alzheimers disease based on pib-pet scans. In: *Image Processing (ICIP), 2017 IEEE International Conference on, Beijing, China*, IEEE (2017).

178. Ismail, M., Soliman, A., Ghazal, M., Switala, A.E., Gimel'farb, G., Barnes, G.N., Khalil, A. and El-Baz, A., 2017. A fast stochastic framework for automatic MR brain images segmentation. PloS one, 12(11), p.e0187391.
179. Ismail, M.M., Keynton, R.S., Mostapha, M.M., ElTanboly, A.H., Casanova, M.F., Gimel'farb, G.L., El-Baz, A.: Studying autism spectrum disorder with structural and diffusion magnetic resonance imaging: a survey. *Frontiers in Human Neuroscience* 10 (2016).
180. Alansary, A., Ismail, M., Soliman, A., Khalifa, F., Nitzken, M., Elnakib, A., Mostapha, M., Black, A., Stinebruner, K., Casanova, M.F., et al.: Infant brain extraction in t1-weighted mr images using bet and refinement using lcdg and mgrf models. *IEEE Journal of Biomedical and Health Informatics* 20(3) (2016) 925–935.
181. Ismail, M., Barnes, G., Nitzken, M., Switala, A., Shalaby, A., Hosseini-Asl, E., Casanova, M., Keynton, R., Khalil, A. and El-Baz, A., 2017, September. A new deep-learning approach for early detection of shape variations in autism using structural mri. In 2017 IEEE International Conference on Image Processing (ICIP) (pp. 1057–1061). IEEE.
182. Ismail, M., Soliman, A., ElTanboly, A., Switala, A., Mahmoud, M., Khalifa, F., Gimel'farb, G., Casanova, M.F., Keynton, R., El-Baz, A.: Detection of white matter abnormalities in mr brain images for diagnosis of autism in children. (2016) 6–9.
183. Ismail, M., Mostapha, M., Soliman, A., Nitzken, M., Khalifa, F., Elnakib, A., Gimel'farb, G., Casanova, M., El-Baz, A.: Segmentation of infant brain mr images based on adaptive shape prior and higher-order mgrf. (2015) 4327–4331.

9

Cardiac Image Segmentation Using Generalized Polynomial Chaos Expansion and Level Set Function

1. C. Petitjean and J.-N. Dacher, "A review of segmentation methods in short axis cardiac MR images," *Medical Image Anlysis*, vol. 2, no. 169–184, p. 15, 2011.
2. M. R. M. Jongbloed, M. J. Schalij, K. Zeppenfled, P. V. Oemrawsingh, E. E. Wall and J. J. Bax, "Clinical applications of intracardiac echocardiography in interventional preocedures," *Heart*, vol. 91, no. 7, pp. 981–990, 2005.
3. T. Gerber, B. Kantor and E. Williamson, Computed tomography of the cardiovascular system, Boca Raton, FL: Taylor & Francis Group, LLC, 2007.
4. M. Dewey, E. Zimmermann, F. Deissenrieder, M. Laule, H. Dubel, P. Schlattmann, F. Knebel, W. Rutsch and B. Hamm, "Noninvasive Coronary Angiography by 320-Row Computed Tomography With Lower Radiation Exposure and Maintained Diagnostic Accuracy," *Circulation*, vol. 120, no. 10, pp. 867–875, 2009.
5. C. Petitjean and J.-N. Dacher, "A review of segmentation methods in short axis cardiac MR images," *Medical Image Analysis*, vol. 15, pp. 169–184, 2011.
6. D. Mahapatra, "Cardiac image segmentation from cine cardiac MRI using graph cuts and shape priors," *Journal of Digital Imaging*, vol. 26, pp. 721–730, 2013.
7. T. Donnell, G. Funka-Lea, H. Tek, M.-P. Jolly, M. Rasch and R. Setser, "Comprehensive cardiovascular image analysis using MR and CT at Siemens Corporate Research," *International Journal of Computer Vision*, vol. 70, no. 2, pp. 165–178, 2006.
8. J. Woo, P. Slomka, J. Kou and B.-W. Hong, "Multiphase segmentation using animplicit dual shape prior: application to detection of left ventricle in cardiac MRI," *Computer Vision and Image Understanding*, vol. 117, pp. 1084–1094, 2013.
9. X. Zhuang, K. S. Rhode and R. S. Razavi, "A registration-based propagation framework for automatic whole heart segmentation of cardiac MRI," *IEEE Transactions on Medical Imaging*, vol. 29, no. 9, pp. 1612–1625, 2010.
10. P. Kalshetti, M. Bundele, P. Rahangdale, D. Jangra, C. Chattopadhyay, G. Harit and A. Elhence, "An interactive medical image segmentation framework using iterative refinement," *Computers in Biology and Medicine*, vol. 83, pp. 22–33, 2017.
11. T. F. Chan and J. Shen, Image Processing and Analysis: Variational, PDE, Wavelet, and Stochastic Methods, Philadelphia, PA: The Society for Industrial and Applied Mathematics, 2005.

12. A. Ziadi, X. Maldague, L. Saucier, C. Duchesne and R. Gosselin, "Visible and near- infrared light transmission: a hybrid imaging method for non-destructive meat quality evaluation," *Infrared Physics & Technology*, vol. 55, no. 5, pp. 412–420, 2012.
13. T. Patz and T. Preusser, "Segmentation of stochastic images using level set propagation with uncertain speed," *Journal of Mathematical Imaging and Vision*, vol. 48, no. 3, pp. 467–487, 2014.
14. T. Preusser, H. Scharr, K. Krajsek and R. M. Kirby, "Building blocks for computer vision with stochastic partial differential equations," *International Journal of Computer Vision*, vol. 80, no. 3, pp. 375–405, 2008.
15. Y. Du, H. Budman and T. Duever, "Classification of normal and apoptotic cells from fluorescence microscopy images using generalized polynomial chaos and level set function," *Microscopy and Microanalysis*, vol. 22, no. 3, pp. 475–486, 2016.
16. D. Xiu, Numerical methods for stochastic computations: a spectral method approach, Princeton, New Jersey: Princeton University Press, 2010.
17. T. Chan and L. Vese, "Active contours without edges," *IEEE Transactions on Image Processing*, vol. 10, no. 2, pp. 266–278, 2001.
18. P. Getreuer, "Chan-Vese segmentation," *Image Processing On Line*, vol. 2, pp. 214–224, 2012.
19. S. Shors, C. Fung, C. Francois, P. Finn and D. Fieno, "Accurate quantification of right ventricular mass at MR imaging by using cine true fast imaging with steady state precession: study in dogs," *Radiology*, vol. 230, no. 2, pp. 383–388, 2004.
20. T. F. Chan and J. Shen, Image processing and analysis variational, PDE, Wavelet, and stochastic methods, Philadelphia, PA: The Society for Industrial and Applied Mathematics, 2005.
21. J. Caudron, J. Fares, F. Bauer and J. N. Dacher, "Left ventricular diastolic function assessment by cardiac MRI," *Radio Graphics*, vol. 31, no. 1, pp. 259–261, 2010.
22. N. Rougon, C. Petitjean, P. Cluzel, F. Preteux and P. Grenier, "A non rigid registration approach for quantifying myocardial contraction in tagged MRI using generalized information measures," *Medical Image Analysis*, vol. 9, no. 4, pp. 353–375, 2005.
23. A. Dervieus and F. Thomasset, "A finite element method for simulation of a Rayleigh- Taylor instability," *Approximation Methods for Navier-Stokes Problems. Lecture notes in Mathematics*, vol. 771, pp. 145–158, 1980.
24. S. Osher and J. A. Sethian, "Fronts propagating with curvature dependent speed: algorithm based on Hamilton-Jacobi formulations," *Journal of Computational Physics*, vol. 79, no. 1, pp. 12–49, 1998.
25. J. A. Sethian, Level set methods and fast marching methods, Cambridge, UK: Cambridge University Press, 1999.
26. S. Osher and J. A. Sethian, "Fronts propagating with curvature dependent speed: algorithms based on Hamilton-Jacobi formulation," *Journal of Computational Physics*, vol. 79, no. 1, pp. 12–49, 1998.
27. C. Li, C. Y. Kao, J. C. Gore and Z. Ding, "Minimization of region scalable fitting energy for image segmentation," *IEEE Transactions on Image Processing*, vol. 17, no. 10, pp. 1940–1949, 2008.
28. R. Malladi, J. A. Sethian and B. C. Vemuri, "Evolutionary fronts for topology independent shape modeling and recovery," in *Proceeding of the Third European Conference on Computer Vision*, Stockholm, Sweden, 1994.

29. V. Caselles, R. Kimmel and G. Sapiro, "Geodesic active contours," *International Journal of Computer Vision*, vol. 22, no. 1, pp. 61–79, 1997.
30. D. Mumford and J. Shah, "Optimal approximation by piecewise smooth functions and associated variational problems," *Communications on Pure and Applied Mathematics*, vol. 42, pp. 577–685, 1989.
31. N. Wiener, "The homogeneous chaos," *American Journal of Mathematics*, vol. 60, no. 4, pp. 897–936, 1938.
32. R. Ghanem and P. Spanos, Stochastic Finite Elements - A Spectral Approach, Mineola, New York, USA: Dover Publications, INC, 1991.
33. Y. Du, H. Budman and T. Duever, "Fault detection and diagnosis with parametric uncertainty using generalized polynomial chaos," *Computers and Chemical Engineering*, vol. 76, pp. 63–75, 2015.
34. L. He and S. Osher, "Solving the Chan-Vese Model by a multiphase level set algorithm based on the topological derivative," in *International Conference on Scale Space and Variational Methods in Computer Vision*, Ischia, Italy, 2007.
35. N. Badshah and K. Chen, "Multigrid method for the Chan-Vese model in variational segmentation," *Communications in Computational Physics*, vol. 4, no. 2, pp. 294–316, 2008.
36. G. Aubert and L. A. Vese, "A variational method in image recovery," *SIAM Journal of Numerical Analysis*, vol. 34, no. 5, pp. 1948–1979, 1997.
37. B. Debsschere, H. Najm, P. Pebay, O. Knio, R. Ghanem and O. Le Maitre, "Numerical challenges in the use of polynomial chaos representations for stochastic processes," *SIAM Journal of Scientific Computation*, vol. 26, no. 2, pp. 698–719, 2004.
38. L. A. Vese and T. F. Chan, "A multiphase level set framework for image segmentation using the Mumford and Shah model," *International Journal of Computer Vision*, vol. 50, no. 3, pp. 271–293, 2002.
39. Y. Du, H. Budman and T. Duever, "Segmentation and quantitative analysis of apoptosis of Chinese Hamster Ovary cells from fluorescence microscopy images," *Microscopy and Miscroanalysis*, vol. 23, no. 3, pp. 569–583, 2017.
40. Y. Du, H. Budman and T. Duever, "Parameter estimation for an inverse nonlinear stochastic problem: reactivity ratio studies in copolymerization," *Macromolecular Theory and Simulations*, vol. 26, no. 2, pp. 1–15, 2017.
41. Jordan, M. Ringenberg, Computerized 3D modeling and simulations of patient-specific cardiac anatomy fUom segmented MRI, Ph.D. Dissertation, The University of Toledo, December 2014.

10

Medical Image Segmentation Approach That Uses Level Sets with Statistical Shape Priors

1. S. Osher and R. P. Fedkiw, "Level set methods: an overview and some recent results," *Journal of Computational Physics*, vol. 169, no. 2, pp. 463–502, 2001.
2. M. Kass, A. Witkin, and D. Terzopoulos, "Snakes: Active contour models," *International Journal of Computer Vision*, vol. 1, no. 4, pp. 321–331, 1988.
3. A. S. El-Baz, A. A. Farag, H. A. El Munim, and S. E. Yuksel, "Level set segmentation using statistical shape priors," in *Computer Vision and Pattern Recognition Workshop, 2006. CVPRW'06. Conference on*. IEEE, 2006, pp. 78–78.
4. A. A. Amini, T. E. Weymouth, and R. C. Jain, "Using dynamic programming for solving variational problems in vision," *IEEE Transactions on Pattern Analysis and Machine Intelligence*, vol. 12, no. 9, pp. 855–867, 1990.
5. D. J. Williams and M. Shah, "A fast algorithm for active contours and curvature estimation," *CVGIP: Image Understanding*, vol. 55, no. 1, pp. 14–26, 1992.
6. Y. Wong, P. C. Yuen, and C. S. Tong, "Segmented snake for contour detection," *Pattern Recognition*, vol. 31, no. 11, pp. 1669–1679, 1998.
7. M. Wang, J. Evans, L. Hassebrook, and C. Knapp, "A multistage, optimal active contour model," *IEEE Transactions on Image Processing*, vol. 5, no. 11, pp. 1586–1591, 1996.
8. A. S. El-Baz, "Novel stochastic models for medical image analysis," Ph.D. dissertation, J.B. Speed School of Engineering, University of Louisville, 2006.
9. M. E. Leventon, W. E. L. Grimson, and O. Faugeras, "Statistical shape influence in geodesic active contours," in *Computer Vision and Pattern Recognition, 2000. Proceedings. IEEE Conference on*, vol. 1. IEEE, 2000, pp. 316–323.
10. D. Shen and C. Davatzikos, "An adaptive-focus deformable model using statistical and geometric information," *IEEE Transactions on Pattern Analysis and Machine Intelligence*, vol. 22, no. 8, pp. 906–913, 2000.
11. A. Tsai, A. Yezzi, W. Wells, C. Tempany, D. Tucker, A. Fan, W. E. Grimson, and A. Willsky, "A shape-based approach to the segmentation of medical imagery using level sets," *IEEE Transactions on Medical Imaging*, vol. 22, no. 2, pp. 137–154, 2003.
12. A. Tsai, W. Wells, C. Tempany, E. Grimson, and A. Willsky, "Mutual information in coupled multi-shape model for medical image segmentation," *Medical Image Analysis*, vol. 8, no. 4, pp. 429–445, 2004.
13. K. Pohl, J. Fisher, M. Shenton, R. McCarley, W. Grimson, R. Kikinis, and W. Wells, "Logarithm odds maps for shape representation," *Medical Image Computing and Computer-Assisted Intervention–MICCAI 2006*, pp. 955–963, 2006.

14. J. Yang and J. S. Duncan, "3d image segmentation of deformable objects with joint shape-intensity prior models using level sets," *Medical Image Analysis*, vol. 8, no. 3, pp. 285–294, 2004.
15. X. Huang, D. Metaxas, and T. Chen, "Metamorphs: Deformable shape and texture models," in *Computer Vision and Pattern Recognition, 2004. CVPR 2004. Proceedings of the 2004 IEEE Computer Society Conference on*, vol. 1. IEEE, 2004, pp. I–I.
16. M. Rousson, N. Paragios, and R. Deriche, "Implicit active shape models for 3d segmentation in mr imaging," in *International Conference on Medical Image Computing and Computer-Assisted Intervention*. Springer, 2004, pp. 209–216.
17. M. E. Leventon, "Statistical models in medical image analysis," Ph.D. dissertation, Citeseer, 2000.
18. T. B. Sebastian, P. N. Klein, and B. B. Kimia, "Recognition of shapes by editing shock graphs." in *ICCV*, vol. 1, 2001, pp. 755–762.
19. K. Siddiqi, A. Shokoufandeh, S. Dickenson, and S. W. Zucker, "Shock graphs and shape matching," in *Computer Vision, 1998. Sixth International Conference on*. IEEE, 1998, pp. 222–229.
20. S. Osher and J. A. Sethian, "Fronts propagating with curvature-dependent speed: algorithms based on hamilton-jacobi formulations," *Journal of Computational Physics*, vol. 79, no. 1, pp. 12–49, 1988.
21. J. A. Sethian, *Level set methods and fast marching methods: evolving interfaces in computational geometry, fluid mechanics, computer vision, and materials science*. Cambridge University Press, 1999, vol. 3.
22. R. Malladi, J. A. Sethian, and B. C. Vemuri, "Shape modeling with front propagation: A level set approach," *IEEE Transactions on Pattern Analysis and Machine Intelligence*, vol. 17, no. 2, pp. 158–175, 1995.
23. J. Gomes and O. Faugeras, "Reconciling distance functions and level sets," in *Biomedical Imaging, 2002. 5th IEEE EMBS International Summer School on*. IEEE, 2002, pp. 15–pp.
24. N. Paragios and R. Deriche, "Unifying boundary and region-based information for geodesic active tracking," in *Computer Vision and Pattern Recognition, 1999. IEEE Computer Society Conference on.*, vol. 2. IEEE, 1999, pp. 300–305.
25. X. Zeng, L. H. Staib, R. T. Schultz, H. Tagare, L. Win, and J. S. Duncan, "A new approach to 3d sulcal ribbon finding from mr images," in *International Conference on Medical Image Computing and Computer-Assisted Intervention*. Springer, 1999, pp. 148–157.
26. R. O. Duda, P. E. Hart, and D. G. Stork, *Pattern classification*. John Wiley & Sons, 2012.
27. C. Samson, L. Blanc-Féraud, G. Aubert, and J. Zerubia, "Multiphase evolution and variational image classification," Ph.D. dissertation, INRIA, 1999.
28. T. K. Moon, "The expectation-maximization algorithm," *IEEE Signal Processing Magazine*, vol. 13, no. 6, pp. 47–60, Nov 1996.
29. G. Gimel'farb, A. A. Farag, and A. El-Baz, "Expectation-maximization for a linear combination of gaussians," in *Proceedings of the 17th International Conference on Pattern Recognition, 2004. ICPR 2004.*, vol. 3, Aug 2004, pp. 422–425 Vol. 3.
30. P. Viola and W. M. Wells, "Alignment by maximization of mutual information," in *Computer Vision, 1995. Proceedings., Fifth International Conference on*. IEEE, 1995, pp. 16–23.

31. S. Ourselin, A. Roche, S. Prima, and N. Ayache, "Block matching: A general framework to improve robustness of rigid registration of medical images," in *International Conference on Medical Image Computing And Computer-Assisted Intervention*. Springer, 2000, pp. 557–566.
32. Y. Zhang, B. J. Matuszewski, L.-K. Shark, and C. J. Moore, "Medical image segmentation using new hybrid level-set method," in *BioMedical Visualization, 2008. MEDIVIS'08. Fifth International Conference*. IEEE, 2008, pp. 71–76.
33. A. M. Ali, A. A. Farag, and A. El-Baz, "Graph cuts framework for kidney segmentation with prior shape constraints," in *Proceedings of International Conference on Medical Image Computing and Computer-Assisted Intervention, (MICCAI'07)*, vol. 1, Brisbane, Australia, October 29–November 2, 2007, pp. 384–392.
34. A. S. Chowdhury, R. Roy, S. Bose, F. K. A. Elnakib, and A. El-Baz, "Non-rigid biomedical image registration using graph cuts with a novel data term," in *Proceedings of IEEE International Symposium on Biomedical Imaging: From Nano to Macro, (ISBI'12)*, Barcelona, Spain, May 2–5, 2012, pp. 446–449.
35. A. El-Baz, A. A. Farag, S. E. Yuksel, M. E. El-Ghar, T. A. Eldiasty, and M. A. Ghoneim, "Application of deformable models for the detection of acute renal rejection," in *Deformable models*. Springer, New York, NY, 2007, pp. 293–333.
36. A. El-Baz, A. Farag, R. Fahmi, S. Yuksel, M. A. El-Ghar, and T. Eldiasty, "Image analysis of renal DCE MRI for the detection of acute renal rejection," in *Proceedings of IAPR International Conference on Pattern Recognition (ICPR'06)*, Hong Kong, August 20–24, 2006, pp. 822–825.
37. A. El-Baz, A. Farag, R. Fahmi, S. Yuksel, W. Miller, M. A. El-Ghar, T. El-Diasty, and M. Ghoneim, "A new CAD system for the evaluation of kidney diseases using DCE-MRI," in *Proceedings of International Conference on Medical Image Computing and Computer-Assisted Intervention, (MICCAI'08)*, Copenhagen, Denmark, October 1–6, 2006, pp. 446–453.
38. A. El-Baz, G. Gimel'farb, and M. A. El-Ghar, "A novel image analysis approach for accurate identification of acute renal rejection," in *Proceedings of IEEE International Conference on Image Processing, (ICIP'08)*, San Diego, California, USA, October 12–15, 2008, pp. 1812–1815.
39. ——, "Image analysis approach for identification of renal transplant rejection," in *Proceedings of IAPR International Conference on Pattern Recognition, (ICPR'08)*, Tampa, Florida, USA, December 8–11, 2008, pp. 1–4.
40. ——, "New motion correction models for automatic identification of renal transplant rejection," in *Proceedings of International Conference on Medical Image Computing and Computer-Assisted Intervention, (MICCAI'07)*, Brisbane, Australia, October 29–November 2, 2007, pp. 235–243.
41. A. Farag, A. El-Baz, S. Yuksel, M. A. El-Ghar, and T. Eldiasty, "A framework for the detection of acute rejection with Dynamic Contrast Enhanced Magnetic Resonance Imaging," in *Proceedings of IEEE International Symposium on Biomedical Imaging: From Nano to Macro, (ISBI'06)*, Arlington, Virginia, USA, April 6–9, 2006, pp. 418–421.
42. F. Khalifa, G. M. Beache, M. A. El-Ghar, T. El-Diasty, G. Gimel'farb, M. Kong, and A. El-Baz, "Dynamic contrast-enhanced MRI-based early detection of acute renal transplant rejection," *IEEE Transactions on Medical Imaging*, vol. 32, no. 10, pp. 1910–1927, 2013.

43. F. Khalifa, A. El-Baz, G. Gimel'farb, and M. A. El-Ghar, "Non-invasive image-based approach for early detection of acute renal rejection," in *Proceedings of International Conference Medical Image Computing and Computer-Assisted Intervention, (MICCAI'10)*, Beijing, China, September 20–24, 2010, pp. 10–18.
44. F. Khalifa, A. El-Baz, G. Gimel'farb, R. Ouseph, and M. A. El-Ghar, "Shape-appearance guided level-set deformable model for image segmentation," in *Proceedings of IAPR International Conference on Pattern Recognition, (ICPR'10)*, Istanbul, Turkey, August 23–26, 2010, pp. 4581–4584.
45. F. Khalifa, M. A. El-Ghar, B. Abdollahi, H. Frieboes, T. El-Diasty, and A. El-Baz, "A comprehensive non-invasive framework for automated evaluation of acute renal transplant rejection using DCE-MRI," *NMR in Biomedicine*, vol. 26, no. 11, pp. 1460–1470, 2013.
46. F. Khalifa, M. A. El-Ghar, B. Abdollahi, H. B. Frieboes, T. El-Diasty, and A. El-Baz, "Dynamic contrast-enhanced MRI-based early detection of acute renal transplant rejection," in *2014 Annual Scientific Meeting and Educational Course Brochure of the Society of Abdominal Radiology, (SAR'14)*, Boca Raton, Florida, March 23–28, 2014, p. CID: 1855912.
47. F. Khalifa, A. Elnakib, G. M. Beache, G. Gimel'farb, M. A. El-Ghar, G. Sokhadze, S. Manning, P. McClure, and A. El-Baz, "3D kidney segmentation from CT images using a level set approach guided by a novel stochastic speed function," in *Proceedings of International Conference Medical Image Computing and Computer-Assisted Intervention, (MICCAI'11)*, Toronto, Canada, September 18–22, 2011, pp. 587–594.
48. F. Khalifa, G. Gimel'farb, M. A. El-Ghar, G. Sokhadze, S. Manning, P. McClure, R. Ouseph, and A. El-Baz, "A new deformable model-based segmentation approach for accurate extraction of the kidney from abdominal CT images," in *Proceedings of IEEE International Conference on Image Processing, (ICIP'11)*, Brussels, Belgium, September 11–14, 2011, pp. 3393–3396.
49. M. Mostapha, F. Khalifa, A. Alansary, A. Soliman, J. Suri, and A. El-Baz, "Computer-aided diagnosis systems for acute renal transplant rejection: Challenges and methodologies," in *Abdomen and Thoracic Imaging*, A. El-Baz and L. saba J. Suri, Eds. Springer, 2014, pp. 1–35.
50. M. Shehata, F. Khalifa, E. Hollis, A. Soliman, E. Hosseini-Asl, M. A. El-Ghar, M. El-Baz, A. C. Dwyer, A. El-Baz, and R. Keynton, "A new non-invasive approach for early classification of renal rejection types using diffusion-weighted mri," in *IEEE International Conference on Image Processing (ICIP), 2016*. IEEE, 2016, pp. 136–140.
51. F. Khalifa, A. Soliman, A. Takieldeen, M. Shehata, M. Mostapha, A. Shaffie, R. Ouseph, A. Elmaghraby, and A. El-Baz, "Kidney segmentation from CT images using a 3D NMF-guided active contour model," in *IEEE 13th International Symposium on Biomedical Imaging (ISBI), 2016*. IEEE, 2016, pp. 432–435.
52. M. Shehata, F. Khalifa, A. Soliman, A. Takieldeen, M. A. El-Ghar, A. Shaffie, A. C. Dwyer, R. Ouseph, A. El-Baz, and R. Keynton, "3d diffusion mri-based cad system for early diagnosis of acute renal rejection," in *Biomedical Imaging (ISBI), 2016 IEEE 13th International Symposium on*. IEEE, 2016, pp. 1177–1180.
53. M. Shehata, F. Khalifa, A. Soliman, R. Alrefai, M. A. El-Ghar, A. C. Dwyer, R. Ouseph, and A. El-Baz, "A level set-based framework for 3d kidney segmentation from diffusion mr images," in *IEEE International Conference on Image Processing (ICIP), 2015*. IEEE, 2015, pp. 4441–4445.

54. M. Shehata, F. Khalifa, A. Soliman, M. A. El-Ghar, A. C. Dwyer, G. Gimel'farb, R. Keynton, and A. El-Baz, "A promising non-invasive cad system for kidney function assessment," in *International Conference on Medical Image Computing and Computer-Assisted Intervention*. Springer, 2016, pp. 613–621.
55. F. Khalifa, A. Soliman, A. Elmaghraby, G. Gimel'farb, and A. El-Baz, "3d kidney segmentation from abdominal images using spatial-appearance models," *Computational and mathematical methods in medicine*, vol. 2017, pp. 1–10, 2017.
56. E. Hollis, M. Shehata, F. Khalifa, M. A. El-Ghar, T. El-Diasty, and A. El-Baz, "Towards non-invasive diagnostic techniques for early detection of acute renal transplant rejection: A review," *The Egyptian Journal of Radiology and Nuclear Medicine*, vol. 48, no. 1, pp. 257–269, 2016.
57. M. Shehata, F. Khalifa, A. Soliman, M. A. El-Ghar, A. C. Dwyer, and A. El-Baz, "Assessment of renal transplant using image and clinical-based biomarkers," in *Proceedings of 13th Annual Scientific Meeting of American Society for Diagnostics and Interventional Nephrology (ASDIN'17), New Orleans, LA, USA, February 10-12, 2017*, 2017.
58. ——, "Early assessment of acute renal rejection," in *Proceedings of 12th Annual Scientific Meeting of American Society for Diagnostics and Interventional Nephrology (ASDIN'16), Pheonix, AZ, USA, February 19-21, 2016*, 2017.
59. F. Khalifa, G. Beache, A. El-Baz, and G. Gimel'farb, "Deformable model guided by stochastic speed with application in cine images segmentation," in *Proceedings of IEEE International Conference on Image Processing, (ICIP'10)*, Hong Kong, September 26–29, 2010, pp. 1725–1728.
60. F. Khalifa, G. M. Beache, A. Elnakib, H. Sliman, G. Gimel'farb, K. C. Welch, and A. El-Baz, "A new shape-based framework for the left ventricle wall segmentation from cardiac first-pass perfusion MRI," in *Proceedings of IEEE International Symposium on Biomedical Imaging: From Nano to Macro, (ISBI'13)*, San Francisco, CA, April 7–11, 2013, pp. 41–44.
61. ——, "A new nonrigid registration framework for improved visualization of transmural perfusion gradients on cardiac first–pass perfusion MRI," in *Proceedings of IEEE International Symposium on Biomedical Imaging: From Nano to Macro, (ISBI'12)*, Barcelona, Spain, May 2–5, 2012, pp. 828–831.
62. F. Khalifa, G. M. Beache, A. Firjani, K. C. Welch, G. Gimel'farb, and A. El-Baz, "A new nonrigid registration approach for motion correction of cardiac first-pass perfusion MRI," in *Proceedings of IEEE International Conference on Image Processing, (ICIP'12)*, Lake Buena Vista, Florida, September 30–October 3, 2012, pp. 1665–1668.
63. F. Khalifa, G. M. Beache, G. Gimel'farb, and A. El-Baz, "A novel CAD system for analyzing cardiac first-pass MR images," in *Proceedings of IAPR International Conference on Pattern Recognition (ICPR'12)*, Tsukuba Science City, Japan, November 11–15, 2012, pp. 77–80.
64. ——, "A novel approach for accurate estimation of left ventricle global indexes from short-axis cine MRI," in *Proceedings of IEEE International Conference on Image Processing, (ICIP'11)*, Brussels, Belgium, September 11–14, 2011, pp. 2645–2649.
65. F. Khalifa, G. M. Beache, G. Gimel'farb, G. A. Giridharan, and A. El-Baz, "A new image-based framework for analyzing cine images," in *Handbook of Multi Modality State-of-the-Art Medical Image Segmentation and Registration Methodologies*, A. El-Baz, U. R. Acharya, M. Mirmedhdi, and J. S. Suri, Eds. Springer, New York, 2011, vol. 2, ch. 3, pp. 69–98.

66. ——, "Accurate automatic analysis of cardiac cine images," *IEEE Transactions on Biomedical Engineering*, vol. 59, no. 2, pp. 445–455, 2012.
67. F. Khalifa, G. M. Beache, M. Nitzken, G. Gimel'farb, G. A. Giridharan, and A. El-Baz, "Automatic analysis of left ventricle wall thickness using short-axis cine CMR images," in *Proceedings of IEEE International Symposium on Biomedical Imaging: From Nano to Macro, (ISBI'11)*, Chicago, Illinois, March 30–April 2, 2011, pp. 1306–1309.
68. M. Nitzken, G. Beache, A. Elnakib, F. Khalifa, G. Gimel'farb, and A. El-Baz, "Accurate modeling of tagged cmr 3D image appearance characteristics to improve cardiac cycle strain estimation," in *Image Processing (ICIP), 2012 19th IEEE International Conference on*. Orlando, Florida, USA: IEEE, Sep. 2012, pp. 521–524.
69. ——, "Improving full-cardiac cycle strain estimation from tagged cmr by accurate modeling of 3D image appearance characteristics," in *Biomedical Imaging (ISBI), 2012 9th IEEE International Symposium on*. Barcelona, Spain: IEEE, May 2012, pp. 462–465, (Selected for oral presentation).
70. M. J. Nitzken, A. S. El-Baz, and G. M. Beache, "Markov-gibbs random field model for improved full-cardiac cycle strain estimation from tagged cmr," *Journal of Cardiovascular Magnetic Resonance*, vol. 14, no. 1, pp. 1–2, 2012.
71. H. Sliman, A. Elnakib, G. Beache, A. Elmaghraby, and A. El-Baz, "Assessment of myocardial function from cine cardiac MRI using a novel 4D tracking approach," *J Comput Sci Syst Biol*, vol. 7, pp. 169–173, 2014.
72. H. Sliman, A. Elnakib, G. M. Beache, A. Soliman, F. Khalifa, G. Gimel'farb, A. Elmaghraby, and A. El-Baz, "A novel 4D PDE-based approach for accurate assessment of myocardium function using cine cardiac magnetic resonance images," in *Proceedings of IEEE International Conference on Image Processing (ICIP'14)*, Paris, France, October 27–30, 2014, pp. 3537–3541.
73. H. Sliman, F. Khalifa, A. Elnakib, G. M. Beache, A. Elmaghraby, and A. El-Baz, "A new segmentation-based tracking framework for extracting the left ventricle cavity from cine cardiac MRI," in *Proceedings of IEEE International Conference on Image Processing, (ICIP'13)*, Melbourne, Australia, September 15–18, 2013, pp. 685–689.
74. H. Sliman, F. Khalifa, A. Elnakib, A. Soliman, G. M. Beache, A. Elmaghraby, G. Gimel'farb, and A. El-Baz, "Myocardial borders segmentation from cine MR images using bi-directional coupled parametric deformable models," *Medical Physics*, vol. 40, no. 9, pp. 1–13, 2013.
75. H. Sliman, F. Khalifa, A. Elnakib, A. Soliman, G. M. Beache, G. Gimel'farb, A. Emam, A. Elmaghraby, and A. El-Baz, "Accurate segmentation framework for the left ventricle wall from cardiac cine MRI," in *Proceedings of International Symposium on Computational Models for Life Science, (CMLS'13)*, vol. 1559, Sydney, Australia, November 27–29, 2013, pp. 287–296.
76. N. Eladawi, M. Elmogy, M. Ghazal, O. Helmy, A. Aboelfetouh, A. Riad, S. Schaal, and A. El-Baz, "Classification of retinal diseases based on oct images," *Front Biosci (Landmark Ed)*, vol. 23, pp. 247–264, 2018.
77. A. ElTanboly, M. Ismail, A. Shalaby, A. Switala, A. El-Baz, S. Schaal, G. Gimel'farb, and M. El-Azab, "A computer-aided diagnostic system for detecting diabetic retinopathy in optical coherence tomography images," *Medical Physics*, vol. 44, no. 3, pp. 914–923, 2017.

78. B. Abdollahi, A. C. Civelek, X.-F. Li, J. Suri, and A. El-Baz, "PET/CT nodule segmentation and diagnosis: A survey," in *Multi Detector CT Imaging*, L. Saba and J. S. Suri, Eds. Taylor , Francis, 2014, ch. 30, pp. 639–651.
79. B. Abdollahi, A. El-Baz, and A. A. Amini, "A multi-scale non-linear vessel enhancement technique," in *Engineering in Medicine and Biology Society, EMBC, 2011 Annual International Conference of the IEEE*. IEEE, 2011, pp. 3925–3929.
80. B. Abdollahi, A. Soliman, A. Civelek, X.-F. Li, G. Gimel'farb, and A. El-Baz, "A novel gaussian scale space-based joint MGRF framework for precise lung segmentation," in *Proceedings of IEEE International Conference on Image Processing, (ICIP'12)*. IEEE, 2012, pp. 2029–2032.
81. B. Abdollahi, A. Soliman, A. Civelek, X.-F. Li, G. Gimel'farb, and A. El-Baz, "A novel 3D joint MGRF framework for precise lung segmentation," in *Machine Learning in Medical Imaging*. Springer, 2012, pp. 86–93.
82. A. M. Ali, A. S. El-Baz, and A. A. Farag, "A novel framework for accurate lung segmentation using graph cuts," in *Proceedings of IEEE International Symposium on Biomedical Imaging: From Nano to Macro, (ISBI'07)*. IEEE, 2007, pp. 908–911.
83. A. El-Baz, G. M. Beache, G. Gimel'farb, K. Suzuki, and K. Okada, "Lung imaging data analysis," *International journal of biomedical imaging*, vol. 2013, pp. 1–2, 2013.
84. A. El-Baz, G. M. Beache, G. Gimel'farb, K. Suzuki, K. Okada, A. Elnakib, A. Soliman, and B. Abdollahi, "Computer-aided diagnosis systems for lung cancer: Challenges and methodologies," *International Journal of Biomedical Imaging*, vol. 2013, pp. 1–46, 2013.
85. A. El-Baz, A. Elnakib, M. Abou El-Ghar, G. Gimel'farb, R. Falk, and A. Farag, "Automatic detection of 2D and 3D lung nodules in chest spiral CT scans," *International Journal of Biomedical Imaging*, vol. 2013, pp. 1–11, 2013.
86. A. El-Baz, A. A. Farag, R. Falk, and R. La Rocca, "A unified approach for detection, visualization, and identification of lung abnormalities in chest spiral CT scans," in *International Congress Series*, vol. 1256. Elsevier, 2003, pp. 998–1004.
87. ——, "Detection, visualization and identification of lung abnormalities in chest spiral CT scan: Phase-I," in *Proceedings of International conference on Biomedical Engineering, Cairo, Egypt*, vol. 12, no. 1, 2002.
88. A. El-Baz, A. Farag, G. Gimel'farb, R. Falk, M. A. El-Ghar, and T. Eldiasty, "A framework for automatic segmentation of lung nodules from low dose chest CT scans," in *Proceedings of International Conference on Pattern Recognition, (ICPR'06)*, vol. 3. IEEE, 2006, pp. 611–614.
89. A. El-Baz, A. Farag, G. Gimel'farb, R. Falk, and M. A. El-Ghar, "A novel level set-based computer-aided detection system for automatic detection of lung nodules in low dose chest computed tomography scans," *Lung Imaging and Computer Aided Diagnosis*, vol. 10, pp. 221–238, 2011.
90. A. El-Baz, G. Gimel'farb, M. Abou El-Ghar, and R. Falk, "Appearance-based diagnostic system for early assessment of malignant lung nodules," in *Proceedings of IEEE International Conference on Image Processing, (ICIP'12)*. IEEE, 2012, pp. 533–536.
91. A. El-Baz, G. Gimel'farb, and R. Falk, "A novel 3D framework for automatic lung segmentation from low dose CT images," in *Lung Imaging and Computer Aided Diagnosis*, A. El-Baz and J. S. Suri, Eds. Taylor , Francis, 2011, ch. 1, pp. 1–16.
92. A. El-Baz, G. Gimel'farb, R. Falk, and M. El-Ghar, "Appearance analysis for diagnosing malignant lung nodules," in *Proceedings of IEEE International Symposium on Biomedical Imaging: From Nano to Macro (ISBI'10)*. IEEE, 2010, pp. 193–196.

93. A. El-Baz, G. Gimel'farb, R. Falk, and M. A. El-Ghar, "A novel level set-based CAD system for automatic detection of lung nodules in low dose chest CT scans," in *Lung Imaging and Computer Aided Diagnosis*, A. El-Baz and J. S. Suri, Eds. Taylor , Francis, 2011, vol. 1, ch. 10, pp. 221–238.
94. ——, "A new approach for automatic analysis of 3D low dose CT images for accurate monitoring the detected lung nodules," in *Proceedings of International Conference on Pattern Recognition, (ICPR'08)*. IEEE, 2008, pp. 1–4.
95. ——, "A novel approach for automatic follow-up of detected lung nodules," in *Proceedings of IEEE International Conference on Image Processing, (ICIP'07)*, vol. 5. IEEE, 2007, pp. V–501.
96. ——, "A new CAD system for early diagnosis of detected lung nodules," in *Image Processing, 2007. ICIP 2007. IEEE International Conference on*, vol. 2. IEEE, 2007, pp. II–461.
97. A. El-Baz, G. Gimel'farb, R. Falk, M. A. El-Ghar, and H. Refaie, "Promising results for early diagnosis of lung cancer," in *Proceedings of IEEE International Symposium on Biomedical Imaging: From Nano to Macro, (ISBI'08)*. IEEE, 2008, pp. 1151–1154.
98. A. El-Baz, G. L. Gimel'farb, R. Falk, M. Abou El-Ghar, T. Holland, and T. Shaffer, "A new stochastic framework for accurate lung segmentation," in *Proceedings of Medical Image Computing and Computer-Assisted Intervention, (MICCAI'08)*, 2008, pp. 322–330.
99. A. El-Baz, G. L. Gimel'farb, R. Falk, D. Heredis, and M. Abou El-Ghar, "A novel approach for accurate estimation of the growth rate of the detected lung nodules," in *Proceedings of International Workshop on Pulmonary Image Analysis*, 2008, pp. 33–42.
100. A. El-Baz, G. L. Gimel'farb, R. Falk, T. Holland, and T. Shaffer, "A framework for unsupervised segmentation of lung tissues from low dose computed tomography images," in *Proceedings of British Machine Vision, (BMVC'08)*, 2008, pp. 1–10.
101. A. El-Baz, G. Gimel'farb, R. Falk, and M. A. El-Ghar, "3D MGRF-based appearance modeling for robust segmentation of pulmonary nodules in 3D LDCT chest images," in *Lung Imaging and Computer Aided Diagnosis*. 2011, ch. 3, pp. 51–63.
102. ——, "Automatic analysis of 3D low dose CT images for early diagnosis of lung cancer," *Pattern Recognition*, vol. 42, no. 6, pp. 1041–1051, 2009.
103. A. El-Baz, G. Gimel'farb, R. Falk, M. A. El-Ghar, S. Rainey, D. Heredia, and T. Shaffer, "Toward early diagnosis of lung cancer," in *Proceedings of Medical Image Computing and Computer-Assisted Intervention, (MICCAI'09)*. Springer, 2009, pp. 682–689.
104. A. El-Baz, G. Gimel'farb, R. Falk, M. A. El-Ghar, and J. Suri, "Appearance analysis for the early assessment of detected lung nodules," in *Lung Imaging and Computer Aided Diagnosis*. 2011, ch. 17, pp. 395–404.
105. A. El-Baz, F. Khalifa, A. Elnakib, M. Nitkzen, A. Soliman, P. McClure, G. Gimel'farb, and M. A. El-Ghar, "A novel approach for global lung registration using 3D Markov Gibbs appearance model," in *Proceedings of International Conference Medical Image Computing and Computer-Assisted Intervention, (MICCAI'12)*, Nice, France, October 1–5, 2012, pp. 114–121.

106. A. El-Baz, M. Nitzken, A. Elnakib, F. Khalifa, G. Gimel'farb, R. Falk, and M. A. El-Ghar, "3D shape analysis for early diagnosis of malignant lung nodules," in *Proceedings of International Conference Medical Image Computing and Computer-Assisted Intervention, (MICCAI'11)*, Toronto, Canada, September 18–22, 2011, pp. 175–182.
107. A. El-Baz, M. Nitzken, G. Gimel'farb, E. Van Bogaert, R. Falk, M. A. El-Ghar, and J. Suri, "Three-dimensional shape analysis using spherical harmonics for early assessment of detected lung nodules," in *Lung Imaging and Computer Aided Diagnosis*. 2011, ch. 19, pp. 421–438.
108. A. El-Baz, M. Nitzken, F. Khalifa, A. Elnakib, G. Gimel'farb, R. Falk, and M. A. El-Ghar, "3D shape analysis for early diagnosis of malignant lung nodules," in *Proceedings of International Conference on Information Processing in Medical Imaging, (IPMI'11)*, Monastery Irsee, Germany (Bavaria), July 3–8, 2011, pp. 772–783.
109. A. El-Baz, M. Nitzken, E. Vanbogaert, G. Gimel'Farb, R. Falk, and M. Abo El-Ghar, "A novel shape-based diagnostic approach for early diagnosis of lung nodules," in *Biomedical Imaging: From Nano to Macro, 2011 IEEE International Symposium on*. IEEE, 2011, pp. 137–140.
110. A. El-Baz, P. Sethu, G. Gimel'farb, F. Khalifa, A. Elnakib, R. Falk, and M. A. El-Ghar, "Elastic phantoms generated by microfluidics technology: Validation of an imaged-based approach for accurate measurement of the growth rate of lung nodules," *Biotechnology Journal*, vol. 6, no. 2, pp. 195–203, 2011.
111. ——, "A new validation approach for the growth rate measurement using elastic phantoms generated by state-of-the-art microfluidics technology," in *Proceedings of IEEE International Conference on Image Processing, (ICIP'10)*, Hong Kong, September 26–29, 2010, pp. 4381–4383.
112. A. El-Baz, P. Sethu, G. Gimel'farb, F. Khalifa, A. Elnakib, R. Falk, and M. A. E.-G. J. Suri, "Validation of a new imaged-based approach for the accurate estimating of the growth rate of detected lung nodules using real CT images and elastic phantoms generated by state-of-the-art microfluidics technology," in *Handbook of Lung Imaging and Computer Aided Diagnosis*, A. El-Baz and J. S. Suri, Eds. Taylor & Francis, New York, 2011, vol. 1, ch. 18, pp. 405–420.
113. A. El-Baz, A. Soliman, P. McClure, G. Gimel'farb, M. A. El-Ghar, and R. Falk, "Early assessment of malignant lung nodules based on the spatial analysis of detected lung nodules," in *Proceedings of IEEE International Symposium on Biomedical Imaging: From Nano to Macro, (ISBI'12)*. IEEE, 2012, pp. 1463–1466.
114. A. El-Baz, S. E. Yuksel, S. Elshazly, and A. A. Farag, "Non-rigid registration techniques for automatic follow-up of lung nodules," in *Proceedings of Computer Assisted Radiology and Surgery, (CARS'05)*, vol. 1281. Elsevier, 2005, pp. 1115–1120.
115. A. S. El-Baz and J. S. Suri, *Lung Imaging and Computer Aided Diagnosis*. CRC Press, 2011.
116. A. oliman, F. Khalifa, A. Shaffie, N. Liu, N. Dunlap, B. Wang, A. Elmaghraby, G. Gimel'farb, and A. El-Baz, "Image-based cad system for accurate identification of lung injury," in *Proceedings of IEEE International Conference on Image Processing, (ICIP'16)*. IEEE, 2016, pp. 121–125.
117. A. Soliman, F. Khalifa, N. Dunlap, B. Wang, M. El-Ghar, and A. El-Baz, "An iso-surfaces based local deformation handling framework of lung tissues," in *Biomedical Imaging (ISBI), 2016 IEEE 13th International Symposium on*. IEEE, 2016, pp. 1253–1259.

118. A. Soliman, F. Khalifa, A. Shaffie, N. Dunlap, B. Wang, A. Elmaghraby, and A. El-Baz, "Detection of lung injury using 4d-ct chest images," in *Biomedical Imaging (ISBI), 2016 IEEE 13th International Symposium on*. IEEE, 2016, pp. 1274–1277.
119. A. Soliman, F. Khalifa, A. Shaffie, N. Dunlap, B. Wang, A. Elmaghraby, G. Gimel'farb, M. Ghazal, and A. El-Baz, "A comprehensive framework for early assessment of lung injury," in *Image Processing (ICIP), 2017 IEEE International Conference on*. IEEE, 2017, pp. 3275–3279.
120. A. Shaffie, A. Soliman, M. Ghazal, F. Taher, N. Dunlap, B. Wang, A. Elmaghraby, G. Gimel'farb, and A. El-Baz, "A new framework for incorporating appearance and shape features of lung nodules for precise diagnosis of lung cancer," in *Image Processing (ICIP), 2017 IEEE International Conference on*. IEEE, 2017, pp. 1372–1376.
121. A. Soliman, F. Khalifa, A. Shaffie, N. Liu, N. Dunlap, B. Wang, A. Elmaghraby, G. Gimel'farb, and A. El-Baz, "Image-based cad system for accurate identification of lung injury," in *Image Processing (ICIP), 2016 IEEE International Conference on*. IEEE, 2016, pp. 121–125.
122. B. Dombroski, M. Nitzken, A. Elnakib, F. Khalifa, A. El-Baz, and M. F. Casanova, "Cortical surface complexity in a population-based normative sample," *Translational Neuroscience*, vol. 5, no. 1, pp. 17–24, 2014.
123. A. El-Baz, M. Casanova, G. Gimel'farb, M. Mott, and A. Switala, "An MRI-based diagnostic framework for early diagnosis of dyslexia," *International Journal of Computer Assisted Radiology and Surgery*, vol. 3, no. 3-4, pp. 181–189, 2008.
124. A. El-Baz, M. Casanova, G. Gimel'farb, M. Mott, A. Switala, E. Vanbogaert, and R. McCracken, "A new CAD system for early diagnosis of dyslexic brains," in *Proc. International Conference on Image Processing (ICIP'2008)*. IEEE, 2008, pp. 1820–1823.
125. A. El-Baz, M. F. Casanova, G. Gimel'farb, M. Mott, and A. E. Switwala, "A new image analysis approach for automatic classification of autistic brains," in *Proc. IEEE International Symposium on Biomedical Imaging: From Nano to Macro (ISBI'2007)*. IEEE, 2007, pp. 352–355.
126. A. El-Baz, A. Elnakib, F. Khalifa, M. A. El-Ghar, P. McClure, A. Soliman, and G. Gimel'farb, "Precise segmentation of 3-D magnetic resonance angiography," *IEEE Transactions on Biomedical Engineering*, vol. 59, no. 7, pp. 2019–2029, 2012.
127. A. El-Baz, A. Farag, G. Gimel'farb, M. A. El-Ghar, and T. Eldiasty, "Probabilistic modeling of blood vessels for segmenting mra images," in *18th International Conference on Pattern Recognition (ICPR'06)*, vol. 3. IEEE, 2006, pp. 917–920.
128. A. El-Baz, A. A. Farag, G. Gimel'farb, M. A. El-Ghar, and T. Eldiasty, "A new adaptive probabilistic model of blood vessels for segmenting mra images," in *Medical Image Computing and Computer-Assisted Intervention–MICCAI 2006*, vol. 4191. Springer, 2006, pp. 799–806.
129. A. El-Baz, A. A. Farag, G. Gimel'farb, and S. G. Hushek, "Automatic cerebrovascular segmentation by accurate probabilistic modeling of tof-mra images," in *Medical Image Computing and Computer-Assisted Intervention–MICCAI 2005*. Springer, 2005, pp. 34–42.
130. A. El-Baz, A. Farag, A. Elnakib, M. F. Casanova, G. Gimel'farb, A. E. Switala, D. Jordan, and S. Rainey, "Accurate automated detection of autism related corpus callosum abnormalities," *Journal of Medical Systems*, vol. 35, no. 5, pp. 929–939, 2011.

131. A. El-Baz, A. Farag, and G. Gimel'farb, "Cerebrovascular segmentation by accurate probabilistic modeling of tof-mra images," in *Image Analysis*, vol. 3540. Springer, 2005, pp. 1128–1137.
132. A. El-Baz, G. Gimel'farb, R. Falk, M. A. El-Ghar, V. Kumar, and D. Heredia, "A novel 3D joint Markov-gibbs model for extracting blood vessels from PC–mra images," in *Medical Image Computing and Computer-Assisted Intervention–MICCAI 2009*, vol. 5762. Springer, 2009, pp. 943–950.
133. A. Elnakib, A. El-Baz, M. F. Casanova, G. Gimel'farb, and A. E. Switala, "Image-based detection of corpus callosum variability for more accurate discrimination between dyslexic and normal brains," in *Proc. IEEE International Symposium on Biomedical Imaging: From Nano to Macro (ISBI'2010)*. IEEE, 2010, pp. 109–112.
134. A. Elnakib, M. F. Casanova, G. Gimel'farb, A. E. Switala, and A. El-Baz, "Autism diagnostics by centerline-based shape analysis of the corpus callosum," in *Proc. IEEE International Symposium on Biomedical Imaging: From Nano to Macro (ISBI'2011)*. IEEE, 2011, pp. 1843–1846.
135. A. Elnakib, M. Nitzken, M. Casanova, H. Park, G. Gimel'farb, and A. El-Baz, "Quantification of age-related brain cortex change using 3D shape analysis," in *Pattern Recognition (ICPR), 2012 21st International Conference on*. IEEE, 2012, pp. 41–44.
136. M. Mostapha, A. Soliman, F. Khalifa, A. Elnakib, A. Alansary, M. Nitzken, M. F. Casanova, and A. El-Baz, "A statistical framework for the classification of infant dt images," in *Image Processing (ICIP), 2014 IEEE International Conference on*. IEEE, 2014, pp. 2222–2226.
137. M. Nitzken, M. Casanova, G. Gimel'farb, A. Elnakib, F. Khalifa, A. Switala, and A. El-Baz, "3D shape analysis of the brain cortex with application to dyslexia," in *Image Processing (ICIP), 2011 18th IEEE International Conference on*. Brussels, Belgium: IEEE, Sep. 2011, pp. 2657–2660, (Selected for oral presentation. Oral acceptance rate is 10 percent and the overall acceptance rate is 35 percent).
138. F. E.-Z. A. El-Gamal, M. M. Elmogy, M. Ghazal, A. Atwan, G. N. Barnes, M. F. Casanova, R. Keynton, and A. S. El-Baz, "A novel cad system for local and global early diagnosis of alzheimer's disease based on pib-pet scans," in *2017 IEEE International Conference on Image Processing (ICIP)*. IEEE, 2017, pp. 3270–3274.
139. M. Ismail, A. Soliman, M. Ghazal, A. E. Switala, G. Gimel'farb, G. N. Barnes, A. Khalil, and A. El-Baz, "A fast stochastic framework for automatic mr brain images segmentation," 2017.
140. M. M. Ismail, R. S. Keynton, M. M. Mostapha, A. H. ElTanboly, M. F. Casanova, G. L. Gimel'farb, and A. El-Baz, "Studying autism spectrum disorder with structural and diffusion magnetic resonance imaging: a survey," *Frontiers in Human Neuroscience*, vol. 10, p. 211, 2016.
141. A. Alansary, M. Ismail, A. Soliman, F. Khalifa, M. Nitzken, A. Elnakib, M. Mostapha, A. Black, K. Stinebruner, M. F. Casanova *et al.*, "Infant brain extraction in t1-weighted mr images using bet and refinement using lcdg and mgrf models," *IEEE Journal of Biomedical and Health Informatics*, vol. 20, no. 3, pp. 925–935, 2016.
142. M. Ismail, A. Soliman, A. ElTanboly, A. Switala, M. Mahmoud, F. Khalifa, G. Gimel'farb, M. F. Casanova, R. Keynton, and A. El-Baz, "Detection of white matter abnormalities in mr brain images for diagnosis of autism in children," pp. 6–9, 2016.

143. M. Ismail, M. Mostapha, A. Soliman, M. Nitzken, F. Khalifa, A. Elnakib, G. Gimel'farb, M. Casanova, and A. El-Baz, "Segmentation of infant brain mr images based on adaptive shape prior and higher-order mgrf," pp. 4327–4331, 2015.
144. A. Mahmoud, A. El-Barkouky, H. Farag, J. Graham, and A. Farag, "A non-invasive method for measuring blood flow rate in superficial veins from a single thermal image," in *Proceedings of the IEEE Conference on Computer Vision and Pattern Recognition Workshops*, 2013, pp. 354–359.
145. A. El-baz, A. Shalaby, F. Taher, M. El-Baz, M. Ghazal, M. A. El-Ghar, A. Takieldeen, and J. Suri, "Probabilistic modeling of blood vessels for segmenting magnetic resonance angiography images," 2017, vol. 5, no. 3.
146. A. S. Chowdhury, A. K. Rudra, M. Sen, A. Elnakib, and A. El-Baz, "Cerebral white matter segmentation from MRI using probabilistic graph cuts and geometric shape priors." in *ICIP*, 2010, pp. 3649–3652.

11

Level Set Method in Medical Imaging Segmentation

1. Ayed B., Mitchie A., and Belhadj Z. Multiregion level-set partitioning of synthetic aperture radar images. *IEEE Trans Pattern Anal Mach Intell.* 2005; 27: 793–800; doi: 10.1109/TPAMI.2005.106.
2. Pham D. L., Xu C., and Prince J. Current methods in medical image segmentation. *Ann Rev Biomed Eng.* 2000; 2: 315–338.
3. Cai Q., Aggarwal J. Human motion analysis: A review. *Comput Vis Image Underst.* 1999; 73: 428–440; doi: 10.1109/NAMW.1997.609859.
4. Zhao T., Nevatia R., Wu B. Segmentation and tracking of multiple humans in crowded environments. *IEEE Trans Pattern Anal Mach Intell.* 2008; 30: 1198–1211; doi: 10.1109/TPAMI.2007.70770.
5. Caselles V., Kimmel R., and Sapiro G. Geodesic active contours. *Int J Comput Vis.* 1997; 22: 61–79; doi: 10.1023/A:10079798.
6. Chan T. and Vese L. Active contours without edges. *IEEE Trans on Image Proc.* 2001; 10: 266–277; doi: 10.1016/S1470-2045(12)70388–1.
7. Li C., Kao C. Y., Gore J. C., Ding Z. Minimization of region-scalable fitting energy for image segmentation. *IEEE Trans on Image Proc.* 2008; 17: 1940–1949; doi: 10.1007/978-3-642–17274-8_12.
8. Mansouri A.-R., Mitiche A., Vazquez C. Multiregion competition: A level set extension of region competition to multiple region image partitioning. *Comput Vis Image Underst*. 2006;101:137–150; doi: 10.1200/JCO.2012.44.0586.
9. Vese L., Chan T. A multiphase level set framework for image segmentation using the Mumford and Shah model. *Int J Comput Vis.* 2002; 50: 271–293; doi: 10.1023/A:1020874308076.
10. Lankton S., Tannenbaum A. Localizing region-based active contours. *IEEE Trans on Image Proc.* 2008; 17 (11): 2029–2039; doi: 10.1109/TIP.2008.2004611.
11. Brox T., Weickert J. Level set segmentation with multiple regions. *IEEE Trans on Image Proc.* 2006; 15(10): 3213–3218; doi: 10.1109/TIP.2006.877481.
12. Cremers D., Rousson M., Deriche R. A review of statistical approaches to level set segmentation: Integrating color, texture, motion and shape. *Int J Comput Vis.* 2007; 72(2): 195–215; doi: 10.1007/s11263-006-8711-1A.
13. Bertelli L., Sumengen B., Manjunath B., Gibou F. A variational framework for multi-region pairwise similarity-based image segmentation. *IEEE Trans Pattern Anal Mach Intell.* 2008; 30(8): 1400–1414; doi: 10.1109/TPAMI.2007.70785.

14. Li C. M., Kao C. Y., Gore J. C., Ding Z. Implicit active contours driven by local binary fitting energy. *Proc of IEEE Conf Comput Vis and Pattern Recog* 2007;1–7; doi: 10.1109/CVPR.2007.383014.
15. Brox T. and Cremers D. On local region models and a statistical interpretation of the piecewise smooth Mumford-Shah functional. *Int J Comput Vis.* 2009; 84(2): 184–193; doi: 10.1007/s11263-008-0153-5.
16. Mumford D., and Shah J. Optimal approximations by piecewise smooth functions and associated variational problems. *Commun Pure Appl Math.* 1989; 42(5): 577–685.
17. Li C. M., Xu C., Gui C., Fox M. D. Level set evolution without re-initialization: A new variational formulation. *Proc of IEEE Conf Comput Vis and Pattern Recog*. 2005; 430–436; doi: 10.1109/CVPR.2005.213.
18. Law Y. N., Lee H. K., Yip A. M. A multiresolution stochastic level set method for Mumford-Shah image segmentation. *IEEE Trans on Image Proc.* 2008; 17(12): 2289–2300; doi: 10.1109/TIP.2008.2005823.
19. Bazi Y., Melgani F., Al-Sharari H. D. Unsupervised change detection in multispectral remotely sensed imagery with level set methods. *IEEE Trans. on Geoscience & Remote Sensing*. 2010; 48(8): 3178–3187; doi: 10.1109/TGRS.2010.2045506.
20. Zhu G. P., Zhang S. Q., Zeng Q. S., Wang C. H. Boundary-based image segmentation using binary level set method. *Opt. Eng.* 2007; 46: 050501; doi: 10.1117/1.2740762.
21. Zhu G. P., Zeng Q. S., Wang C. H. Dual geometric active contour for image segmentation. *Opt. Eng.* 2006; 45: 080505; doi: 10.1117/1.2333566.
22. Liu F., Luo Y. Q., Hu D. C. Adaptive level set image segmentation using the Mumford and Shah functional. *Opt. Eng.* 2002; 41: 3002–3003; doi: 10.1117/1.1519542.
23. Zhu S. C., Yuille A. Region competition: unifying snakes, region growing, and Bayes/MDL for multiband image segmentation. *IEEE Trans Pattern Anal Mach Intell.* 1996; 18(9): 884–900; doi: 10.1109/34.537343.
24. Martin P., Refregier P., Goudail F., Guerault F. Influence of the noise model on level set active contour segmentation. *IEEE Trans Pattern Anal Mach Intell.* 2004; 26(6): 799–803; doi: 10.1109/TPAMI.2004.11.
25. Kim J., Fisher J. W., Yezzi A., Cetin M. Nonparametric methods for image segmentation using information theory and curve evolution. In *Int. Conf. on Image Processing.* 2002; 3: 797–800; doi: 10.1109/ICIP.2002.1039092.
26. Ayed I. B., Mitiche A. A region merging prior for variational level set image segmentation. *IEEE Trans on Image Proc.* 2008; 17(12): 2301–2311; doi: 10.1109/TIP.2008.2006425.
27. Salah M. Ben, Mitiche A., Ayed I. B. Effective level set image segmentation with a kernel induced data term. *IEEE Trans on Image Proc.* 2010; 19(1): 220-232; doi: 10.1109/TIP.2009.2032940.

12

Image Segmentation With B-Spline Level Set

1. M. Unser, "Splines: a perfect fit for signal and image processing," *IEEE Signal Processing Magazine*, vol. 16, pp. 22–38, 1999.
2. B. K. P. Horn, *Robot vision*. New York: MIT Press, 1986.
3. M. Eden, M. Unser, and R. Leonardi, "Polynomial representation of pictures," *Signal Processing*, vol. 10, pp. 385–393, 1986.
4. V. Torre and T. A. Poggio, "On edge detection," *IEEE Transactions on Pattern Analysis and Machine Intelligence*, vol. 8, pp. 147–163, 1986.
5. M. Unser, A. Aldroubi, and M. Eden, "B-spline signal processing: part I-Theory," *Signal Processing IEEE Transactions on*, vol. 41, pp. 821–833, 1993.
6. J. Kittler, "On the accuracy of the Sobel edge detector," *Image and Vision Computing*, vol. 1, pp. 37–42, 1983.
7. Hueckel and H. Manfred, "A Local Visual Operator Which Recognizes Edges and Lines," *Journal of the Association for Computing Machinery*, vol. 20, pp. 634–647, 1973.
8. C. De Boor, *A practical guide to splines*. New York: Springer Verlag, 1978.
9. V. Caselles, R. Kimmel, and G. Sapiro, "Geodesic active contours," *International Journal of Computer Vision*, vol. 22, pp. 61–79, 1997.
10. N. Paragios and R. Deriche, "Geodesic Active Contours and Level Sets for the Detection and Tracking of Moving Objects," *IEEE Transactions on Pattern Analysis and Machine Intelligence*, vol. 22, pp. 266–280, 2000.
11. D. Lingrand, A. Charnoz, P. M. Koulibaly, J. Darcourt, and J. Montagnat, "Toward Accurate Segmentation of the LV Myocardium and Chamber for Volumes Estimation in Gated SPECT Sequences," in *European Conference on Computer Vision*, 2004, pp. 267–278.
12. N. Paragios, M. Rousson, and V. Ramesh, "Knowledge-based Registration & Segmentation of the Left Ventricle: A Level Set Approach," in *IEEE Workshop on Applications of Computer Vision*, 2002, p. 37.
13. J. Park, S. Park, and W. Cho, "Medical Image Segmentation Using Level Set Method with a New Hybrid Speed Function Based on Boundary and Region Segmentation," *Ieice Transactions on Information and Systems*, vol. 95, pp. 2133–2141, 2012.
14. T. Mcinerney and D. Terzopoulos, "Deformable models in medical image analysis: a survey," in *Mathematical Methods in Biomedical Image Analysis, 1996., Proceedings of the Workshop on*, 2002, pp. 171–180.
15. B. S. Morse, W. Liu, T. S. Yoo, and K. Subramanian, "Active contours using a constraint-based implicit representation," in *ACM SIGGRAPH*, 2005, p. 252.

16. A. Gelas, O. Bernard, D. Friboulet, and R. Prost, "Compactly supported radial basis functions based collocation method for level-set evolution in image segmentation," *IEEE Transactions on Image Processing*, vol. 16, pp. 1873–1887, 2007.
17. O. Bernard, D. Friboulet, P. Thevenaz, and M. Unser, "Variational B-spline level-set method for fast image segmentation," in *IEEE International Symposium on Biomedical Imaging: From Nano To Macro*, 2008, pp. 177–180.
18. O. Bernard, D. Friboulet, P. Thevenaz, and M. Unser, "Variational B-Spline Level-Set: A Linear Filtering Approach for Fast Deformable Model Evolution," *IEEE Transactions on Image Processing A Publication of the IEEE Signal Processing Society*, vol. 18, pp. 1179–1191, 2009.
19. R. Cipolla and A. Blake, "The dynamic analysis of apparent contours," *Proceedings Third International Conference on Computer Vision*, 1990, pp. 616–623.
20. S. Menet, P. Saint-Marc, and G. Medioni,"B-snakes: implementation and application to stereo," *IEEE Transactions on Image Processing*, vol. 9, pp. 720–726, 1990.
21. G. E. Hinton, C. K. I. Williams, and M. D. Revow, "Adaptive elastic models for hand-printed character recognition," in *International Conference on Neural Information Processing Systems*, 1992, pp. 512–519.
22. D. Cremers, F. Tischhäuser, J. Weickert, and C. Schnörr, "Diffusion Snakes: Introducing Statistical Shape Knowledge into the Mumford-Shah Functional," *International Journal of Computer Vision*, vol. 50, pp. 295–313, 2002.
23. D. Mumford and J. Shah, "Optimal approximations by piecewise smooth functions and associated variational problems," *Communications on Pure and Applied Mathematics*, vol. 42, pp. 577–685, 1989.
24. É. Debreuve, M. Gastaud, M. Barlaud, and G. Aubert, "Using the Shape Gradient for Active Contour Segmentation: from the Continuous to the Discrete Formulation," *Journal of Mathematical Imaging and Vision*, vol. 28, pp. 47–66, 2007.
25. P. M. Prenter, *Splines and variational methods*. New York: Wiley, 1975.
26. A. Goshtasby, F. Cheng, and B. A. Barsky, "B -spline curves and surfaces viewed as digital filters," *Computer Vision Graphics & Image Processing*, vol. 52, pp. 264–275, 1990.
27. M. Unser, A. Aldroubi, and M. Eden, "Fast B-spline Transforms for Continuous Image Representation and Interpolation," *IEEE Trans. Pattern Anal. Mach. Intell.*, vol. 13, pp. 277–285, 1991.
28. M. Unser, A. Aldroubi, and M. Eden, "B-spline signal processing: part II-Efficiency design and applications," *IEEE Transactions on Signal Processing*, vol. 41, pp. 834–848, 2002.
29. T. F. Chan and L. A. Vese, "Active contours without edges," *IEEE Transactions on Image Processing*, vol. 10, pp. 266–277, 2001.
30. T.-T. Tran, V.-T. Pham, and K.-K. Shyu, "Moment-based alignment for shape prior with variational B-spline level set," *Machine Vision and Applications*, vol. 24, pp. 1075–1091, 2013.
31. T. T. Tran, V. T. Pham, and K. K. Shyu, *Moment-based alignment for shape prior with variational B-spline level set*: Springer-Verlag New York, Inc., 2013.
32. J. G. Leu, "Shape normalization through compacting," *Pattern Recognition Letters*, vol. 10, pp. 243–250, 1989.
33. S. C. Pei and C. N. Lin, "Image normalization for pattern recognition," *Image & Vision Computing*, vol. 13, pp. 711–723, 1995.

34. H. Ming-Kuei, "Visual pattern recognition by moment invariants," *IRE Transactions on Information Theory*, vol. 8, pp. 179–187, 1962.
35. L. Chunming, X. Chenyang, G. Changfeng, and M. D. Fox, "Level set evolution without re-initialization: a new variational formulation," in *2005 IEEE Computer Society Conference on Computer Vision and Pattern Recognition (CVPR'05)*, vol. 1, pp. 430–436, 2005.
36. D. Cremers, S. J. Osher, and S. Soatto, "Kernel Density Estimation and Intrinsic Alignment for Shape Priors in Level Set Segmentation," *International Journal of Computer Vision*, vol. 69, pp. 335–351, 2006.
37. A. Tsai, A. Yezzi, W. Wells, C. Tempany, D. Tucker, A. Fan, *et al.*, "A shape-based approach to the segmentation of medical imagery using level sets," *IEEE Transactions on Medical Imaging*, vol. 22, pp. 137–154, 2003.
38. W. Liu, Y. Shang, X. Yang, R. Deklerck, and J. Cornelis, "A shape prior constraint for implicit active contours," *Pattern Recognition Letters*, vol. 32, pp. 1937–1947, 2011.
39. V.-T. Pham, T.-T. Tran, K.-K. Shyu, L.-Y. Lin, Y.-H. Wang, and M.-T. Lo, "Multiphase B-spline level set and incremental shape priors with applications to segmentation and tracking of left ventricle in cardiac MR images," *Machine Vision and Applications*, vol. 25, pp. 1967–1987, November 01 2014.
40. M. E. Leventon, W. E. L. Grimson, and O. Faugeras, "Statistical shape influence in geodesic active contours," in *5th IEEE EMBS International Summer School on Biomedical Imaging, 2002*.
41. D. A. Ross, J. Lim, R. S. Lin, and M. H. Yang, "Incremental Learning for Robust Visual Tracking," *International Journal of Computer Vision*, vol. 77, pp. 125–141, 2008.
42. L. A. Vese and T. F. Chan, "A Multiphase Level Set Framework for Image Segmentation Using the Mumford and Shah Model," *International Journal of Computer Vision*, vol. 50, pp. 271–293, 2002.
43. N. Vu and B. S. Manjunath, "Shape prior segmentation of multiple objects with graph cuts," in *Computer Vision and Pattern Recognition, 2008. CVPR 2008. IEEE Conference on*, 2008, pp. 1–8.
44. J. Woo, P. J. Slomka, C. C. J. Kuo, and B. W. Hong, "Multiphase segmentation using an implicit dual shape prior: Application to detection of left ventricle in cardiac MRI," *Computer Vision & Image Understanding*, vol. 117, pp. 1084–1094, 2013.
45. S. Zheng, B. Fang, L. Li, M. Gao, R. Chen, and K. Peng, "B-Spline based globally optimal segmentation combining low-level and high-level information," *Pattern Recognition*, vol. 73, pp. 144–157, 2018.
46. T. F. Chan, S. Esedoglu, and M. Nikolova, "Algorithms for Finding Global Minimizers of Image Segmentation and Denoising Models," *SIAM Journal on Applied Mathematics*, vol. 66, pp. 1632–1648, 2006.
47. T. Goldstein and S. Osher, "The Split Bregman Method for L1-Regularized Problems," *SIAM Journal on Imaging Sciences*, vol. 2, pp. 323–343, 2009.
48. C. Li, C. Xu, C. Gui, and M. D. Fox, "Distance Regularized Level Set Evolution and Its Application to Image Segmentation," *IEEE Transactions on Image Processing*, vol. 19, pp. 3243–3254, 2010.
49. L. Wang, L. He, A. Mishra, and C. Li, "Active contours driven by local Gaussian distribution fitting energy," *Signal Processing*, vol. 89, pp. 2435–2447, 2009.

50. M. Jung, G. Peyré, and L. D. Cohen, "Nonlocal Active Contours," *SIAM Journal on Imaging Sciences*, vol. 5, pp. 1022–1054, 2012.
51. V. Estellers, D. Zosso, R. Lai, S. Osher, J. P. Thiran, and X. Bresson, "Efficient Algorithm for Level Set Method Preserving Distance Function," *IEEE Transactions on Image Processing*, vol. 21, pp. 4722–4734, 2012.
52. J. Wang and K. L. Chan, "Incorporating Patch Subspace Model in Mumford–Shah Type Active Contours," *IEEE Transactions on Image Processing*, vol. 22, pp. 4473–4485, 2013.
53. L. Dai, J. Ding, and J. Yang, "Inhomogeneity-embedded active contour for natural image segmentation," *Pattern Recognition*, vol. 48, pp. 2513–2529, 2015.
54. K. Zhang, L. Zhang, K. M. Lam, and D. Zhang, "A Level Set Approach to Image Segmentation With Intensity Inhomogeneity," *IEEE Transactions on Cybernetics*, vol. 46, pp. 546–557, 2016.